University of Alberta

Cytotoxicity, mutagenicity, and genotoxicity of emerging drinking water disinfection byproducts

by

Claire Frances McGuigan

A thesis submitted to the Faculty of Graduate Studies and Research
in partial fulfillment of the requirements for the degree of

Doctor of Philosophy

in

Medical Sciences – Laboratory Medicine & Pathology

This thesis is dedicated
to my family,
and to the people of the
Town of High River
for whom everything
changed
on June 20, 2013.

"High River Strong"

Abstract

Drinking water disinfection byproducts (DBPs) are formed unintentionally when organic matter in raw water reacts with disinfectants used to kill pathogens. Epidemiological studies have shown that an increased risk of bladder cancer is associated with consumption of chlorinated water, but little is known of the toxicity of many DBPs. This thesis examined the cytotoxic, mutagenic, and genotoxic properties of phenazine and halobenzoquinone (HBQ) DBPs in human cells. Cytotoxicity was examined with an impedance-based real-time cell analysis (RTCA) instrument, mutagenicity was examined with the Ames test (bacterial reverse mutation assay), and genotoxicity was examined with the alkaline comet assay. Phenazine showed differential toxicity in human cell lines, producing an antiproliferative cytotoxic effect in HepG2 cells but a genotoxic effect in T24 cells. The BJ/XPA RTCA *in vitro* assay was developed and validated to provide high-throughput screening of cytotoxicity and nucleotide excision repair (NER)-mediated DNA damage simultaneously. Selected HBQs were examined with the BJ/XPA assay; the position, type, and number of substitutions on the benzoquinone ring affected cytotoxicity. All tested HBQs caused substitution mutations in the Ames test under at least some of the experimental conditions. 2,6-dichloro-3-methyl-1,4-benzoquinone (DCMBQ) was the most potent HBQ compound tested, demonstrating cytotoxicity, mutagenicity, and genotoxicity. Follow-up experiments indicated that N-acetylcysteine, a ROS scavenger, reduced cytotoxicity and genotoxicity when added concomitantly with DCMBQ. Both the cytotoxic and genotoxic effects of DCMBQ appeared to be mediated, at least in

part, by the formation of reactive oxygen species. DCMBQ-induced genotoxicity appeared to be refractory to repair and may involve formation of complex oxidatively generated clustered lesions. Additional *in vitro* and *in vivo* studies are required for HBQ DBPs, particularly DCMBQ, to further determine their toxic effects. In summary, the original contributions of this research are: 1) the development of a novel *in vitro* method to simultaneously assess cytotoxicity and NER-mediated genotoxicity; 2) new information on the cytotoxic, mutagenic, and genotoxic properties of halobenzoquinone DBPs; 3) discovery of cytotoxic and genotoxic properties of phenazine; and 4) evidence of potential toxic mechanisms of action of DCMBQ.

Acknowledgements

Table of Contents

List of Tables

List of Figures

List of abbreviations

2,5DBBQ: 2,5-dibromo-1,4-benzoquinone

2,6DBBQ: 2,6-dibromo-1,4-benzoquinone

8OHdG: 8-hydroxy-2'-deoxyguanosine

95% CI: 95% confidence interval

AC: alternating current

ANOVA: analysis of variance

ATCC: American Type Culture Collection

ATP: adenosine-5'-triphosphate

B(a)P: benzo(a)pyrene

BER: base excision repair

BPDE: benzo(a)pyrene diolepoxide

BrdU: 5-bromo-2'-deoxyuridine

CAS: Chemical Abstracts Service

CHO: Chinese hamster ovary

CI: cell index

DAR: transcription-coupled domain repair

DBP: drinking water disinfection byproduct

DCBQ: 2,6-dichloro-1,4-benzoquinone

DCFDA: 2',7' –dichlorofluorescein diacetate

DCMBQ: 2,6-dichloro-3-methyl-1,4-benzoquinone

DMSO: dimethyl sulfoxide

DNA: deoxyribonucleic acid

DPBS: Dulbecco's phosphate-buffered saline

EDTA: ethylenediaminetetraacetic acid

ELISA: enzyme-linked immunosorbent assay

EMEM: Eagle's minimal essential medium

FBS: fetal bovine serum

FITC: fluorescein isothiocyanate

GGR: global genome repair

HAA: haloacetic acid

HBQ: halobenzoquinone

hOGG1: human 8-oxoguanine DNA glycosylase 1

IARC: International Agency for Research on Cancer

IC_{50}: inhibitory concentration (50%)

kDa: kilodaltons

kHz: kilohertz

LDH: lactate dehydrogenase

LOAEL: lowest observed adverse effect level

MEM: minimum essential medium

mRNA: messenger ribonucleic acid

MTT: 3-(4,5-dimethylthiazol-2-yl)-2,5-diphenyltetrazolium bromide

NDMA: N-Nitrosodimethylamine

NER: nucleotide excision repair

NIGMS: National Institute of General Medical Sciences

NOM: natural organic matter

ODN: oligodeoxynucleotides

PARP: poly (ADP-ribose) polymerase

PBS: phosphate-buffered saline

PBST: phosphate-buffered saline with Tween 20

PCNA: proliferating cell nuclear antigen

P_{OW}: octanol-water partition coefficient

PZ: phenazine (unsubstituted unless otherwise specified)

QSTR: quantitative structure-toxicity relationship

ROS: reactive oxygen species

RTCA: real-time cell analysis

RT-CES: real-time cell electronic sensing

SDS-PAGE: sodium dodecyl sulfate polyacrylamide gel electrophoresis

SEM: standard error of the mean

$t_{1/2}$: half-life

TCBQ: 2,3,6-trichloro-1,4-benzoquinone

TCR: transcription-coupled repair

THM: trihalomethane

TOBr: total organic bromine

TOCl: total organic chlorine

TOX: total organic halide

U: units

UV: ultraviolet

XP: xeroderma pigmentosum

XTT: (2,3-bis-(2-methoxy-4-nitro-5-sulfophenyl)-2H-tetrazolium-5-carboxanilide)

Chapter 1: Introduction[1]

1.1   History & background: drinking water disinfection byproducts (DBPs)

The advent of drinking water disinfection has resulted in dramatically reduced mortality from water-borne microbiological diseases. Widely considered one of the most important public health advances, drinking water disinfection is vital to protecting public safety and community health (1). The drinking water treatment process normally consists of several steps, including pretreatment (to remove large debris), coagulation/flocculation/sedimentation (to bind, precipitate, and remove suspended particles), filtration (to remove additional suspended particles), and disinfection (to kill or disable pathogenic microorganisms) (2, 3). The amount of chemical disinfectant is adjusted to ensure that a disinfectant residual remains as the treated water moves throughout the distribution system. By ensuring an adequate concentration of disinfectant remains in the water until it reaches the consumer, safe, high-quality drinking water free of pathogenic microorganisms may be provided to the public.

Drinking water disinfection byproducts (DBPs) are unintentionally produced from reactions between chemical and/or physical disinfectants and organic materials in raw water. Naturally-occurring organic matter (NOM) and anthropogenic contaminants (pharmaceuticals, pesticides, etc.) can react with common disinfectants, including chlorine, chloramine, chlorine dioxide, ozone, and UV light, to produce a large variety of DBPs. Initial interest in DBPs began in 1974 with the discovery of chloroform and trihalomethane (THM) DBPs in disinfected water (1-3) and the first US Environmental Protection Agency survey of municipal drinking waters for halogenated organic compounds, which discovered that chloroform and other THMs were widespread in chlorinated American drinking water (4). Chloroform was initially found to be carcinogenic in rodents

---

[1] A version of **Section 1.7** of this chapter has been accepted for publication. Moe B, McGuigan CF, Dabek-Zlotorzynska E, Gabos S, Li XF. 2013. Encyclopedia of Analytical Chemistry. Hoboken, NJ: John Wiley and Sons, Inc.

(5), but it was later discovered that the dosing protocol in these studies had significantly contributed to the observed toxicity (6), as other studies using a different dosing vehicle did not show carcinogenicity (7). Due to concerns about potentially toxic DBPs, regulatory agencies began to develop maximum allowable concentrations of specific DBPs in finished water, and research expanded to include other newly-discovered DBP compounds and classes. In the 1980s and 1990s, the identification of haloacetic acids (8), the genotoxic halofuranones (e.g. MX) (9), and the carcinogenic nitrosamines (e.g. nitrosodimethylamine, NDMA) (10) as DBPs spurred further interest in DBP research and regulation. The identification of NDMA and other nitrosamines revealed that DBPs could also include *non*-halogenated compounds, creating further avenues of research. In subsequent decades, the numbers of newly-discovered DBPs increased rapidly due to improvements in isolation, detection, and analytical methods. Recent approaches in DBP research include using computational chemistry principles to predict the formation and toxicity of possible byproducts (11, 12). DBP publications have steadily increased since the 1970s; as of July 23, 2013, of the 650+ entries in PubMed pertaining to "drinking water disinfection byproducts", over 480 were published in the last 10 years. A more detailed review of the history of DBPs, including risk assessment and public health considerations, is available (13). Although significant progress has been made in DBP research over the past 40 years, enormous challenges lie ahead.

1.2   Challenges in DBP research

A major challenge in DBP research is the sheer number of known and predicted DBPs. Over 600 DBPs have been discovered; however, these likely represent only 25-50% of all existing DBPs (14). A mass-balance experiment which monitored total organic halogen (TOX), total organic bromine (TOBr), and total organic chlorine (TOCl) in US drinking water treatment plants revealed that only 30% of TOX, 39% of TOBr, and 24% of TOCl was incorporated into identified halogenated DBPs; the identity of the remainder was unknown (15). These

findings indicate that there are hundreds, if not thousands, of unidentified DBPs potentially present in drinking water. Determining the toxicity or potential public health impact of so many unknown compounds poses an enormous challenge. Efforts are underway to identify and predict the formation of DBPs, but this is a resource-intensive process. Even many recently identified DBPs have little or no toxicological information available. The traditional approach of testing compounds first with *in vitro* assays, then *in vivo* rodent bioassays is not feasible for DBP research, due to the time- and resource-intensive nature of *in vivo* testing and the large number of DBPs. Therefore, a new method must be developed for efficient screening and identification of toxic DBPs, while providing data suitable for regulatory decision-making.

The highly variable nature of DBP formation also poses significant challenges; the composition and concentrations of DBPs may be influenced by disinfectant type, contact time, source water conditions, temperature, pH, and other factors (11, 16, 17). Because so many factors are involved, not all identified DBPs will be present in all drinking water systems, and changing conditions within a drinking water system over time will influence the composition of resulting DBPs. The development of analytical methods for unknown DBPs is also challenging, as the chemical properties (structure, polarity, stability, etc.) of these substances are not known. Existing analytical methods may not provide an accurate assessment of all DBPs in a sample. As an example, our research group discovered several new nitrosamine DBPs using a new analytical method. These thermally unstable nitrosamines could not be detected using the previously accepted analytical method because they were destroyed during the separation process (18). The sheer number of unknown DBPs and the variable nature of DBP formation create unique and difficult challenges in determining the composition, toxicity, and potential public health impact of these substances.

1.3 Toxicity of DBPs

As DBPs are discovered, they may be assessed for toxicity using *in vitro* and *in vivo* methods. However, as previously stated, the large numbers of identified DBPs pose a challenge, as the time required for toxicity testing (especially for *in vivo* studies) is unable to match the pace of DBP identification. Therefore, there are many identified DBPs which have little to no toxicological information available. The most comprehensive examination of DBP toxicology to date is a review published in 2007 (14), which discusses the genotoxicity and carcinogenicity of 85 DBPs, 11 of which are subject to regulation in the United States. This study found that most of the 85 DBPs examined, including many regulated DBPs, had gaps in the available toxicological data, and different methods to examine mutagenicity and genotoxicity had been used for some compounds. Of the regulated DBPs, most were shown to have mutagenic, genotoxic, and/or carcinogenic properties in *in vitro* and *in vivo* assays. Ten of the 11 regulated DBPs (except bromoacetic acid) were tested in 2-year *in vivo* rodent bioassays for carcinogenicity, and nine of these demonstrated evidence of carcinogenicity. However, many *in vivo* rodent studies performed with DBPs indicated that tumours formed at different sites than those expected from the epidemiological findings (e.g. liver tumours instead of bladder or colorectal tumours) (14).

Based on existing data for emerging *unregulated* DBPs, it appears these substances have varying cytotoxic, genotoxic, mutagenic, and carcinogenic effects (14). However, several patterns have emerged, based on a "cyto- & genotoxicity index" allowing relative comparison of toxicity of different DBPs on CHO cells (14, 19). For both cytotoxicity and genotoxicity of halogenated DBPs, iodinated DBPs appear to be the most toxic, followed by brominated DBPs, then chlorinated DBPs. DBP species that contain nitrogen appear to be more cytotoxic and genotoxic compared to species which contain carbon but not nitrogen. When comparing DBP classes, the halonitromethanes, haloacetamides, and haloacetonitriles are more genotoxic and cytotoxic than the haloacetic acids or

4

halomethanes. Although these observations may be helpful in predicting the relative toxicity of new DBPs, significant knowledge gaps still remain and hundreds to thousands of DBPs have yet to be identified.

Since 2007, many studies have examined cytotoxicity and genotoxicity of individual DBPs and DBP mixtures. Many emerging DBPs have been tested for genotoxicity and cytotoxicity using Chinese hamster ovary (CHO) cells, including haloacetamides (20), iodinated DBPs (21), nitrosamines (22), and haloacetic acids (23, 24). Similar methodology has been used to examine samples of disinfected water from swimming pools and hot tubs (25, 26), disinfected waters containing iodinated X-ray contrast media (27), and organic fractions of water disinfected with or without chlorine and UV light (28). In all the studies described above, the DBPs or DBP mixtures were cytotoxic and/or genotoxic to the CHO cells under at least some of the experimental conditions. A similar study found that selected haloacetic acid DBPs were both cytotoxic and mutagenic in CHO cells *in vitro* (29). The presence of microcystins, a common water contaminant arising from algae, caused a greater-than-additive increase in genotoxicity and mutagenicity of the halofuranone DBP MX in CHO cells, as measured by the comet assay and Ames test; this toxicity is thought to involve the presence of reactive oxygen species (30). Because CHO cells were frequently used for DBP toxicity testing, known and newly-discovered DBPs can be tested in the same system to determine their relative toxicity, as described previously (14, 19).

Other mammalian cell types have been used to examine DBP toxicity. Monohaloacetic acid DBPs were genotoxic and clastogenic in primary human lymphocyte cells *in vitro* (31), but other experiments exposing a human lymphoblastoid cell line to monohaloacetic acids showed no significant genotoxicity (32). In a panel of 15 compounds, representing trihalomethanes, haloacetic acids, haloacetonitriles, furanone, and acetaldehyde DBPs, iodinated DBPs were found to be the most genotoxic to HepG2 cells, as measured by the alkaline comet assay (33). Iodoacetic acid was cytotoxic and genotoxic to mouse fibroblast cells *in vitro*, and was also tumorigenic in nude mice *in vivo* in a 30-day

5

study (34). Genotoxicity of selected nitrosamine DBPs to human lymphocytes and lymphoblastoid cells was observed only at high (millimolar) concentrations (35). Our research group found that selected nitrosamine DBPs were cytotoxic to CHO cells, as well as human liver, bladder, and lung cancer cell lines; N-nitrosodiphenylamine was found to cause cell cycle arrest in CHO cells (36). Other members of our research group determined that selected halobenzoquinone DBPs were cytotoxic to human bladder cancer cells via induction of reactive oxygen species production, leading to oxidative damage of DNA and cellular proteins (37). Four of 16 organic N-chloramine DBPs tested were genotoxic and cytotoxic to human lymphoblastoid cells *in vitro* (38), and hydroxyfuranone DBPs also showed genotoxicity in human lymphoblastoid cells (39). Concentrates of surface waters disinfected with chlorination were genotoxic and induced oxidative stress in a human liver cell line (40), but in other experiments, human colon and breast cancer cell lines showed little cytotoxicity and oxidative stress when exposed to enriched fractions of chlorinated and/or chloraminated water, except at high levels of enrichment (41, 42). From these results, it appears that DBPs can cause cytotoxicity and genotoxicity in a variety of cell types, but these effects may not necessarily result from environmentally relevant exposures.

Many DBPs have been investigated for mutagenicity, especially with the Ames test. Besides the mutagenicity assays mentioned above, there have been a number of other studies in this area. Mutagenicity studies published before 2007 are reviewed in detail elsewhere (14); generally, mutagenicity was observed for many regulated and emerging unregulated DBPs, as well as extracts or concentrated samples of chlorinated water. More recently, six DBPs from the halonitromethane, halogenated acetaldehyde, and hydroxyfuranone classes were tested in a mouse lymphoma mutagenicity assay, but only mucobromic acid (a hydroxyfuranone) caused mutagenicity at the highest tested concentration (43). Mutagenicity testing of five nitrosamine DBPs with a specialized *Salmonella* strain sensitive to alkylating agents revealed four were mutagenic, but only upon metabolic activation with S9 fraction (22). A survey of five drinking water treatment facilities in the United States found correlations between the

mutagenicity of concentrated disinfected water samples and the total organic carbon in the raw water plus the total chlorine dose, the concentration of total organic halides in the finished water, and haloacetic acid concentration in the finished water (44). Testing of both volatilized and liquid-concentrated components of disinfected drinking water revealed that chlorination produced more mutagenic products compared to water disinfected with ozone followed by chlorination, as measured by the Ames test (45). Concentrated extracts of swimming pool water treated with either chlorinated or brominated disinfectants produced significant mutagenicity in the Ames test, with over 100 different DBPs identified in the samples; the degree of mutagenicity was similar to that of disinfected drinking water (46). As extracts of treated water appear to be consistently mutagenic in the Ames test, mutagenicity testing of individual compounds will be an important tool to discover the DBP classes responsible for this effect.

In vivo studies of DBPs as mixtures, thought to be a more environmentally relevant model for toxicity, are also underway (47). Administration of concentrated disinfected drinking water to pregnant Sprague-Dawley rats did not appear to have adverse developmental effects on offspring (48), but pregnant F344 rats exposed to mixtures of regulated DBPs experienced pregnancy loss and eye malformations in offspring at high DBP concentrations (49). Related *in vivo* experiments showed reduced pup weight and increased incidence of eye malformation in offspring of F344 rats exposed to DBP mixtures while pregnant; Sprague-Dawley rats exposed while pregnant experienced increased perinatal mortality of pups and lower pup weight compared to the unexposed control group (50). Although the sheer number of DBPs precludes performing *in vivo* rodent assays for each compound, DBPs that appear toxic in *in vitro* assays should be subjected to *in vivo* screening in order to obtain appropriate data for risk assessment.

Based on the results from both *in vitro* and *in vivo* toxicity assays, many of the regulated and newly-emerging DBPs may be cytotoxic, genotoxic, mutagenic, or

carcinogenic under specific experimental conditions. Individual DBPs as well as concentrated extracts from disinfected waters were capable of producing deleterious effects in experimental systems. However, it is important to note that these experiments used high DBP concentrations that would not be found in actual water samples, and *in vitro* or *in vivo* experiments are not necessarily accurate models of environmentally relevant exposure in humans. Many DBPs still have little or no toxicological information available, but it appears that some emerging DBPs could possess equal or greater toxicity compared to the currently-regulated DBPs. Additional *in vivo* studies are required to examine effects of DBPs in intact organisms, particularly for those shown to be toxic in *in vitro* studies.

1.4   Human exposure and epidemiological studies

When considering human exposure to DBPs, it is important to consider all potential exposure routes. Initial investigations into DBPs primarily focused on oral consumption of drinking water. However, dermal and inhalational exposure to DBPs may result from the use of treated water for bathing, showering, and swimming (51-54). Swimming pools and hot tubs maintain a higher disinfectant residual compared to drinking water, in order to deal with organic substances (personal care products, bodily fluids, epithelial cells, etc.) introduced into the water by bathers ('bather load'). DBP composition in pools or hot tubs may be different than that found in drinking water due to the different disinfectants potentially in use (e.g. the use of brominated disinfectant systems in swimming pools and hot tubs) (46). These potential sources and routes of exposure should also be considered when determining total exposure to DBPs.

Several studies have examined the *in vivo* effects of DBPs on humans in realistic exposure situations. Lymphocytes from human volunteers who swam in a chlorinated indoor pool for 40 minutes did not show increased DNA damage compared to lymphocytes collected before swimming, as measured by the comet

assay; however, urine from the post-swimming participants was shown to be more mutagenic in the Ames test compared to urine collected prior to swimming (55). In a similar study, 6 of 10 human volunteers dermally administered the DBP bromodichloromethane, and 3 of 8 volunteers with oral administration, showed significantly increased mutagenicity of post-exposure urine samples compared to pre-exposure samples, as assessed by the Ames test (56). Toxicity of brominated THM DBPs in humans may be correlated with activity of the glutathione transferase theta 1 (GSTT1) metabolic enzyme, as these compounds are bioactivated by this enzyme (57). Functional GSTT1 polymorphisms (as opposed to the null GSTT1 genotype) were associated with an increased risk of bladder cancer with THM exposure in a recent case-control study (58). Although few *in vivo* studies with humans have been performed, they are important for determining the toxicokinetics and possible toxic effects of environmentally relevant DBP exposure.

Epidemiological studies have been conducted to examine health effects associated with exposure to disinfected drinking water. The primary concern over DBPs arises from a number of studies which have linked chlorinated water exposure to a variety of adverse health effects. The overall odds ratios reported in epidemiological studies investigating the association between exposure to disinfected water and cancer generally range between 1-3 (11), indicating a moderate increase in risk at most. However, a small yet consistent association between exposure to chlorinated water and an increased risk of bladder cancer has been observed in several cohort and case-control studies (51, 59-62). Other epidemiological studies have examined the associations between exposure to chlorinated water or specific disinfection byproducts and brain cancer (63), colorectal cancer (64, 65), congenital anomalies (66-68), and adverse effects on fetal growth or maturity (69, 70), but little to no excess risk has been observed for most studies (61). However, a recent investigation revealed a significant association between exposure of pregnant women to high levels of chlorate and chlorite in drinking water and increased risk of congenital abnormalities in their children (71). The authors caution that more research is required to confirm this

9

hypothesis as some potentially confounding variables were not incorporated in the study. In general, public health-based decisions on DBPs focus on bladder cancer risk, as it is the strongest and most consistent association observed to date.

1.5 Regulatory control of DBPs

Relatively few DBPs are currently subject to regulatory limits in drinking water. Health Canada legislates the Maximum Acceptable Concentration (MAC) of bromate (0.01 mg/L), chlorate (1 mg/L), chlorite (1 mg/L), five haloacetic acids (monochloroacetic acid, dichloroacetic acid, trichloroacetic acid, monobromoacetic acid, and dibromoacetic acid; total 0.08 mg/L as a running annual average of quarterly samples), N-nitrosodimethylamine (NDMA; 40 ng/L), and four trihalomethanes (bromodichloromethane, bromoform, dibromochloromethane, and chloroform; total 0.1 mg/L as a running annual average of quarterly samples). The guideline value for haloacetic acids also indicates concentrations of these compounds should be as low as reasonably achievable (ALARA) without adversely affecting water disinfection (72). In the United States, similar Maximum Contaminant Level (MCL) values from the Environmental Protection Agency are in place for bromate, chlorite (0.8 mg/L), the five haloacetic acids (total 0.06 mg/L as a running annual average), and four trihalomethanes (total 0.08 mg/L as a running annual average) (73). Additional DBPs will be considered for future MCL development as part of the Contaminant Candidate List 3 (74).

While THMs and HAAs represent ~25% of all halogenated DBPs by mass, they do not account for the increased risks observed in epidemiological studies. The risk of bladder cancer observed in epidemiological studies is 20-fold greater than the calculated risk of all cancers in experimental animals treated with regulated DBPs. Current data indicate that THMs and HAAs are likely not sufficiently potent and are not present in sufficient concentrations to be responsible for the observed association with bladder cancer risk (11, 14). Furthermore, relying

10

solely on measures of THMs and HAAs to determine water quality may underestimate the risk of more toxic DBPs in drinking water (12). Water utilities switching from chlorine to chloramine disinfectant to reduce THM and HAA concentrations has resulted in formation of more toxic DBPs (e.g. nitrosamines and halobenzoquinones) in some systems (14). To set more appropriate water quality standards, and minimize the risk of adverse effects, better toxicological data for DBPs are urgently required.

1.6 Computational approaches in DBP research

As previously stated, the large number of unknown and newly-discovered DBPs presents a difficult challenge for toxicity testing and regulation. A novel approach to identifying toxic DBPs uses quantitative-structure toxicity relationship (QSTR) prediction to identify potentially toxic DBPs prior to laboratory testing (11, 12). This method uses organic chemistry principles to predict the structure of DBPs that could form based on the disinfectant in use and the natural organic material (NOM) structures present in the incoming raw water. A QSTR program then analyzes the chemical and structural properties of the proposed DBPs to predict the molecular interactions it may have *in vivo*. These properties are compared to databases of compounds with known toxicological properties, including toxic and non-toxic compounds. The QSTR program uses the degree of similarity of the proposed DBP to compounds in the databases in order to predict its toxic properties, such as carcinogenicity or developmental toxicity. The program also generates a predicted chronic rat lowest observed adverse effect level (LOAEL) for each compound. This value indicates the lowest amount of continuous exposure which could case adverse health effects in rats, and can be used for comparing the potency of compounds to one another.

While this approach works well for straightforward receptor-chemical interactions, it is less successful for predicting more complex outcomes like carcinogenicity; the primary value of QSTR in these situations is to determine the

11

relative potency of predicted compounds (11, 12). As the carcinogenicity databases are composed of *in vivo* rodent studies, the predictions have limited applicability to humans due to significant differences in human vs. rodent anatomy and physiology. As the databases that QSTR uses have different characteristics (test species, endpoint, experimental conditions), they can produce conflicting results. Not all chemical structures are represented in the databases, so the predictive ability of the program may be poor for certain classes of compounds. This issue is particularly relevant for DBPs, as many newly-discovered DBPs have unique structures that are not currently represented in toxicity databases, preventing accurate toxicity predictions by QSTR (11, 12). While this approach has successfully predicted the presence of some DBP species in finished water (e.g. halobenzoquinones (75)), the lack of appropriate toxicological data for the QSTR program limits its ability to accurately predict DBP toxicity.

1.7   *In vitro* **assay development for DBP screening**

Due to the limitations of predictive computational toxicology methods, additional screening assays for DBP toxicity are desired, and empirically-derived toxicity data from newly-discovered DBP species are required. The use of *in vitro* toxicity assays is particularly well-suited for this application, as these assays are often relatively inexpensive, can examine many compounds simultaneously, and can make use of standardized cell lines. Results from *in vitro* assays may be used to prioritize newly-discovered DBPs for further testing, allowing identification of compounds of concern. These results will also allow relative comparison of DBP toxicity, both within and between chemical classes; comparison with QSTR toxicity predictions may also be performed. In this thesis, several established *in vitro* methods have been used to examine the cytotoxicity, mutagenicity, and genotoxicity of several newly-discovered DBPs.

However, traditional *in vitro* cytotoxicity assays have several disadvantages. Many of these assays are 'endpoint-based', providing data for only a single exposure timepoint per experiment. Assays may be specific for individual parameters of cell function, such as proliferation, metabolic capacity, morphology, etc. An individual culture often cannot be used for measurements of multiple effects or at multiple timepoints; thus, a different set of cells is required for each individual experiment. This may lead to increased inter-experimental variability, preventing identification of subtle effects (76). Endpoint-based assays often rely on indirect measurements of cell function, using dyes or labels. For example, common dye- or label-based cytotoxicity assays rely on dye exclusion (trypan blue) (77), dye retention (Neutral Red Uptake) (78), metabolic activation (resazurin (79), MTT (80)), or incorporation of a detectable label (5-bromo-2-deoxyuridine, BrdU) (81)). Depending on the assay, substantial sample processing time may be required before data are collected. While dye- and label-based endpoint assays are widely used, they may not provide a rapid, sensitive, and high-throughput method of measuring cell response.

However, an alternative cell monitoring technology, known as impedance-based assays, provide another approach for measuring cell response. One such system is known as real time cell analysis (RTCA), manufactured by ACEA Biosciences, Inc. (San Diego, CA). (The technology is also known by the names real-time cell electronic sensing (RT-CES) and xCELLigence^{TM}; however, the acronym RTCA will be used in this thesis.) The basic concept of the technology is as follows (76, 82): adherent cells are cultured in specialized multiwell plates which contain electrodes embedded in the bottom surface (**Figure 1-1A**). The cells attach to the plate surface and the embedded electrodes. The plates are connected to a system which generates a low-voltage (<20mV) alternating (AC) current and measures electrical impedance across the electrodes. The current is applied at user-defined intervals both before and after the desired treatment is applied, allowing real-time monitoring of cell response. The number of cells and the degree of contact they have with the electrodes will affect the way the current flows through the electrodes. Increased cell-electrode contact, through increased cell number (via

proliferation) and/or greater contact of individual cells with the electrodes (via changes in morphology) will result in increased impedance. Conversely, decreased cell-electrode contact, through cell death, detachment from the electrodes, or morphological changes resulting in less contact of each cell with the electrodes result in decreased impedance.

In the RTCA system, impedance is not reported directly. Instead, a unitless parameter termed "cell index" (CI) is used to describe the interaction of the cells with the electrodes. CI is automatically calculated by the RTCA system and, because it is unitless, it is used to facilitate comparisons between experiments. The equation used to calculate cell index is:

$$CI = \max_{i=1...N} \left(\frac{R_{cell}(f_i)}{R_0(f_i)} - 1 \right)$$

where CI is cell index, N refers to the number of frequencies at which impedance is measured (N=3: 10kHz, 25kHz, and 50kHz), $R_{cell}(f_i)$ is the resistance of the electrodes at a given frequency with cells present in the well, and $R_0(f_i)$ is the resistance of the electrodes at a given frequency when no cells are present in the well (83). Multiple frequencies are used in impedance measurements because the behaviour of a current in this system will depend on the frequency of the applied current. Currents will flow between and around cells at low frequencies, while higher frequencies generate currents which flow directly across cell membranes (84). As with impedance, an increased CI indicates greater cell-electrode contact due to cell viability, proliferation, or adhesion; a decreased CI indicates reduced cell-electrode contact due to cell death, detachment, or induction of a cytostatic state (**Figure 1-1B**). In this way, CI values represent a blended measurement of cell number, proliferation, and morphology, and are thought to be a more comprehensive measurement of cell health compared to traditional dye- and label-based assays (85).

I have used the RTCA system to develop and validate a new high-throughput *in vitro* assay (the BJ/XPA RTCA *in vitro* assay), capable of simultaneously

examining cytotoxicity and specific types of DNA damage. This novel method continuously monitors human cell lines exposed to potentially toxic DBPs. The resulting assay is simple, quick to perform, capable of screening many compounds simultaneously, and is able to generate continuous data from a single plating of cells. The development of this new *in vitro* assay could be a valuable addition to the predictive and computational toxicity testing methods already in use, and the results obtained from this testing could be used to design future *in vivo* assays, resulting in more efficient use of limited testing resources.

A)

ACEA Biosciences, www.aceabio.com
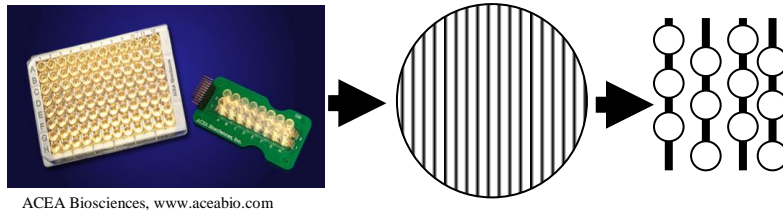
B)
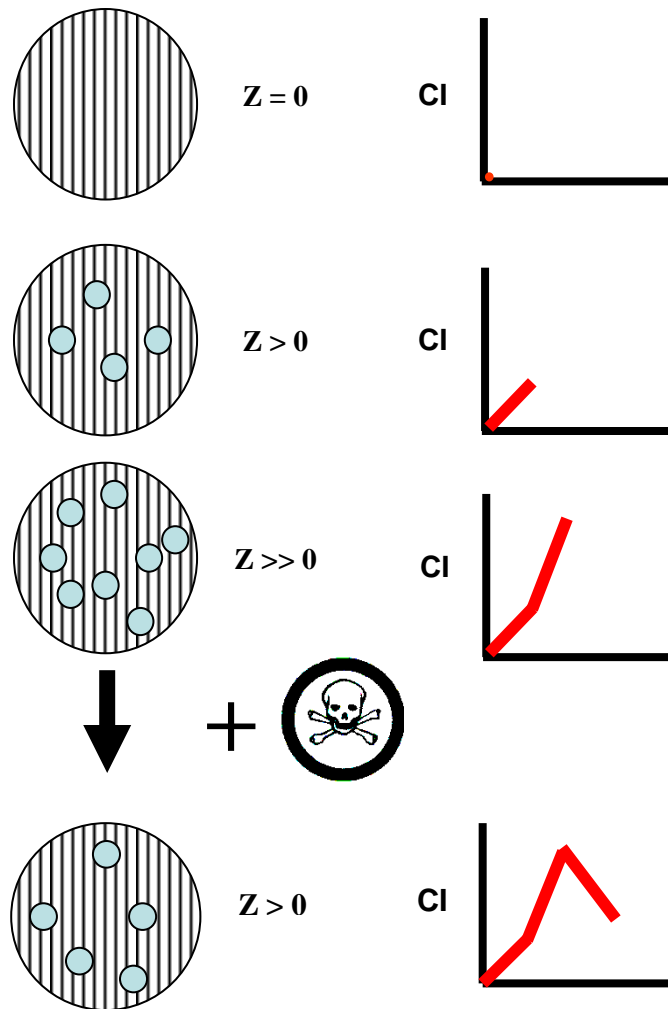
Figure 1-1: The RTCA system

A): The bottom surface of each well in an RTCA plate (left) is lined with ~2000 gold microelectrodes, arranged in a linear pattern (centre). Upon closer examination (right), the electrodes are aligned in a circle-on-line format,

permitting the electrodes to cover over 80% of the bottom surface of the well (82). (Note that drawings are not to scale.) **B**): A visual representation of the relationship between cell-electrode interaction and CI. Before cells are added to the plate, there is no impedance (Z) of the current, so CI=0. After cells are added and attach to the bottom of the plate, the impedance and CI increase. As the cells proliferate, the impedance and CI continue to increase. However, when a cytotoxic substance (represented by the skull and crossbones) is added which causes cells to die and/or detach from the plate, the impedance and CI decrease.

1.8   DNA repair pathways

Through the use of the RTCA system and other experimental protocols, this thesis also explores the contributions of DNA damage and repair to the toxicity of DBPs. Two major DNA repair pathways were examined: nucleotide excision repair (NER) and base excision repair (BER). These specific pathways were selected because they repair a wide range of DNA lesions which may be caused by emerging DBPs (e.g. adduct formation, oxidative damage). Several excellent review articles exist for NER (86-89) and BER (86, 87, 89, 90); the following overview represents a summary of these sources.

The nucleotide excision repair (NER) pathway (86-89) primarily repairs bulky adducts, DNA cross-linking, and photodimers caused by exposure to UV light. However, NER may also repair oxidative damage, either by repairing specific oxidative lesions (91, 92) and/or by acting as a backup pathway to the base excision repair (BER) pathway (93), which repairs most oxidative DNA lesions. The primary proteins involved in NER are known as XP proteins, named after xeroderma pigmentosum, a genetic disorder arising from defective NER.

There are two types of NER: global genome repair (GGR), which occurs continuously in the entire genome; and transcription-coupled repair (TCR), which occurs when an unrepaired lesion is detected during transcription. **Figure 1-2** details the steps of both GGR and TCR. GGR begins when a distortion is detected

17

in the double-helix structure by a protein triad composed of XPC, HR23B, and centrin 2. XPC has a strong affinity for damaged DNA and will cause the triad to bind to the damaged site. Some lesions repaired by NER, such as cyclobutane pyrimidine dimers, do not distort the helix sufficiently to attract the XPC complex. In these cases, the damaged DNA binding (DDB) complex, which includes the XPE protein, will bind to the DNA and deliberately distort the helix so it may be detected by the XPC complex. Once the XPC complex has bound to the damaged site, the DNA around the lesion is unwound by the TFIIH complex, which includes the XPB and XPD helicase proteins. Next, the XPA protein binds to the damaged site and displaces the XPC triad complex. The precise role of XPA in NER is unclear, but NER is unable to proceed without functional XPA protein. The endonuclease proteins XPF and XPG then incise the damaged strand on either side of the lesion. A strip of ~25-30 nucleotides is removed, with the lesion normally located ~5 bases from the 3' side and ~24 bases from the 5' side. DNA polymerase δ or ε, along with proliferating cell nuclear antigen (PCNA), fills the resulting gap with the proper sequence of nucleotides, using the undamaged strand as a template. DNA ligase then repairs the nicks in the DNA to complete the NER process.

TCR bypasses the initial steps of the GGR pathway, since TCR is initiated on an emergency basis when RNA polymerase encounters a transcription-blocking lesion. After transcription is halted, additional enzymes such as XAB2, CSA, and CSB are recruited to the damaged site. The precise function of these enzymes is unclear, but they are required to recruit or initiate the binding of the TFIIH complex as described above. The remainder of TCR then proceeds through the same steps as GGR, starting with the binding of the TFIIH complex. Therefore, the TCR pathway bypasses the requirement for the XPC or XPE proteins, since it initiates the NER process later in the pathway. This feature may be exploited experimentally; for example, TCR alone may be studied by using cells deficient in functional XPC or XPE proteins, since these are required for GGR but not TCR. Conversely, all NER may be eliminated in cells deficient in a protein

central to both TCR and GGR, such as XPA. The latter approach was used in this thesis to study the ability of emerging DBPs to cause DNA lesions repaired by NER; please see **Chapter 3** for details.
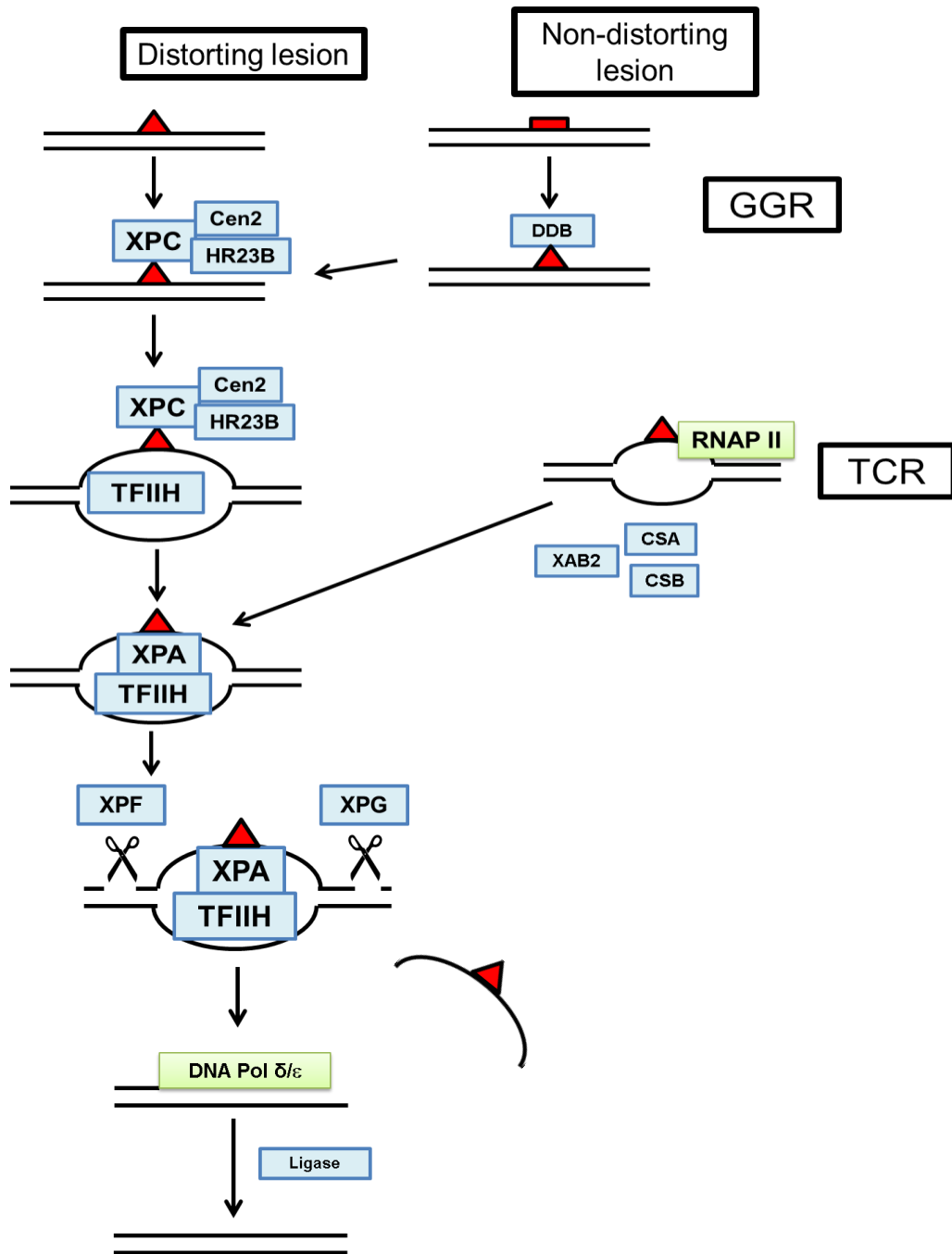
Figure 1-2: Nucleotide excision repair pathways

This figure shows simplified global genome repair (GGR) and transcription-coupled repair (TCR), as described above. The red triangle represents a helix-distorting lesion, while the red rectangle represents a non-helix-distorting lesion that is repaired by NER. The scissors icon indicates an endonuclease incision. RNAP II: RNA polymerase II, DNA Pol δ/ε: DNA polymerase delta or epsilon

Conversely, the base excision repair (BER) pathway primarily repairs small, non-distorting lesions such as oxidized, alkylated, and deaminated bases; missing bases; and the inappropriate incorporation of uracil into DNA (86, 87, 89, 90). First described by Tomas Lindahl in 1974 (94), the BER pathway consists of five steps. Two varieties of BER exist: the more common short-patch pathway (seen on the left side of **Figure 1-3**), which replaces a single nucleotide; and the long-patch pathway, which replaces two to ten nucleotides (seen on the right side of **Figure 1-3**). For both types of BER, initial recognition of damaged bases is performed by glycosylase enzymes. Many different glycosylases exist, each specific for certain DNA lesions. This is in contrast to NER, which uses the same cellular machinery for all lesions falling under the NER pathway. The appropriate glycosylase will remove the damaged base by cleaving the N-glycosidic bond, which results in formation of an apyrimidinic or apurinic site. Next, a nick is made in the DNA backbone at the AP site by either AP endonuclease or DNA AP lyase. In some cases, the corresponding glycosylase can perform this activity; in other cases, involvement of a separate enzyme is required. Action of an exonuclease enzyme, such as DNA deoxyribophosphodiesterase, may be required to prepare the resulting gap for the replacement of the correct base by DNA polymerase.

At this point, the short-patch and long-patch BER pathways diverge. For short-patch BER, DNA polymerase β will insert a single nucleotide to replace the missing base. For long-patch BER, DNA polymerase β or δ (in conjunction with PCNA) will insert a string of two to ten nucleotides, beginning at the position of the missing base. This will create a "flap" of nucleotides, as DNA polymerase will displace the existing nucleotides as it inserts the new string (see **Figure 1-3**). A flap endonuclease protein then cleaves the DNA backbone to remove the extraneous string of nucleotides. In both pathways, once the correct base(s) have been inserted, DNA ligase will repair the nick in the DNA backbone, completing the BER process.

Short-patch BER is the more common form of BER, and is preferred when ATP is abundant. The less-common long-patch pathway is preferred when a single-strand break is present or when ATP levels are low. Long-patch BER requires the involvement of additional enzymes compared to short-patch BER, such as proliferating cell nuclear antigen (PCNA), and flap endonucleases. (For additional details on long-patch BER, please see the review papers by Hoeijmakers (87) and Robertson and colleagues (90)). While the individual contributions of short- and long-patch BER to emerging DBP toxicity were not considered in this thesis, some of the suspected mechanisms of toxicity of emerging DBPs cause lesions repaired by the BER pathway (e.g. oxidative damage). Therefore, the potential contribution of the BER pathway to emerging DBP toxicity will be discussed later in this thesis (see **Chapter 5**).
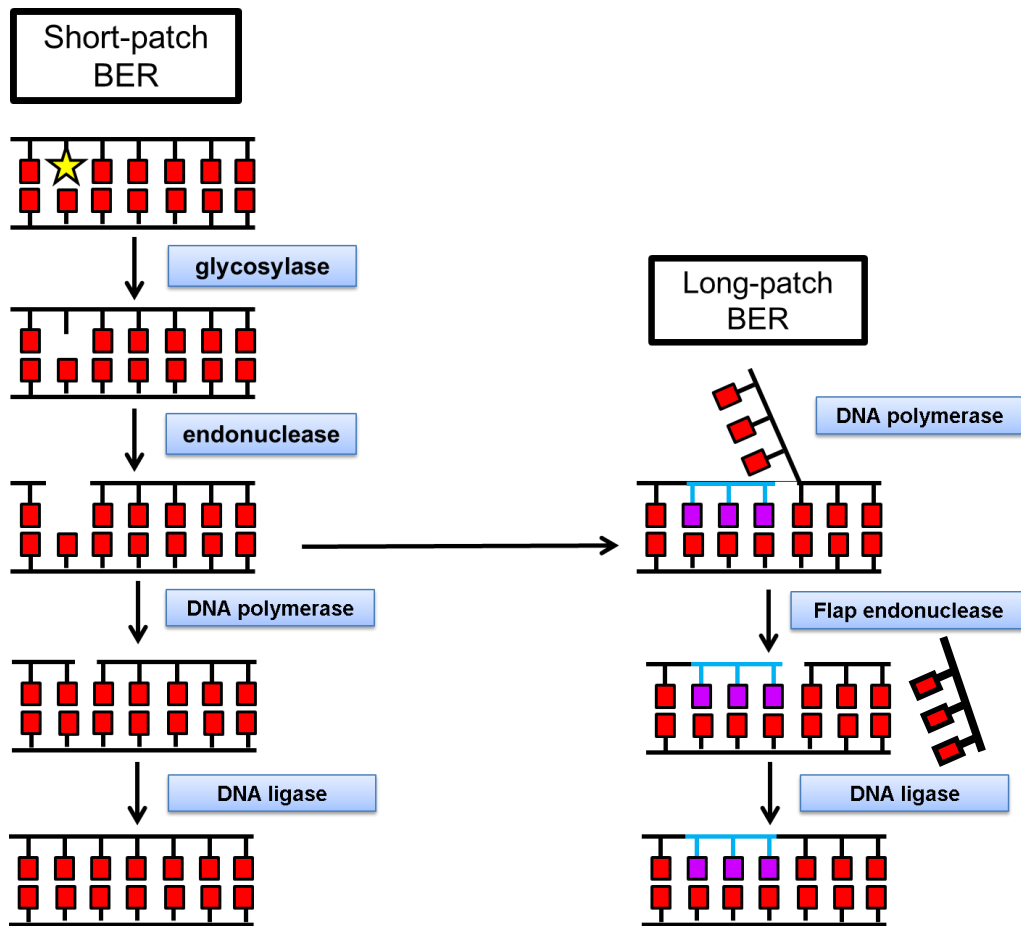
Figure 1-3: Base excision repair pathways

This figure shows simplified short-patch and long-patch BER, as described above. The yellow star represents a damaged base, the red squares represent undamaged bases, and the purple squares and blue lines represent newly-inserted nucleotides in long-patch BER. After the endonuclease has incised the DNA backbone, repair may occur either through the short-patch pathway (shown on the left) or through the long-patch pathway (shown on the right). (Note: for clarity and simplicity, enzyme family names and some associated proteins (e.g. PCNA during long-patch BER) are not shown.)

1.9 Specific focus: phenazine and halobenzoquinone DBPs

This work will focus primarily on two newly discovered classes of DBPs, phenazine and the halobenzoquinones. Phenazine, as a disinfection byproduct, was discovered by members of our research group (95), and is unique in that it may be formed by chemical or biological processes, or a combination of the two (see **Chapter 2** for further details). Phenazine is an N-heterocyclic polyaromatic hydrocarbon which may be substituted with halogens or other compounds. The halobenzoquinones we have examined here (see **Chapters 4&5**) are aromatic p-benzoquinone compounds with varying numbers and positions of chlorine or bromine substitutions, which arise from their interaction with disinfectants and compounds present in raw waters. (Other benzoquinone compounds, including o-benzoquinones, have been identified; however, this thesis will be restricted to discussion of p-benzoquinone compounds only.) The formation and toxic potential of some halobenzoquinones was predicted by QSTR (11, 12) and several have been confirmed to occur in finished North American drinking water (96, 97). The halobenzoquinone class has been identified as a research priority as QSTR predictions have identified several members of this class as potential potent carcinogens, particularly 2,6-dichloro-3-methyl-1,4-benzoquinone (DCMBQ) (12). In both cases, toxicological data for these compounds are either extremely limited or non-existent. As these compounds have been detected in finished drinking water samples, there is an urgent need for toxicological characterization to determine if they pose any potential risk to human health, and to determine their toxic mechanisms of action.

1.10 Hypotheses and objectives of this research

Based on the limited toxicological information in the scientific literature and the existing QSTR predictions (11, 12), the following hypotheses were formulated: 1) phenazine and halobenzoquinone DBPs will cause cytotoxicity in human cell lines in a concentration-dependent manner; 2) phenazine and halobenzoquinone

DBPs will cause DNA damage in mammalian cell lines; 3) DNA damage caused by phenazine and halobenzoquinone DBPs will contribute to the overall cytotoxicity in mammalian cell lines, as measured by real-time cell analysis (RTCA); and 4) of the halobenzoquinone DBPs tested in these experiments, DCMBQ will demonstrate the greatest overall *in vitro* toxicity under these experimental conditions.

More specifically, the objectives of this research were to: 1) investigate the *in vitro* cytotoxicity and genotoxicity of phenazine and halobenzoquinone DBPs, using human cell lines; 2) develop and validate a high-throughput, real-time *in vitro* system for the simultaneous detection of cytotoxicity and nucleotide excision repair-mediated DNA damage using human cell lines proficient and deficient in nucleotide excision repair (the BJ/XPA RTCA *in vitro* assay); 3) determine the mutagenicity of several halobenzoquinone DBPs; and 4) examine the mechanism of action of toxic halobenzoquinone DBPs, especially the formation of reactive oxygen species and the mechanism by which DNA damage is produced. These objectives were achieved through the use of *in vitro* methods using mammalian cells (with the exception of the Ames test in **Chapter 4**, which uses bacterial strains), with emphasis on using real-time cell analysis (RTCA), a high-throughput method, where possible.

In summary, this research represents a significant contribution to the field of drinking water disinfection byproduct research. These results will provide urgently-needed *in vitro* toxicity information on phenazine and halobenzoquinone DBPs, which may be used to prioritize these compounds for further testing. In addition, the *in vitro* method described in this thesis could be adapted to screen other classes of DBPs for cytotoxicity and genotoxicity. This could result in more rapid and efficient identification and reduction of potentially toxic DBPs, permitting the continued provision of safe, clean drinking water to the public.

1.11 References

1. Rook JJ. Formation of haloforms during chlorination of natural waters. Water treatment and examination. 1974;24:234-43.

2. Bellar TA, Lichtenberg JJ, Kroner RC. The occurrence of organohalides in chlorinated drinking waters. 1974.

3. Kopfler FC, Melton RG, Lingg RD, Colem WE. GC-MS determination of volatiles for the national organics reconnaissance survey (NORS) of drinking water. In: Keith LH, editor. Identification and analysis of organic pollutants in water. Ann Arbor, MI: Ann Arbor Science; 1976.

4. Symons JM, Bellar TA, Carswell JK, DeMarco J, Kropp KL, Robeck GG, et al. National organics reconnaissance survey for halogenated organics in drinking water. Cincinnati, OH: United States Environmental Protection Agency; 1975.

5. National Cancer Institute. REPORT ON THE CARCINOGENESIS BIOASSAY OF CHLOROFORM. Bethesda, Maryland: 1976.

6. Bull RJ, Brown JM, Meierhenry EA, Jorgenson TA, Robinson M, Stober JA. Enhancement of the hepatotoxicity of chloroform in B6C3F1 mice by corn oil: Implications for chloroform carcinogenesis. Environ Health Perspect. 1986 Nov;69:49-58.

7. Jorgenson TA, Meierhenry EF, Rushbrook CJ, Bull RJ, Robinson M. Carcinogenicity of chloroform in drinking water to male osborne-mendel rats and female B6C3F1 mice. Fundamental and Applied Toxicology. 1985;5(4):760-9.

8. Coleman WE, Melton RG, Kopfler FC, Barone KA, Aurand TA, Jellison MG. Identification of organic compounds in a mutagenic extract of a surface drinking water by a computerized gas chromatography/mass spectrometry system (GC/MS/COM). Environ Sci Technol. 1980;14(5):576-88.

9. Meier JR, Knohl RB, Coleman WE, Ringhand HP, Munch JW, Kaylor WH, et al. Studies on the potent bacterial mutagen, 3-chloro-4-(dichloromethyl)-5-hydroxy-2 (5H)-furanone: Aqueous stability, XAD recovery and analytical determination in drinking water and in chlorinated humic acid solutions. Mutation Research/Genetic Toxicology. 1987;189(4):363-73.

10. Mitch WA, Sharp JO, Trussell RR, Valentine RL, Alvarez-Cohen L, Sedlak DL. N-nitrosodimethylamine (NDMA) as a drinking water contaminant: A review. Environ Eng Sci. 2003;20(5):389-404.

11. Bull RJ, Awwa Research Foundation, United States. Environmental Protection Agency. Use of toxicological and chemical models to prioritize DBP research. Denver, CO: Awwa Research Foundation; 2006.

12. Bull RJ, Reckhow DA, Li X, Humpage AR, Joll C, Hrudey SE. Potential carcinogenic hazards of non-regulated disinfection by-products: Haloquinones, halo-cyclopentene and cyclohexene derivatives, N-halamines, halonitriles, and heterocyclic amines. Toxicology. 2011 Aug 15;286(1-3):1-19.

13. Hrudey SE. Chlorination disinfection by-products, public health risk tradeoffs and me. Water Res. 2009 May;43(8):2057-92.

14. Richardson SD, Plewa MJ, Wagner ED, Schoeny R, Demarini DM. Occurrence, genotoxicity, and carcinogenicity of regulated and emerging disinfection by-products in drinking water: A review and roadmap for research. Mutat Res. 2007 Nov-Dec;636(1-3):178-242.

15. Krasner SW, Weinberg HS, Richardson SD, Pastor SJ, Chinn R, Sclimenti MJ, et al. Occurrence of a new generation of disinfection byproducts. Environ Sci Technol. 2006 Dec 1;40(23):7175-85.

16. Hua G, Reckhow DA. DBP formation during chlorination and chloramination: Effect of reaction time, pH, dosage, and temperature. Journal - American Water Works Association. 2008;100(8):82-95.

17. United States Environmental Protection Agency. Initial distribution system evaluation guidance manual for the final stage 2 disinfectants and disinfection byproducts rule. Washington, DC: 2006. Report No.: EPA 815-B-06-002.

18. Zhao YY, Boyd J, Hrudey SE, Li XF. Characterization of new nitrosamines in drinking water using liquid chromatography tandem mass spectrometry. Environ Sci Technol. 2006 Dec 15;40(24):7636-41.

19. Plewa MJ, Wagner ED, Muellner MG, Hsu KM, Richardson SD. Chapter 3: Comparative mammalian cell toxicity of N-DBPs and C-DBPs. In: Karanfil T, Krasner SW, Westerhoff P, Xie YF, editors. Disinfection by-products in drinking water: occurrence, formation, health effects, and control. Washington, DC; New York: American Chemical Society; 2008. p. 36-50.

20. Plewa MJ, Muellner MG, Richardson SD, Fasano F, Buettner KM, Woo YT, et al. Occurrence, synthesis, and mammalian cell cytotoxicity and genotoxicity of haloacetamides: An emerging class of nitrogenous drinking water disinfection byproducts. Environ Sci Technol. 2008 Feb 1;42(3):955-61.

21. Richardson SD, Fasano F, Ellington JJ, Crumley FG, Buettner KM, Evans JJ, et al. Occurrence and mammalian cell toxicity of iodinated disinfection byproducts in drinking water. Environ Sci Technol. 2008 Nov 15;42(22):8330-8.

22. Wagner ED, Hsu KM, Lagunas A, Mitch WA, Plewa MJ. Comparative genotoxicity of nitrosamine drinking water disinfection byproducts in salmonella and mammalian cells. Mutat Res. 2012 Jan 24;741(1-2):109-15.

23. Komaki Y, Pals J, Wagner ED, Marinas BJ, Plewa MJ. Mammalian cell DNA damage and repair kinetics of monohaloacetic acid drinking water disinfection by-products. Environ Sci Technol. 2009 Nov 1;43(21):8437-42.

24. Plewa MJ, Simmons JE, Richardson SD, Wagner ED. Mammalian cell cytotoxicity and genotoxicity of the haloacetic acids, a major class of drinking water disinfection by-products. Environ Mol Mutagen. 2010 Oct-Dec;51(8-9):871-8.

25. Liviac D, Wagner ED, Mitch WA, Altonji MJ, Plewa MJ. Genotoxicity of water concentrates from recreational pools after various disinfection methods. Environ Sci Technol. 2010 May 1;44(9):3527-32.

26. Plewa MJ, Wagner ED, Mitch WA. Comparative mammalian cell cytotoxicity of water concentrates from disinfected recreational pools. Environ Sci Technol. 2011 May 1;45(9):4159-65.

27. Duirk SE, Lindell C, Cornelison CC, Kormos J, Ternes TA, Attene-Ramos M, et al. Formation of toxic iodinated disinfection by-products from compounds used in medical imaging. Environ Sci Technol. 2011 Aug 15;45(16):6845-54.

28. Plewa MJ, Wagner ED, Metz DH, Kashinkunti R, Jamriska KJ, Meyer M. Differential toxicity of drinking water disinfected with combinations of ultraviolet radiation and chlorine. Environ Sci Technol. 2012 Jul 17;46(14):7811-7.

29. Zhang SH, Miao DY, Liu AL, Zhang L, Wei W, Xie H, et al. Assessment of the cytotoxicity and genotoxicity of haloacetic acids using microplate-based cytotoxicity test and CHO/HGPRT gene mutation assay. Mutat Res. 2010 Dec 21;703(2):174-9.

30. Wang S, Tian D, Zheng W, Jiang S, Wang X, Andersen ME, et al. Combined exposure to 3-chloro-4-dichloromethyl-5-hydroxy-2(5H)-furanone and

microsytin-LR increases genotoxicity in Chinese hamster ovary cells through oxidative stress. Environ Sci Technol. 2013 Feb 5;47(3):1678-87.

31. Escobar-Hoyos LF, Hoyos-Giraldo LS, Londono-Velasco E, Reyes-Carvajal I, Saavedra-Trujillo D, Carvajal-Varona S, et al. Genotoxic and clastogenic effects of monohaloacetic acid drinking water disinfection by-products in primary human lymphocytes. Water Res. 2013 Jun 15;47(10):3282-90.

32. Liviac D, Creus A, Marcos R. Genotoxicity testing of three monohaloacetic acids in TK6 cells using the cytokinesis-block micronucleus assay. Mutagenesis. 2010 Sep;25(5):505-9.

33. Zhang L, Xu L, Zeng Q, Zhang SH, Xie H, Liu AL, et al. Comparison of DNA damage in human-derived hepatoma line (HepG2) exposed to the fifteen drinking water disinfection byproducts using the single cell gel electrophoresis assay. Mutat Res. 2012 Jan 24;741(1-2):89-94.

34. Wei X, Wang S, Zheng W, Wang X, Liu X, Jiang S, et al. Drinking water disinfection byproduct iodoacetic acid induces tumorigenic transformation of NIH3T3 cells. Environ Sci Technol. 2013 Jun 4;47(11):5913-20.

35. Liviac D, Creus A, Marcos R. Genotoxic evaluation of the non-halogenated disinfection by-products nitrosodimethylamine and nitrosodiethylamine. J Hazard Mater. 2011 Jan 30;185(2-3):613-8.

36. Boyd JM, Huang L, Xie L, Moe B, Gabos S, Li XF. A cell-microelectronic sensing technique for profiling cytotoxicity of chemicals. Anal Chim Acta. 2008 May 12;615(1):80-7.

37. Du H, Li J, Moe B, McGuigan CF, Shen S, Li XF. Cytotoxicity and oxidative damage induced by halobenzoquinones to T24 bladder cancer cells. Environ Sci Technol. 2013 Mar 19;47(6):2823-30.

38. Laingam S, Froscio SM, Bull RJ, Humpage AR. In vitro toxicity and genotoxicity assessment of disinfection by-products, organic N-chloramines. Environ Mol Mutagen. 2012 Mar;53(2):83-93.

39. Liviac D, Creus A, Marcos R. Genotoxicity analysis of two hydroxyfuranones, byproducts of water disinfection, in human cells treated in vitro. Environ Mol Mutagen. 2009 Jun;50(5):413-20.

40. Xie SH, Liu AL, Chen YY, Zhang L, Zhang HJ, Jin BX, et al. DNA damage and oxidative stress in human liver cell L-02 caused by surface water extracts during drinking water treatment in a waterworks in China. Environ Mol Mutagen. 2010 Apr;51(3):229-35.

41. Neale PA, Antony A, Bartkow ME, Farre MJ, Heitz A, Kristiana I, et al. Bioanalytical assessment of the formation of disinfection byproducts in a drinking water treatment plant. Environ Sci Technol. 2012 Sep 18;46(18):10317-25.

42. Farre MJ, Day S, Neale PA, Stalter D, Tang JY, Escher BI. Bioanalytical and chemical assessment of the disinfection by-product formation potential: Role of organic matter. Water Res. 2013 Jun 19.

43. Liviac D, Creus A, Marcos R. Mutagenic analysis of six disinfection by-products in the tk gene of mouse lymphoma cells. J Hazard Mater. 2011 Jun 15;190(1-3):1045-52.

44. Schenck KM, Sivaganesan M, Rice GE. Correlations of water quality parameters with mutagenicity of chlorinated drinking water samples. J Toxicol Environ Health A. 2009;72(7):461-7.

45. Claxton LD, Pegram R, Schenck KM, Simmons JE, Warren SH. Integrated disinfection by-products research: Salmonella mutagenicity of water concentrates disinfected by chlorination and ozonation/postchlorination. J Toxicol Environ Health A. 2008;71(17):1187-94.

46. Richardson SD, DeMarini DM, Kogevinas M, Fernandez P, Marco E, Lourencetti C, et al. What's in the pool? A comprehensive identification of disinfection by-products and assessment of mutagenicity of chlorinated and brominated swimming pool water. Environ Health Perspect. 2010 Nov;118(11):1523-30.

47. Simmons JE, Teuschler LK, Gennings C, Speth TF, Richardson SD, Miltner RJ, et al. Component-based and whole-mixture techniques for addressing the toxicity of drinking-water disinfection by-product mixtures. J Toxicol Environ Health A. 2004 Apr 23-May 28;67(8-10):741-54.

48. Narotsky MG, Best DS, Rogers EH, McDonald A, Sey YM, Simmons JE. Integrated disinfection by-products mixtures research: Assessment of developmental toxicity in Sprague-Dawley rats exposed to concentrates of water disinfected by chlorination and ozonation/postchlorination. J Toxicol Environ Health A. 2008;71(17):1216-21.

49. Narotsky MG, Best DS, McDonald A, Godin EA, Hunter ES,3rd, Simmons JE. Pregnancy loss and eye malformations in offspring of F344 rats following gestational exposure to mixtures of regulated trihalomethanes and haloacetic acids. Reprod Toxicol. 2011 Jan;31(1):59-65.

50. Narotsky MG, Pressman JG, Miltner RJ, Speth TF, Teuschler LK, Rice GE, et al. Developmental toxicity evaluations of whole mixtures of disinfection by-products using concentrated drinking water in rats: Gestational and lactational effects of sulfate and sodium. Birth Defects Res B Dev Reprod Toxicol. 2012 Jun;95(3):202-12.

51. Villanueva CM, Cantor KP, Grimalt JO, Malats N, Silverman D, Tardon A, et al. Bladder cancer and exposure to water disinfection by-products through ingestion, bathing, showering, and swimming in pools. Am J Epidemiol. 2007 Jan 15;165(2):148-56.

52. Zwiener C, Richardson SD, DeMarini DM, Grummt T, Glauner T, Frimmel FH. Drowning in disinfection byproducts? assessing swimming pool water. Environ Sci Technol. 2007 Jan 15;41(2):363-72.

53. Xu X, Weisel CP. Dermal uptake of chloroform and haloketones during bathing. J Expo Anal Environ Epidemiol. 2005 Jul;15(4):289-96.

54. Xiao F, Zhang X, Zhai H, Lo IM, Tipoe GL, Yang M, et al. New halogenated disinfection byproducts in swimming pool water and their permeability across skin. Environ Sci Technol. 2012 Jul 3;46(13):7112-9.

55. Kogevinas M, Villanueva CM, Font-Ribera L, Liviac D, Bustamante M, Espinoza F, et al. Genotoxic effects in swimmers exposed to disinfection by-products in indoor swimming pools. Environ Health Perspect. 2010 Nov;118(11):1531-7.

56. Leavens TL, Blount BC, DeMarini DM, Madden MC, Valentine JL, Case MW, et al. Disposition of bromodichloromethane in humans following oral and dermal exposure. Toxicol Sci. 2007 Oct;99(2):432-45.

57. Ross MK, Pegram RA. Glutathione transferase theta 1-1-dependent metabolism of the water disinfection byproduct bromodichloromethane. Chem Res Toxicol. 2003 Feb;16(2):216-26.

58. Cantor KP, Villanueva CM, Silverman DT, Figueroa JD, Real FX, Garcia-Closas M, et al. Polymorphisms in GSTT1, GSTZ1, and CYP2E1, disinfection by-products, and risk of bladder cancer in spain. Environ Health Perspect. 2010 Nov;118(11):1545-50.

59. Villanueva CM, Cantor KP, Grimalt JO, Castano-Vinyals G, Malats N, Silverman D, et al. Assessment of lifetime exposure to trihalomethanes through different routes. Occup Environ Med. 2006 Apr;63(4):273-7.

60. Villanueva CM, Cantor KP, Cordier S, Jaakkola JJ, King WD, Lynch CF, et al. Disinfection byproducts and bladder cancer: A pooled analysis. Epidemiology. 2004 May;15(3):357-67.

61. IARC Working Group on the Evaluation of Carcinogenic Risks to Humans. Some drinking-water disinfectants and contaminants, including arsenic. Lyon, France: International Agency for Research on Cancer Press (IARCPress); 2004.

62. Costet N, Villanueva CM, Jaakkola JJ, Kogevinas M, Cantor KP, King WD, et al. Water disinfection by-products and bladder cancer: Is there a european specificity? A pooled and meta-analysis of european case-control studies. Occup Environ Med. 2011 May;68(5):379-85.

63. Cantor KP, Lynch CF, Hildesheim ME, Dosemeci M, Lubin J, Alavanja M, et al. Drinking water source and chlorination byproducts in iowa. III. risk of brain cancer. Am J Epidemiol. 1999 Sep 15;150(6):552-60.

64. Rahman MB, Driscoll T, Cowie C, Armstrong BK. Disinfection by-products in drinking water and colorectal cancer: A meta-analysis. Int J Epidemiol. 2010 Jun;39(3):733-45.

65. Bove GE,Jr, Rogerson PA, Vena JE. Case control study of the geographic variability of exposure to disinfectant byproducts and risk for rectal cancer. Int J Health Geogr. 2007 May 29;6:18.

66. Nieuwenhuijsen MJ, Martinez D, Grellier J, Bennett J, Best N, Iszatt N, et al. Chlorination disinfection by-products in drinking water and congenital anomalies: Review and meta-analyses. Environ Health Perspect. 2009 Oct;117(10):1486-93.

67. Wigle DT, Arbuckle TE, Walker M, Wade MG, Liu S, Krewski D. Environmental hazards: Evidence for effects on child health. J Toxicol Environ Health B Crit Rev. 2007 Jan-Mar;10(1-2):3-39.

68. Iszatt N, Nieuwenhuijsen MJ, Nelson P, Elliott P, Toledano MB. Water consumption and use, trihalomethane exposure, and the risk of hypospadias. Pediatrics. 2011 Feb;127(2):e389-97.

69. Grellier J, Bennett J, Patelarou E, Smith RB, Toledano MB, Rushton L, et al. Exposure to disinfection by-products, fetal growth, and prematurity: A systematic review and meta-analysis. Epidemiology. 2010 May;21(3):300-13.

70. Levallois P, Gingras S, Marcoux S, Legay C, Catto C, Rodriguez M, et al. Maternal exposure to drinking-water chlorination by-products and small-for-gestational-age neonates. Epidemiology. 2012 Mar;23(2):267-76.

71. Righi E, Bechtold P, Tortorici D, Lauriola P, Calzolari E, Astolfi G, et al. Trihalomethanes, chlorite, chlorate in drinking water and risk of congenital anomalies: A population-based case-control study in northern Italy. Environ Res. 2012 Jul;116:66-73.

72. Health Canada. Guidelines for Canadian drinking water quality: Summary table. Ottawa, Ontario: Water, Air and Climate Change Bureau, Healthy Environments and Consumer Safety Branch, Health Canada; 2012.

73. Basic information about disinfection byproducts in drinking water: Total trihalomethanes, haloacetic acids, bromate, and chlorite [Internet]. Washington, DC: United States Environmental Protection Agency; 2012. Available from: http://water.epa.gov/drink/contaminants/basicinformation/disinfectionbyproducts.cfm.

74. Contaminant candidate list 3 - CCL [Internet]. Washington, DC: United States Environmental Protection Agency; 2012. Available from: http://water.epa.gov/scitech/drinkingwater/dws/ccl/ccl3.cfm.

75. Zhao Y, Qin F, Boyd JM, Anichina J, Li XF. Characterization and determination of chloro- and bromo-benzoquinones as new chlorination

disinfection byproducts in drinking water. Anal Chem. 2010 Jun 1;82(11):4599-605.

76. Atienza JM, Zhu J, Wang X, Xu X, Abassi Y. Dynamic monitoring of cell adhesion and spreading on microelectronic sensor arrays. J Biomol Screen. 2005 Dec;10(8):795-805.

77. Freshney RI. Culture of animal cells : A manual of basic technique. 3rd ed. New York: Wiley-Liss; 1994.

78. Borenfreund E, Puerner JA. Toxicity determined in vitro by morphological alterations and neutral red absorption. Toxicol Lett. 1985 Feb-Mar;24(2-3):119-24.

79. Liu D. A rapid biochemical test for measuring chemical toxicity. Bull Environ Contam Toxicol. 1981 Feb;26(2):145-9.

80. Mosmann T. Rapid colorimetric assay for cellular growth and survival: Application to proliferation and cytotoxicity assays. J Immunol Methods. 1983 12/16;65(1-2):55-63.

81. Leif RC, Stein JH, Zucker RM. A short history of the initial application of anti-5-BrdU to the detection and measurement of S phase. Cytometry A. 2004 Mar;58(1):45-52.

82. Atienza JM, Yu N, Kirstein SL, Xi B, Wang X, Xu X, et al. Dynamic and label-free cell-based assays using the real-time cell electronic sensing system. Assay Drug Dev Technol. 2006 Oct;4(5):597-607.

83. Solly K, Wang X, Xu X, Strulovici B, Zheng W. Application of real-time cell electronic sensing (RT-CES) technology to cell-based assays. Assay Drug Dev Technol. 2004 Aug;2(4):363-72.

84. McGuinness R. Impedance-based cellular assay technologies: Recent advances, future promise. Curr Opin Pharmacol. 2007 Oct;7(5):535-40.

85. Xing JZ, Zhu L, Jackson JA, Gabos S, Sun XJ, Wang XB, et al. Dynamic monitoring of cytotoxicity on microelectronic sensors. Chem Res Toxicol. 2005 Feb;18(2):154-61.

86. Friedberg EC, Walker GC, Siede W. DNA repair and mutagenesis. Washington, D.C.: ASM Press; 1995.

87. Hoeijmakers JH. Genome maintenance mechanisms for preventing cancer. Nature. 2001 May 17;411(6835):366-74.

88. Nouspikel T. DNA repair in mammalian cells : Nucleotide excision repair: Variations on versatility. Cell Mol Life Sci. 2009 Mar;66(6):994-1009.

89. Friedberg EC, Walker GC, Siede W. DNA repair and mutagenesis. 2nd ed. Washington, D.C.: ASM Press; 2006.

90. Robertson AB, Klungland A, Rognes T, Leiros I. DNA repair in mammalian cells: Base excision repair: The long and short of it. Cell Mol Life Sci. 2009 Mar;66(6):981-93.

91. Kuraoka I, Bender C, Romieu A, Cadet J, Wood RD, Lindahl T. Removal of oxygen free-radical-induced 5',8-purine cyclodeoxynucleosides from DNA by the nucleotide excision-repair pathway in human cells. Proc Natl Acad Sci U S A. 2000 Apr 11;97(8):3832-7.

92. Brooks PJ, Wise DS, Berry DA, Kosmoski JV, Smerdon MJ, Somers RL, et al. The oxidative DNA lesion 8,5'-(S)-cyclo-2'-deoxyadenosine is repaired by the nucleotide excision repair pathway and blocks gene expression in mammalian cells. J Biol Chem. 2000 Jul 21;275(29):22355-62.

93. Moller P, Wallin H. Adduct formation, mutagenesis and nucleotide excision repair of DNA damage produced by reactive oxygen species and lipid peroxidation product. Mutat Res. 1998 Jun;410(3):271-90.

94. Lindahl T. An N-glycosidase from escherichia coli that releases free uracil from DNA containing deaminated cytosine residues. Proc Natl Acad Sci U S A. 1974 Sep;71(9):3649-53.

95. Zhou WJ, Boyd JM, Qin F, Hrudey SE, Li XF. Formation of N-nitrosodiphenylamine and two new N-containing disinfection byproducts from chloramination of water containing diphenylamine. Environ Sci Technol. 2009 Nov 1;43(21):8443-8.

96. Zhao Y, Qin F, Boyd JM, Anichina J, Li XF. Characterization and determination of chloro- and bromo-benzoquinones as new chlorination disinfection byproducts in drinking water. Anal Chem. 2010 Jun 1;82(11):4599-605.

97. Zhao Y, Anichina J, Lu X, Bull RJ, Krasner SW, Hrudey SE, et al. Occurrence and formation of chloro- and bromo-benzoquinones during drinking water disinfection. Water Res. 2012 Sep 15;46(14):4351-60.

Chapter 2: Cytotoxicity and genotoxicity of phenazine[1]

2.1 Introduction

Our research group has recently identified phenazine (PZ), an N-heterocyclic polyaromatic hydrocarbon (**Figure 2-1, Table 2-1**), as a drinking water disinfection byproduct (DBP) (1). Phenazine and N-chlorinated phenazine were detected by LC/MS/MS after raw water containing diphenylamine was exposed to chloramine. This finding, and previous descriptions of halogen-substituted PZ derivatives (2), suggests halogen-containing disinfectants may interact with PZ, creating new halogenated DBPs. Other halogenated PZ DBPs may exist, but are currently unidentified. (*Note: Henceforth, "phenazine" (PZ) will refer to unsubstituted phenazine (**Figure 2-1**), while "phenazine derivatives" and specific compound names will indicate substituted phenazine compounds.*)
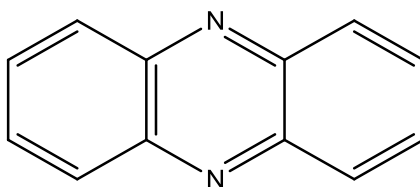
Figure 2-1: Structure of phenazine

Structure generated using the Molinspiration WebME Molecule Editor (http://www.molinspiration.com/docu/webme/).

Table 2-1: Chemical properties of phenazine

	CAS #	Molecular Formula	Molecular Weight (g/mol)	Source and Purity	log P_{OW}
Phenazine (PZ)	92-82-0	$C_{12}H_8N_2$	180.2090	Acros Organics, 98%	3.237

Note: Log P_{OW} values were calculated using Molinspiration software (www.molinspiration.com).

---

[1] A version of of this chapter has been accepted for publication. McGuigan CF & Li XF. 2014. Cytotoxicity and genotoxicity of phenazine in two human cell lines. Toxicology *In Vitro*. (in press)

Although PZ was recently identified as a DBP, phenazines are well-known secondary metabolites in many bacterial species (3). Some bacterial species can produce natural precursors to PZ DBPs (1). Bacteria in drinking water distribution system biofilms (4, 5), especially *Pseudomonas* and *Streptomyces* spp, (3) may be capable of producing PZ or its precursors (1). Therefore, PZ and its derivatives are unique DBPs, as several processes may contribute to their formation: first, as a chemical byproduct from the interaction of chemical precursors in raw water and disinfectants; second, as a biological product from bacteria in distribution system biofilms; and third, as a product of disinfectant residuals reacting with phenazine precursors secreted by distribution system biofilms.

Little is known about the toxicity of PZ; it is mutagenic in *Drosophila* but not *Salmonella* TA98 at low micromolar concentrations (6). More is known about phenazine derivatives, which show antibiotic, antitumor, anti-malarial, and anti-parasitic effects (7). Pyocyanin, a phenazine derivative, is antiproliferative in human cells (8), and induces senescence in the A549 cell line (9, 10). Pyocyanin has also been found to have negative effects on immune system function, through a variety of mechanisms (11-13). 1-hydroxyphenazine interferes with cellular respiration by acting as an electron acceptor, preventing ATP generation (14, 15). PZ derivative mixtures can produce reactive oxygen species *in vitro* (16). Other phenazine derivatives may penetrate cellular membranes and intercalate DNA due to their planar structure and hydrophobicity (7, 8). The objective of this study is to understand the potential toxicity of PZ itself.

Based on these findings, I predicted that PZ may be cytotoxic and genotoxic in mammalian cells. Therefore, I chose to examine phenazine *in vitro* to determine cytotoxicity and genotoxicity, and thus assess the potential need for future investigations (e.g. *in vivo* bioassays). (N-chlorophenazine, which was also detected as a DBP, was not examined here as no chemical standards are available.) I also examined cell proliferation and viability to examine the

mechanism of action of PZ cytotoxicity. HepG2 (human hepatocarcinoma) and T24 (human bladder cancer) cell lines were selected for these assays to represent potential target organs (liver and bladder) for PZ toxicity.

Cytotoxic properties of PZ were investigated using an impedance-based cell sensing technology, called real-time cell analysis (RTCA). As detailed in **Chapter 1, Section 1.7**, RTCA provides a continuous blended measurement of cell number, proliferation, and morphology in real-time, without use of dyes or labels. This system monitors the electrical impedance caused by cells bound to gold microelectrodes which line specialized multiwell plates. Impedance measurements are automatically converted to a unitless measurement called cell index (CI) (17). Increasing CI values over time are associated with cell proliferation and/or a greater degree of individual cell-electrode contact. Decreasing or static CI values over time may indicate cell death, detachment from the electrodes, morphological changes resulting in less cell-electrode contact, and/or induction of a cytostatic state. To confirm the RTCA results and provide additional information on the mechanism of toxicity, follow-up experiments for cell proliferation (5-bromo-2'-deoxyuridine enzyme-linked immunosorbent assay (BrdU ELISA) (18, 19)) and viability (3-(4,5-Dimethylthiazol-2-yl)-2,5-diphenyltetrazolium bromide assay (MTT) (20)) were conducted. (MTT was chosen to examine viability because it does not use phenazine derivatives, unlike other cytotoxicity assays (Neutral Red, XTT, etc.); this avoided confounding with exogenous phenazines.)

As some phenazine compounds are known to cause DNA damage (7), PZ was tested for genotoxicity using the alkaline comet assay (single cell gel electrophoresis). To my knowledge, this is the first reported examination of phenazine genotoxicity in human cell lines. The comet assay detects single and double-stranded breaks, abasic sites, and alkali-labile adducts (21-23). I developed a method to use RTCA data for determination of appropriate PZ

concentrations for the comet assay, which requires a high proportion of viable cells (24).

Based on the available data for PZ and its derivatives, I hypothesized that PZ would have concentration-dependent cytotoxicity to HepG2 and T24 cells, possibly through an antiproliferative mechanism. I also predicted that PZ would evoke DNA damage in these cell lines under these experimental conditions. Therefore, the objective of this study was to evaluate the cytotoxicity and genotoxicity of phenazine using a novel RTCA method and the alkaline comet assay, respectively, to assess potential toxicity of phenazine in drinking water.

2.2 Materials and Methods

2.2.1 Cell lines and culture conditions

Human hepatocarcinoma (HepG2; HB-8065) and human bladder carcinoma (T24; HTB-4) cell lines were obtained from the American Type Culture Collection (ATCC). Cell lines were maintained in a humidified 37°C incubator, with 5% CO_2, in Eagle's Minimum Essential Medium (ATCC; #30-2003) supplemented with 10% fetal bovine serum (Sigma; #F1051) and 1% of 10000 U penicillin/10000 μg streptomycin solution (Gibco; #15140-122). Cells were subcultured when confluence was 80-95%, and culture medium was refreshed at least twice per week. Cell line passage numbers were restricted (≤15 passages per individual set of cell cultures) to minimize effects of genetic drift. All manipulations of cell cultures were performed in a biosafety cabinet (Thermo Scientific Forma Class 2 A2; #1284) under aseptic conditions. Manipulation of cell lines was performed in compliance with the University of Alberta "Working with Biohazardous Materials" policy.

2.2.2 Reagents and toxicant solutions

Phenazine was obtained from Acros Organics (New Jersey, USA; 130150050). DMSO was obtained from Fisher Scientific (Ottawa, Ontario; BP231-1). As phenazine has a very low solubility in water ($P_{OW} = 10^3$), a concentrated stock

solution in sterile DMSO was prepared fresh for each experiment and diluted to the desired concentration in cell culture medium. A DMSO-spiked sample of culture medium, equivalent to the volume of the most concentrated PZ solution (0.1%), was used as a solvent control treatment. Treatment concentrations ranged from 1.9-123 μM; higher concentrations were not used due to the limited solubility of PZ in DMSO and limitations of DMSO concentrations to prevent solvent toxicity.

2.2.3 RTCA cytotoxicity assay

HepG2 and T24 cells were harvested using a 0.05% trypsin-0.53 mM EDTA solution (Gibco; #25300-05) and plated into 16-well RTCA E-plates at a density of 13000 and 5000 cells per well, respectively. Both cell lines were used in each replicate, with half of the available wells plated with each cell type. Using the RTCA software (ACEA RT-CES SP v5.3, ACEA Biosciences), diagnostic assays were performed on all plates prior to use; if any well failed quality control tests, results from that well were discarded. If multiple bad wells were found on a plate, the plate was discarded. Cell index (CI) measurements were collected hourly. Cells were allowed to equilibrate in the E-plates without treatment until reaching a CI value of ~1, corresponding to ~40-50% confluence (25), within 18-24 hours post-plating. Any wells showing abnormal cell growth were not used for treatment or control groups. Plates were then removed from the incubator, and culture medium was removed. Each well was treated with a 200 μL aliquot of PZ solution (1.9-123 μM), DMSO solvent control solution, or culture medium (negative control group). The treatment layout was randomized for each replicate to avoid layout-related artifacts. After treatment, plates were returned to the RTCA unit in the incubator and monitored hourly until a growth plateau had been reached, usually ~72 hours post-treatment. All cell index values were "normalized" to a value of 1 at the time of treatment by the RTCA software in order to accurately compare relative differences in signal between the wells after treatment.

2.2.4 5-bromo-2'-deoxyuridine enzyme-linked immunosorbent assay (BrdU ELISA)

A BrdU cell proliferation kit was used to perform these experiments (Cell proliferation ELISA, BrdU (colorimetric), Roche Applied Science), following a previously described method (18, 19). Cells were plated into clear 96-well plates (#3596, Corning), at a density of 5000 cells/mL for HepG2 and 3750 cells/mL for T24. Appropriate control wells were maintained as per kit instructions. Cells were treated with PZ (1.9-123 µM), DMSO solvent control solution, or culture medium (negative control group) and incubated until two hours prior to the desired exposure time. 10 µL of BrdU label was added, and plates were incubated for the remaining two hours (total exposure time: 24 or 48 hours). The labeling medium was removed, plates were wrapped in foil, and stored at 4°C for up to one week. When analysis resumed, cells were fixed and denatured, labeled with anti-BrdU peroxidase solution for two hours, and washed three times. Peroxidase substrate solution was added, and plates were permitted to develop the blue colorimetric product (approximately 10-15 minutes). A 25 µM H_2SO_4 stop solution was added, plates were gently shaken for one minute, and then measured with a spectrophotometer (Benchmark Plus, Bio-Rad) at 450nm (reference wavelength 690nm).

2.2.5 3-(4,5-Dimethylthiazol-2-yl)-2,5-diphenyltetrazolium bromide assay (MTT)

The MTT assay was performed using the *In Vitro* Toxicology Assay Kit (MTT based, TOX-1) from Sigma, following previously established protocols (20). HepG2 and T24 cells were plated in clear 96-well plates (#3596, Corning) at a density of 10000 and 7500 cells per well, respectively, and treated with desired phenazine concentrations (1.9-123 µM), DMSO solvent control solution, or culture medium (negative control group). Appropriate control wells were reserved as per kit instructions. Two hours prior to the end of the exposure period, plates were removed from the incubator and the MTT label was added. Plates were returned to the incubator for the remaining two hours, for a total exposure time of

24 or 48 hours. Next, the treatment/label medium was removed, and solubilization solution (acidified isopropanol) was added to dissolve the formazan crystals. Plates were gently shaken for 3 minutes to dissolve the crystals, then measured with a spectrophotometer (Benchmark Plus, Bio-Rad) at 570nm, with a subtracted reference wavelength of 690nm.

2.2.6 Selection of appropriate phenazine concentrations for comet assay

For accurate results, substances tested with the comet assay must produce at least 80% cell viability at the desired exposure time. This prevents false positive results from DNA fragmentation due to necrosis or apoptosis (24, 26). To determine appropriate PZ concentrations for the comet assay, RTCA cell index data were used. Cell Index (CI) values were selected as a surrogate measurement of viability, since CI provides a blended measurement of cell number, proliferation, and contact with plate electrodes. Cell index values for PZ-treated cells were expressed as a percentage of the solvent control group CI value at each time point, using the equation below. Only PZ concentrations producing at least 80% of the solvent control cell index value at the 24 hour timepoint were deemed suitable for use in the comet assay.

$$solvent - normalized\ CI = \left(\frac{PZ\ treatment\ group\ CI}{DMSO\ control\ group\ CI}\right) \times 100$$

Where:

Solvent-normalized CI	= percentage of CI for the PZ treatment group as compared to the CI for the DMSO control group cell index at 24 hours
PZ treatment group CI	= cell index of phenazine-treated cells at 24 hours
DMSO control group CI	= cell index of DMSO control group cells at 24 hours

2.2.7 Alkaline comet assay

The alkaline comet assay, or single cell gel electrophoresis assay, was performed as previously described (21), using a CometAssay® kit (Trevigen, # 4250-050-K). HepG2 and T24 cells were treated with appropriate phenazine (HepG2: 1.9-30.8 μM; T24: 7.7-123 μM) or 0.1% DMSO solutions for 24 hours. (Although the phenazine concentrations used for the comet assay in each cell line are different, these concentrations produce equivalent degrees of cytotoxicity.) Control groups included a negative control (culture medium only), solvent control (DMSO volume equal to the most concentrated treatment group = 0.1%), and positive DNA damage control (cells exposed to 0.003% v/v hydrogen peroxide in culture medium for 20 minutes at 4°C).

After treatment, cells were harvested, suspended 1:10 in molten LMAgarose, and spread on provided CometSlides™. Slides were held at 4°C until agarose solidification, immersed in provided Lysis Solution at 4°C, then immersed in room-temperature 200 mM NaOH + 1 mM EDTA solution to permit DNA unwinding. Electrophoresis (constant voltage of 22V, current ~300 mA) was performed at 4°C with an opaque 20-slide comet assay horizontal electrophoresis tank (Scie-Plas, #QCOMET20), using a 200 mM NaOH + 1 mM EDTA electrophoresis solution, for 30 minutes. After electrophoresis, slides were immersed in deionized water and dried in 70% ethanol. Slides were allowed to dry flat overnight, and were stored in a dry, dark environment until imaging, for no longer than two weeks.

For imaging, cells were stained with 1x SYBR Green I (Life Technologies, #S-7563) in Tris-EDTA buffer (pH 7.5) (Promega; #PRA2651. Imaging was performed on an inverted fluorescence microscope with a fluorescein filter (Axiovert 200M, Zeiss) and MetaMorph® software (MDS Analytical Technologies). 100 randomly selected comets from each treatment group were scored for tail moment values with CometScore™ software (Tri-Tek). Tail moment values were used as the metric of DNA fragmentation, and were

calculated automatically by the CometScore[TM] program using the following formula:

$$T_M = \%DNA_{Tail} \times Length_{Tail}$$

Where:

T$_M$ = tail moment

%DNA$_{Tail}$ = percent of comet DNA contained in the tail (compared to comet head)

Length$_{Tail}$ = length of comet tail (in pixels)

2.2.8 Data analysis

Statistical analyses were performed with Prism® software (GraphPad Software) and Microsoft Excel® (Microsoft Corporation). Three replicates were performed for each experiment; mean values from these combined replicates were used for data analysis. Data for RTCA, BrdU, and MTT experiments were analyzed via log-transformation of the concentration values, normalization to the solvent control group values, and fitting of a non-linear sigmoidal dose-response curve (variable slope). Experiment values from BrdU and MTT experiments were expressed as a percentage of the control group absorbance for each replicate to reduce inter-experiment variability. IC$_{50}$ values over time were calculated from this curve, where possible. Data for BrdU, MTT, and comet assay experiments were analyzed via one-way ANOVA with Dunnett's post-hoc analysis, using the DMSO-treated group as the control group. Results were considered statistically significant if $p<0.05$. While all experiments were conducted with a negative control (consisting only of culture medium), these results were virtually identical to those of the solvent group; therefore, only the solvent control data are shown.

2.3 Results

2.3.1 RTCA cytotoxicity assay

47

Figures 2-2 & 2-3 demonstrate the effects of PZ on cell index in HepG2 and T24 cells, respectively. **Figure 2-2A** clearly demonstrates a concentration-dependent decrease in cell index (CI) of HepG2 cells, indicative of cytotoxicity, evident at approximately 15 hours post-exposure (**Figure 2-2A**). IC_{50} values for HepG2 cells over the exposure period ranged from 1651 µM (24 hours) to 100 µM (60 hours); see **Table 2-2 and Figure 2-2B**. The IC_{50} values estimated from the cells treated for shorter durations (e.g. 24 and 36 hours) fall outside the range of tested concentrations, and these values are provided solely for reference. Only the IC_{50} values obtained ≥53 hours post-exposure are within the range of tested concentrations. Conversely, T24 cells experienced little decline in CI over the course of the experiment, except for those treated with 123 µM PZ. This decline was evident approximately 25 hours post-exposure (**Figure 2-3**). Due to the low toxicity of phenazine to T24 cells, no meaningful IC_{50} values could be calculated for this experiment.
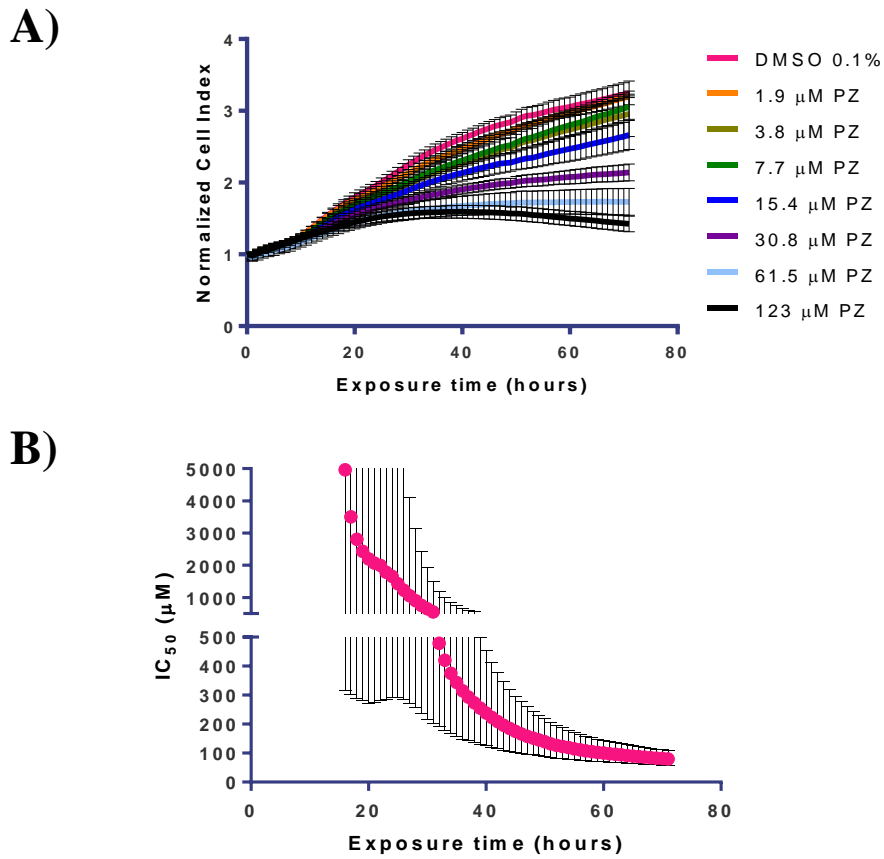
Figure 2-2: Effect of phenazine on cell index and IC$_{50}$ values of HepG2 cells, measured by RTCA

RTCA data (**A**) were obtained from HepG2 cells exposed to phenazine, with calculation of IC$_{50}$ values over time (**B**). DMSO 0.1% represents the solvent control group. Data shown represent the mean of three independent experiments, with error bars representing the standard error of the mean (SEM) in Panel A and 95% confidence intervals in Panel B.

Table 2-2: RTCA IC$_{50}$ values and 95% confidence intervals of HepG2 cells exposed to phenazine for 24, 36, 48, and 60 hours

HepG2 + PZ	24 hours	36 hours	48 hours	60 hours
IC$_{50}$ value (µM)	1651	314	152	100
95% confidence interval (µM)	292-9352	148-664	94-244	70-144

Note: Projected IC$_{50}$ and confidence interval values may fall outside of tested concentration range; these values should be interpreted with caution.
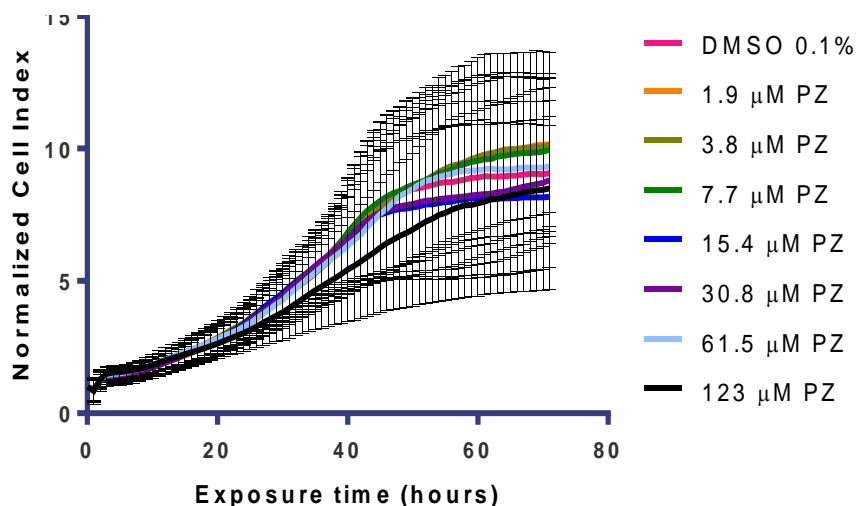
Figure 2-3: Effect of phenazine on cell index of T24 cells, measured by RTCA
RTCA data (**A**) were obtained from T24 cells exposed to phenazine. DMSO 0.1% represents the solvent control group. Data shown represent the mean of three independent experiments, with error bars representing the standard error of the mean (SEM). Due to the low cytotoxicity of PZ to T24 cells, no meaningful IC$_{50}$ values could be calculated.

2.3.2 5-bromo-2'-deoxyuridine enzyme-linked immunosorbent assay (BrdU ELISA)

As shown in **Figure 2-4**, PZ significantly reduced proliferation in both HepG2 (**A**) and T24 (**B**) cells after a 24-hour exposure. HepG2 cells experienced significantly decreased proliferation compared to the solvent control group at all tested phenazine concentrations (1.9-123 µM) (**Figure 2-4A**). However, T24 cells

experienced significantly decreased proliferation only with ≥ 30.8 µM PZ (**Figure 2-4B**). In both cell lines, the reduction in proliferation activity was concentration-dependent, although the effect in HepG2 cells was greater than that observed for T24 cells. IC_{50} values were 11 µM (95% confidence interval: 8.7-13 µM) for HepG2 cells and 47 µM (95% confidence interval: 38 to 57 µM) for T24 cells in the 24-hour exposure (**Figure 2-4C & Table 2-3**). A similar pattern of response was observed in HepG2 and T24 cells exposed to the same PZ concentrations for 48 hours, although higher PZ concentrations were required to significantly depress proliferation in HepG2 cells. Significant reductions in proliferation were observed in both HepG2 and T24 cells exposed to ≥ 15.4 µM PZ (**Figure 2-5 A&B**). IC_{50} values were 7.8 µM (95% confidence interval: 5.2 to 12 µM) for HepG2 cells and 17 µM (95% confidence interval: 14 to 20 µM) for T24 cells in the 48-hour exposure (**Figure 2-5C & Table 2-3**).

A)

B)

C)
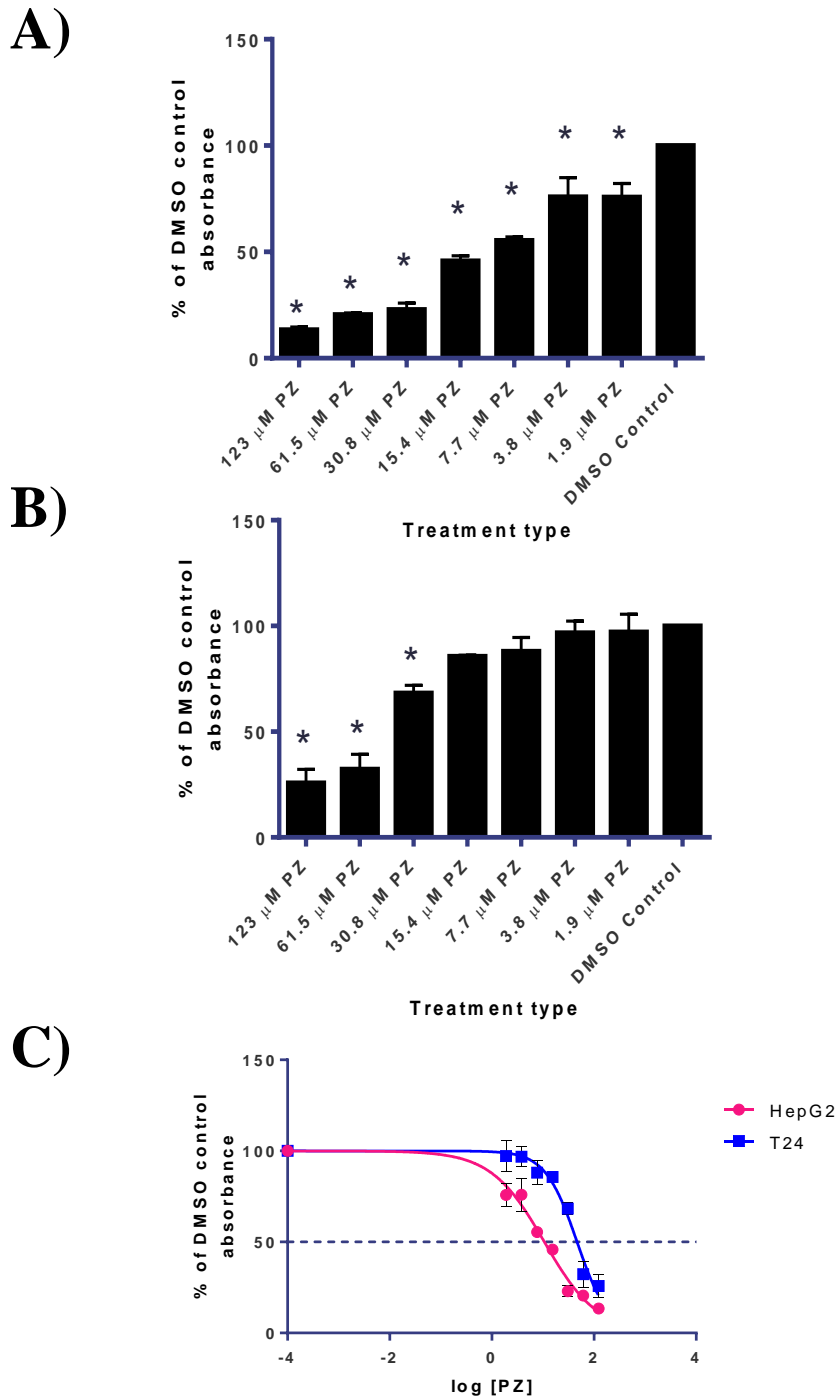
Figure 2-4: Effect of 24-hour phenazine exposure on proliferation of HepG2 and T24 cells, measured by BrdU ELISA

BrdU ELISA proliferation data were obtained from HepG2 (**A**) and T24 (**B**) cells exposed to phenazine for 24 hours, with proliferation expressed as a percentage of the DMSO control group (**C**). Data shown represent the mean of three

independent experiments, with error bars representing the standard error of the mean (SEM). Significantly depressed proliferation compared to the control group was observed in HepG2 cells at all tested concentrations (1.9-123 µM) and T24 cells exposed to 30.8-123 µM phenazine (* = $p<0.05$). Interpolated IC_{50} values from the graph in Panel C are 11 µM (95% confidence interval: 8.7-13 µM) for HepG2 cells and 47 µM (95% confidence interval: 38-57 µM) for T24 cells.
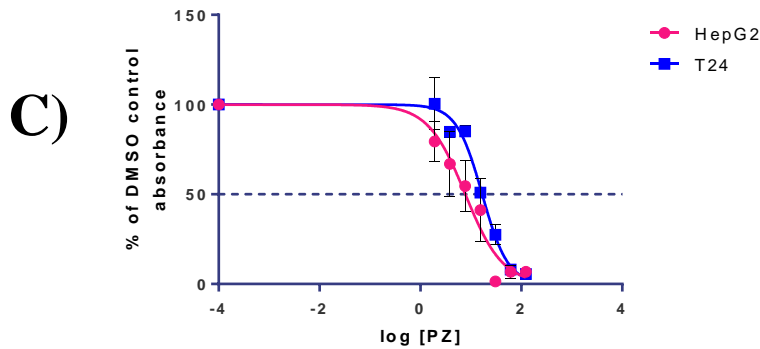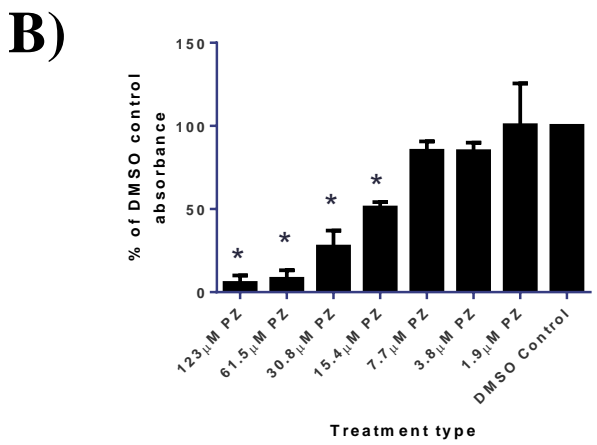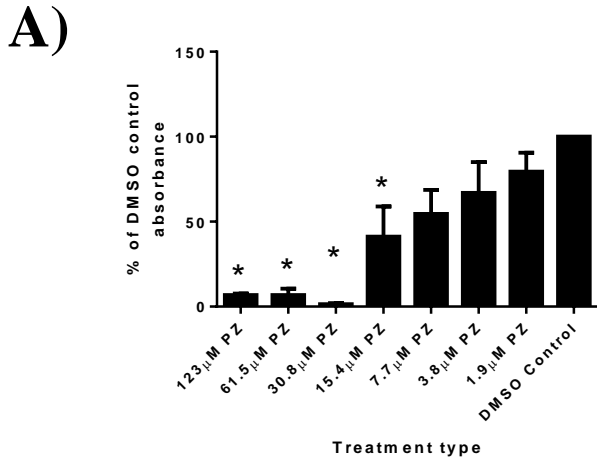
Figure 2-5: Effect of 48-hour phenazine exposure on proliferation of HepG2 and T24 cells, measured by BrdU ELISA

BrdU ELISA proliferation data were obtained from HepG2 (**A**) and T24 (**B**) cells exposed to phenazine for 48 hours, with proliferation expressed as a percentage of the DMSO control group (**C**). Data shown represent the mean of three independent experiments, with error bars representing the standard error of the mean (SEM). Significantly depressed proliferation compared to the control group

was observed in HepG2 cells at 15.4-123 μM and T24 cells exposed to 15.4-123 μM phenazine (* = $p < 0.05$). Interpolated IC_{50} values from the graph in Panel C are 7.8 μM (95% confidence interval: 5.2-12 μM) for HepG2 cells and 17 μM (95% confidence interval: 14-20 μM) for T24 cells.

Table 2-3: BrdU IC_{50} values and 95% confidence intervals of HepG2 & T24 cells exposed to phenazine for 24 and 48 hours

BrdU Assay	HepG2	T24	δIC50 (T24-HepG2)/ IC50 T24 (%)
24h IC_{50} (μM)	11	47	77
24h 95% confidence interval (μM)	8.7 – 13	38 – 57	-
48h IC_{50} (μM)	7.8	17	54
48h 95% confidence interval (μM)	5.2 – 12	14 – 20	-

Note: δIC50 = percentage difference in T24 IC_{50} values vs. HepG2 IC_{50} values

2.3.3 3-(4,5-Dimethylthiazol-2-yl)-2,5-diphenyltetrazolium bromide assay (MTT)

As shown in **Figure 2-6**, PZ appeared to reduce viability in HepG2 cells to a greater extent compared to T24 cells in both 24- and 48-hour exposures. Significantly reduced viability compared to the solvent control group was observed in HepG2 cells exposed to ≥15.4 μM phenazine for 24 hours (**Figure 2-6A**). Conversely, decreased viability in T24 cells treated for 24 hours was observed only at 123 μM, the highest tested concentration (**Figure 2-6B**). IC_{50} values for 24 hour PZ exposures were 115 μM for HepG2 cells (95% confidence interval: 70 to 188 μM) and 368 μM for T24 cells (95% confidence interval: 114 to 1189 μM) (**Figure 2-6C & Table 2-4**). (Note that, due to the lack of effect in T24 cells, the calculated IC_{50} value is beyond the tested concentration range and the confidence interval is large.) For 48 hour PZ exposures, significantly reduced viability compared to the solvent control was observed at ≥7.7 μM for HepG2 cells and ≥61.5 μM for T24 cells (**Figure 2-7 A&B**). IC_{50} values for 48 hour PZ

exposures were 23 µM for HepG2 cells (95% confidence interval: 17 to 31 µM) and 82 µM for T24 cells (95% confidence interval: 49 to 136 µM) (**Figure 2-7C & Table 2-4**).
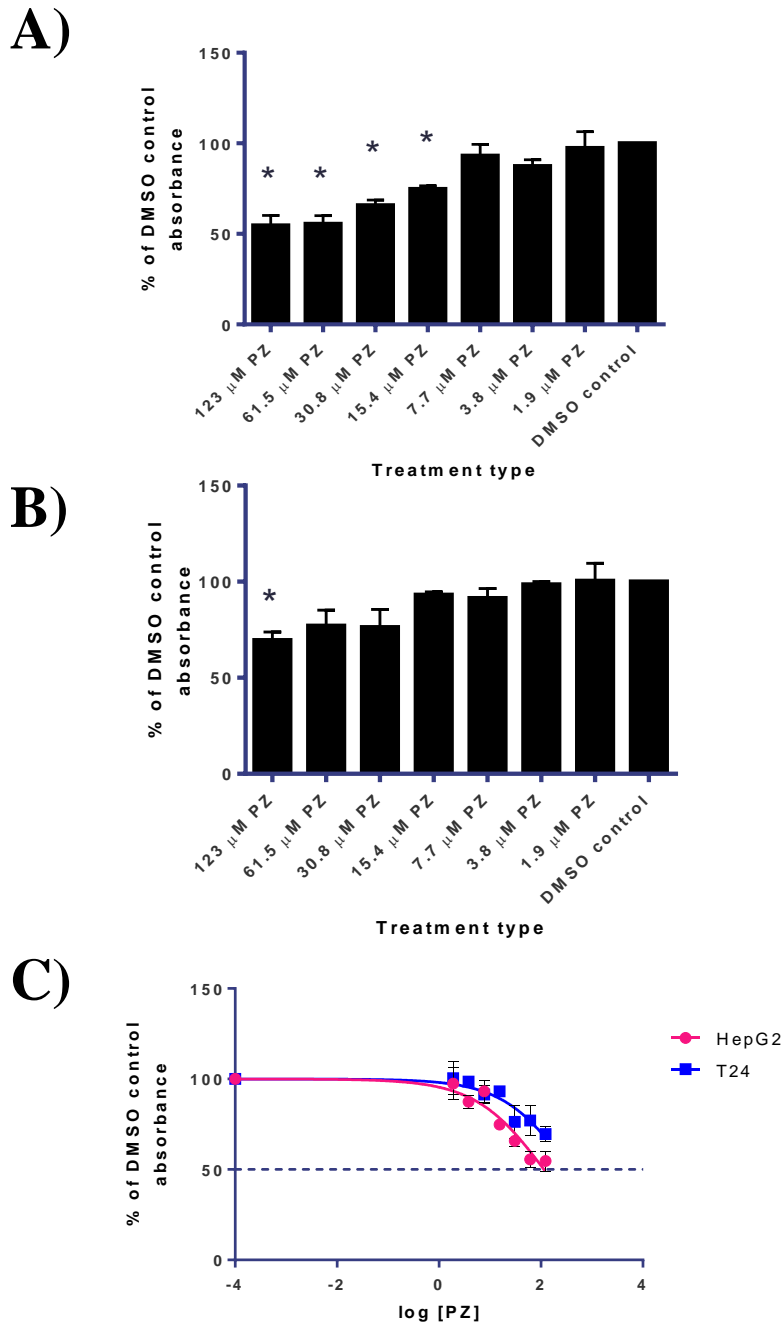
Figure 2-6: Effect of 24-hour phenazine exposure on viability of HepG2 and T24 cells, measured by MTT assay

MTT viability data were obtained from HepG2 (**A**) and T24 (**B**) cells exposed to phenazine for 24 hours, with viability expressed as a percentage of the DMSO control group (**C**). Data shown represent the mean of three independent experiments, with error bars representing the standard error of the mean (SEM).

Significantly depressed viability compared to the control group was observed in HepG2 cells at 15.4-123 µM and T24 cells exposed to 123 µM phenazine (* = $p<0.05$). Interpolated IC_{50} values from the graph in Panel C are 115 µM for HepG2 cells (95% confidence interval: 70-188 µM) and 368 µM for T24 cells (95% confidence interval: 114-1189 µM).
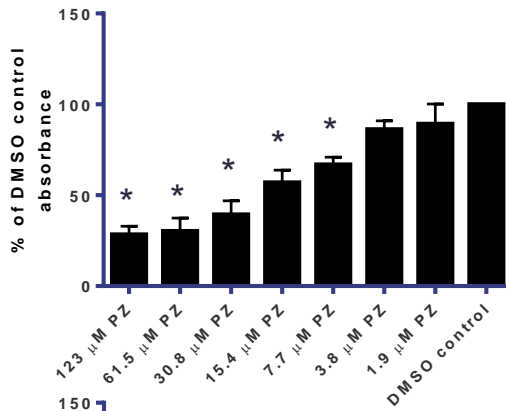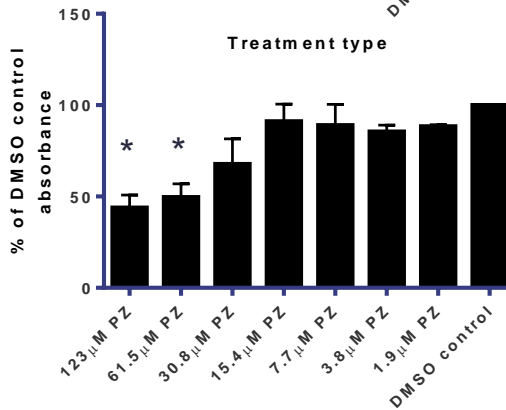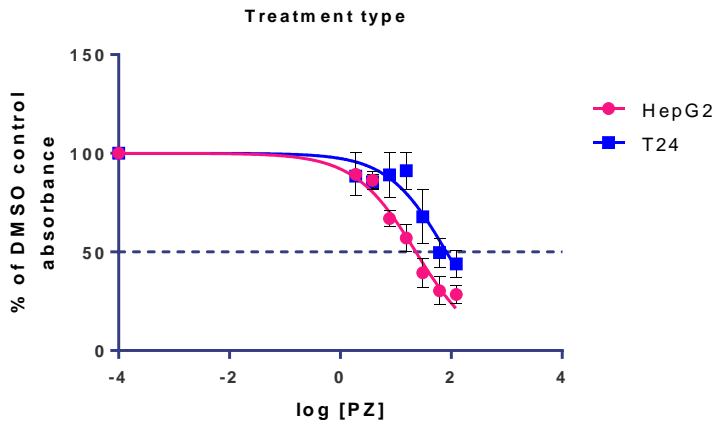
Figure 2-7: Effect of 48-hour phenazine exposure on viability of HepG2 and T24 cells, measured by MTT assay

MTT viability data were obtained from HepG2 (**A**) and T24 (**B**) cells exposed to phenazine for 48 hours, with viability expressed as a percentage of the DMSO control group (**C**). Data shown represent the mean of three independent experiments, with error bars representing the standard error of the mean (SEM). Significantly depressed viability compared to the control group was observed in HepG2 cells at 7.7-123 μM and T24 cells exposed to 61.5-123 μM phenazine (* =

p<0.05). Interpolated IC_{50} values from the graph in Panel C are 23 µM for HepG2 cells (95% confidence interval: 17-31 µM) and 82 µM for T24 cells (95% confidence interval: 49-136 µM).

Table 2-4: MTT IC_{50} values and 95% confidence intervals of HepG2 & T24 cells exposed to phenazine for 24 and 48 hours

MTT Assay	HepG2	T24	δIC50 (T24-HepG2)/ IC50 T24 (%)
24h IC_{50} (µM)	115	368	69
24h 95% confidence interval (µM)	70 – 188	114 - 1189	-
48h IC_{50} (µM)	23	82	72
48h 95% confidence interval (µM)	17– 31	49 – 136	-

Note: δIC50 = percentage difference in T24 IC_{50} values vs. HepG2 IC_{50} values

2.3.4 Selection of appropriate phenazine concentrations for comet assay

Data obtained from the RTCA experiments described above were used to determine appropriate phenazine concentrations for the comet assay. Only PZ concentrations producing ≥80% of the solvent control group cell index value at 24 hours were considered suitable for use in the comet assay. As shown in **Figure 2-8**, ≥80% cell index values compared to the solvent control group were obtained for HepG2 cells treated with ≤30.8 µM phenazine (**A**); all phenazine concentrations tested in T24 cells produced ≥80% cell index values compared to the solvent control group (**B**). Therefore, in the subsequent comet assay experiments, HepG2 cells were exposed to 1.9-30.8 µM PZ, and T24 cells were exposed to 7.7-123 µM PZ. Although the concentration ranges for each cell line are not the same, they produce an equivalent degree of cytotoxicity. The use of different concentration ranges for each cell type is necessary to avoid false positive results in the comet assay arising from cell death-induced DNA fragmentation.
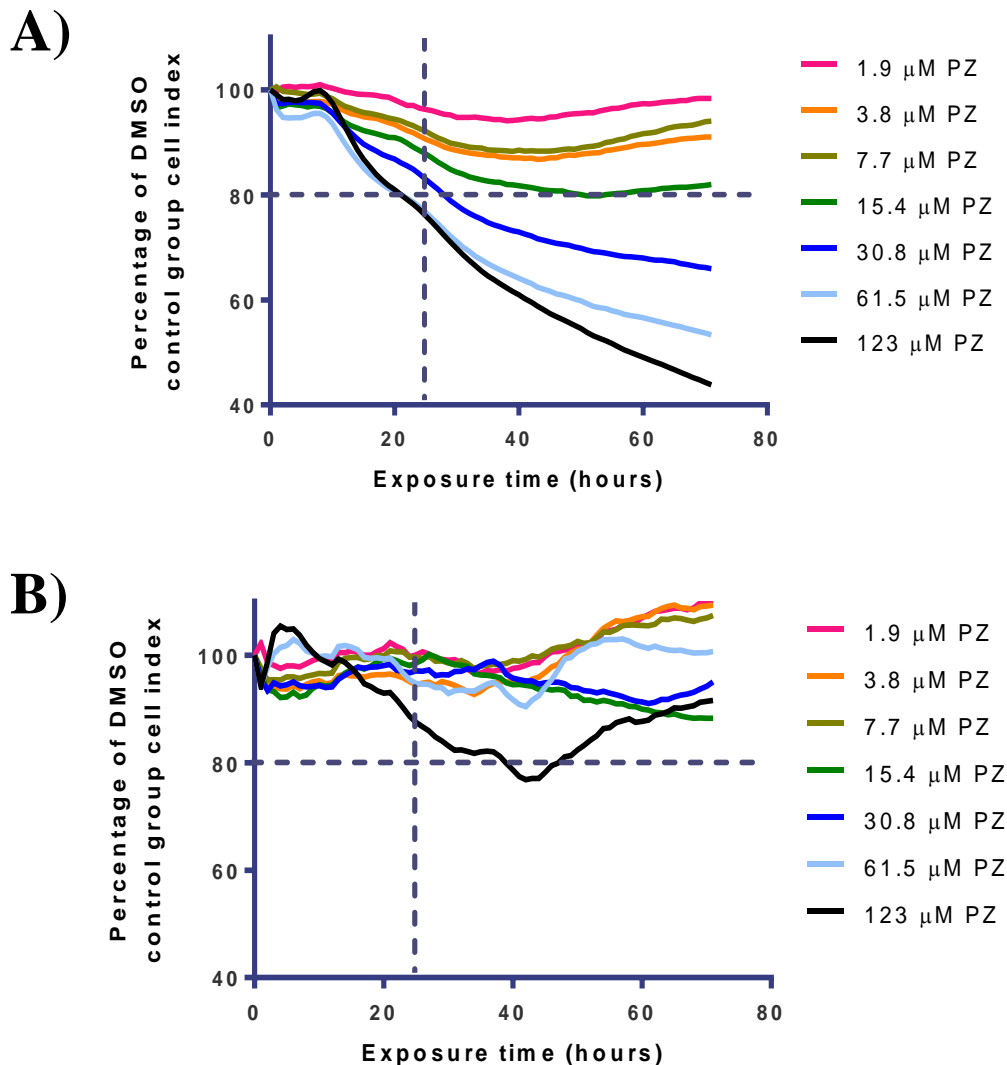
Figure 2-8: Determining appropriate concentrations for alkaline comet assay from RTCA data for HepG2 and T24 cells

Selection of appropriate PZ concentrations for the comet assay, using Cell Index (CI) data generated from RTCA experiments (**Figures 2-2 & 2-3**). All CI values were expressed as a percentage of the control (DMSO) group CI at each timepoint. The horizontal dashed line represents 80% of control group CI, the cutoff value used for PZ concentration suitability. The vertical dashed line represents 24 hours post-PZ exposure, the same exposure period used for the comet assay. Appropriate PZ concentrations fall above the horizontal dashed line at the point where it crosses the vertical dashed line, since this represents 80% control group CI values at 24 hours post-exposure. In HepG2 cells (**A**), PZ

concentrations ≤30.8 µM are suitable for the comet assay; in T24 cells (**B**), all phenazine concentrations tested (≤123 µM) were suitable.

2.3.5 Alkaline comet assay

DNA fragmentation, as measured by tail moment values, was not significantly elevated in HepG2 cells exposed to 1.9-30.8 µM PZ for 24 hours, compared to the solvent control group (**Figure 2-9A**). However, T24 cells treated with ≥61.5 µM PZ for 24 hours showed significantly increased tail moment values compared to the solvent control group (**Figure 2-9B**).

A)
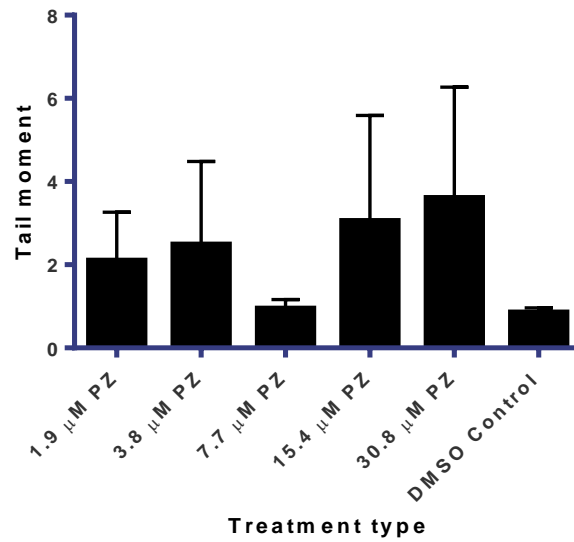
B)
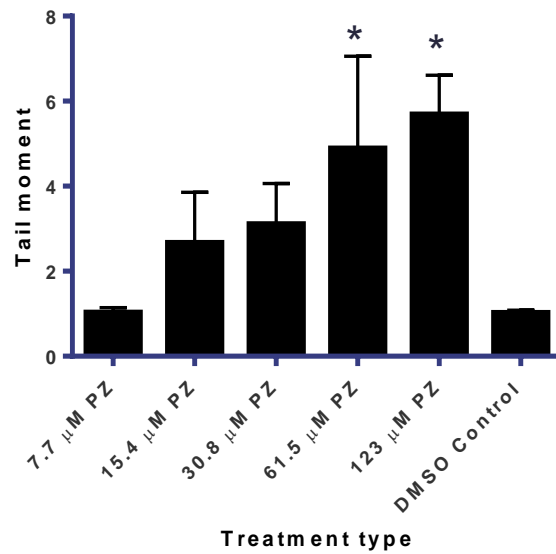
Figure 2-9: Tail moment values of HepG2 and T24 cells exposed to phenazine for 24 hours

Tail moment data were obtained from HepG2 (**A**) and T24 (**B**) cells exposed to phenazine for 24 hours. A solvent control group was treated only with 0.1% DMSO, the highest concentration used in the treatment groups. Data shown represent the mean of three independent experiments, with error bars representing the standard error of the mean (SEM). Statistical significance was determined by performing a one-way ANOVA with Dunnett's post-hoc analysis, using the

DMSO Control group as the comparison (control) group. * = p<0.05 compared to DMSO Control group

2.4 Discussion

Based on these findings, phenazine appears to have a different manifestation of toxicity in each cell line. Under these experimental conditions, HepG2 cells experienced greater overall cytotoxicity than T24 cells exposed to the same concentrations of PZ. This difference is indicated by the greater concentration-dependent cytotoxicity observed in the RTCA assays (**Figures 2-2 & 2-3**), and the more profound effects observed on both cell proliferation (**Figures 2-4 & 2-5**) and viability (**Figures 2-6 & 2-7**) of the HepG2 cells compared to those of the T24 cells. IC_{50} values for cell proliferation (BrdU) and viability (MTT) were 54-77% lower in HepG2 cells compared to T24 cells for the same exposure time (**Tables 2-3 & 2-4**). Moreover, cytotoxicity observed in both HepG2 and T24 cells appears to be primarily an antiproliferative effect, as shown by the lower IC_{50} values and greater proportion of significantly depressed signal for the BrdU assay compared to the MTT assay (**Figures 2-4 to 2-7; Tables 2-3 & 2-4**). In both cell lines, IC_{50} values for cell proliferation were 66-90% lower than those for cell viability when compared against the same cell line and exposure time (**Tables 2-3 & 2-4**). This finding is consistent with the data obtained from the HepG2 RTCA cell index curves (**Figure 2-2**). At elevated phenazine concentrations (≥ 30.8 μM), the curves appear to become static with little net change in cell index. A stable cell index over time could suggest a cytostatic state. If a compound caused negative effects on cell viability, a profound decrease in cell index would be expected, as dead/dying cells would detach from the plate electrodes, reducing impedance. As a dramatic decrease in CI was not observed in the RTCA experiments, and the effect observed in the BrdU assay was generally greater compared to the MTT assay, I propose that the cytotoxic effect of phenazine observed in these experiments is primarily an antiproliferative effect. These findings are consistent with previous research, which has found that phenazine derivatives may have an antiproliferative effect (8-11).

64

However, the comet assay indicates that T24 cells experience greater PZ-induced genotoxicity compared to HepG2 cells at PZ concentrations that produce equivalent cytotoxicity (**Figure 2-9**). Different concentration ranges for each cell type were required due to the difference in sensitivity to the cytotoxic effects of PZ, but they produce an equivalent degree of cytotoxicity in each cell line. For accurate results in the comet assay, a high degree of cell viability is required (24, 26); therefore, RTCA data were used to select PZ concentrations producing ≥80% of solvent control group cell index at the same exposure time in each cell line (**Figure 2-8**). To my knowledge, this is the first reported use of RTCA results to select appropriate concentrations for the comet assay; I believe that these data represent a more comprehensive measurement of cell health compared to traditional dye- or label-based cytotoxicity assays, which often only measure a single parameter of cell health. No significantly elevated DNA fragmentation was observed in HepG2 cells in these experiments, but T24 cells showed significantly increased DNA fragmentation at 61.5 and 123 µM PZ. As the RTCA and MTT assays for T24 cells show relatively low toxicity after a 24-hour exposure at these concentrations (**Figures 2-4 to 2-7**), it appears that non-lethal DNA damage may be occurring in these cells, potentially leading to errors in DNA replication and mutation events. However, it is important to note that no significant genotoxic response was observed in either cell line ≤30.8 µM PZ. The presence of an apparent genotoxic response also conforms with previous findings of phenazine (6) and its derivatives (7). The planar structure of phenazine has been proposed to act as an DNA intercalating agent (7), which could produce the DNA damage observed here. However, as the comet assay does not provide information on the type of detected DNA lesions, additional investigation would be required to determine if intercalation or a different genotoxic effect is responsible for the observed damage.

The differing toxicity profiles in HepG2 and T24 cells may indicate a cell- or tissue-specific response. There may be differences in metabolic capacity between

the two cell lines which affect phenazine metabolism, leading to differences in bioactivation or detoxification. It is possible that the metabolic product produced in HepG2 cells is cytotoxic but not genotoxic under these experimental conditions, while in T24 cells a different metabolite is produced with the opposite effect. The cell lines may also have inherently different susceptibility to the toxic effects of phenazine. Phenazine compounds are known to inhibit oxygen uptake in mouse liver mitochondria (14), and liver-derived HepG2 cells may be particularly susceptible to the same effect due to the large amount of mitochondria present in hepatocytes. However, greater information on the metabolic pathways of phenazine and the metabolic capabilities of the HepG2 and T24 cell lines would be required to more accurately explain the observed differences in toxicity.

A recently published work used the MTT assay to examine the cytotoxicity of phenazine to HepG2 and T24 cells (27). In contrast to the results presented in this chapter, they found that phenazine was more cytotoxic to T24 cells compared to HepG2 cells. However, the authors note that several concentrations of phenazine that did not completely dissolve in DMSO were used to construct the IC_{50} curves for each cell line. Due to the toxic effects of the high concentrations of phenazine, these values greatly influenced the shape of the IC_{50} curves. In addition, those authors used a relatively high DMSO concentration approaching 1% for their experiments, but do not present cytotoxicity data for the solvent control group individually. In addition, the IC_{50} values in that work are presented without confidence intervals or other measures of variance or error. It is possible that these aspects of experimental design may have influenced the observed results. The experiments in this chapter used only concentrations of phenazine that dissolved completely in DMSO, and restricted DMSO to ≤0.1% to avoid solvent-induced toxicity (29), in order to avoid confounding factors. While the results between the previous experiments and the work in this chapter are different, it is possible that aspects of the experimental design may explain the discrepancy.

As phenazine is a newly-identified DBP, I chose to examine its toxicity on HepG2 and T24 cells as these cell lines are derived from potential target organs (liver and bladder). An increased risk of bladder cancer has been associated with consumption of chlorinated water in several epidemiological studies (30-34). Although cyto- and genotoxicity were observed in these experiments, the results should be considered in the proper context. The purpose of these experiments was not to provide data directly for human risk assessment, but rather to perform an initial investigation of phenazine toxicity in standardized cell lines. While the use of cancer cell lines is a well-established practice in *in vitro* toxicity testing, they are not suitable direct surrogates for normal human responses due to potentially differing metabolic enzyme profiles (35-38) and regulation of cellular processes (39). However, cell lines provide a standardized model for regulatory toxicity testing due to the different target organs and tissues available, their ability to proliferate *in vitro*, and the absence of inter-individual variation within a cell line. These *in vitro* results may be used to design additional experiments in different systems, such as primary cell lines or *in vivo* rodent bioassays. Likewise, while DNA damage in the T24 bladder cell line was observed in these experiments, it does not conclusively indicate that phenazine is the DBP responsible for the increased risk of bladder cancer in epidemiological studies. The extremely low concentrations of DBPs in finished water pose a difficult challenge in establishing a causative relationship between increased bladder cancer risk and the presence of one or more DBPs (40). However, it may be prudent to further examine the mechanism by which phenazine causes DNA damage in T24 cells, as it may provide valuable information on other potentially toxic DBPs.

Consideration should also be given to the concentration range of phenazine selected for these experiments. While there are no extensive data available on phenazine concentrations in finished drinking water other than the low ng/L concentration obtained experimentally by our research group (41), it is unlikely that it is present in the μM concentrations (≈ high μg/L to low mg/L) used in these experiments. Because little data were available on the toxic effects of phenazine, a

high concentration range was deliberately selected in order to provoke a toxic response. As phenazine is not water-soluble, its limited solubility in DMSO and the maximum tolerable concentration of DMSO to these cells limited the upper range of the concentrations used. However, because depressed proliferation was seen in the 24 hour BrdU experiments on HepG2 cells even at the lowest concentration tested (1.9 µM, ≈ 346 µg/L), it may indicate that phenazine is capable of depressing cell proliferation even at very low concentrations. The extent of this antiproliferative ability is unknown, but further experiments with lower concentrations of phenazine are clearly indicated.

As shown here, impedance-based cell sensing technologies, such as RTCA, can be useful in conducting *in vitro* toxicity testing of chemical agents. Without requiring the use of a dye or label, RTCA represents a significant improvement to other *in vitro* cytotoxicity methods because it provides a continuous overall measurement of cell growth, proliferation, and morphology in real-time (17). Where traditional *in vitro* assays can often provide data for only one exposure time, RTCA can collect many data points at user-defined intervals throughout the course of a single experiment. Although RTCA cannot definitively distinguish between effects on cell number, proliferation, and morphology, follow-up experiments with more traditional assays may be performed if desired, as was done here with the BrdU and MTT assays. The RTCA system also provides high-throughput capacity; different instrument formats can monitor between 48 and 576 individual microwells at a time (42). In applications where large numbers of potential toxicants must be screened to identify compounds of concern, such as regulatory DBP testing, RTCA results can be used to triage compounds for further testing priority. This will result in more efficient use of limited testing resources, and possible reduction in unnecessary *in vivo* testing. In the future, impedance-based *in vitro* technologies could also represent a potential tool in the reduction or elimination of animal experimentation.

In conclusion, phenazine exerted different toxic effects on HepG2 and T24 cell lines under these experimental conditions. A cytotoxic concentration-dependent reduction of proliferation occurs in HepG2 cells, which may enter a cytostatic state at elevated phenazine concentrations. However, no significant genotoxic response was observed for HepG2 cells. Conversely, T24 cells showed a minor cytotoxic antiproliferative effect, but did experience significant genotoxicity at concentrations which were not cytotoxic. While these effects were seen at phenazine concentrations likely above those found in disinfected water, the persistence of the antiproliferative effect even at low concentrations deserves further study. Additional investigation is required to further determine the biological effects of phenazine as a DBP and bacterial metabolite.

2.5 References

1. Zhou WJ, Boyd JM, Qin F, Hrudey SE, Li XF. Formation of N-nitrosodiphenylamine and two new N-containing disinfection byproducts from chloramination of water containing diphenylamine. Environ Sci Technol. 2009 Nov 1;43(21):8443-8.

2. Cross B, Dunn CL, Payne DH, Tipton JD. Synthesis and pesticidal activity of phenazines. II. alkyl, alkoxy, alkylthio and alkylsulphonyl phenazines. J Sci Food Agric. 1969 Jun;20(6):340-4.

3. Turner JM, Messenger AJ. Occurrence, biochemistry and physiology of phenazine pigment production. Adv Microb Physiol. 1986;27:211-75.

4. Ridgway HF, Olson BH. Scanning electron microscope evidence for bacterial colonization of a drinking-water distribution system. Appl Environ Microbiol. 1981 Jan;41(1):274-87.

5. Wingender J, Flemming H. Contamination potential of drinking water distribution network biofilms. van Loosdrecht MCM and Picioreanu C, editors. Alliance House 12 Caxton Street London SW1H 0QS UK: IWA Publishing; 2004.

6. Watanabe T, Kasai T, Arima M, Okumura K, Kawabe N, Hirayama T. Genotoxicity in vivo of phenazine and aminophenazines assayed in the wing spot test and the DNA-repair test with *Drosophila melanogaster*. Mutat Res. 1996 Jul 10;369(1-2):75-80.

7. Laursen JB, Nielsen J. Phenazine natural products: Biosynthesis, synthetic analogues, and biological activity. Chem Rev. 2004 Mar;104(3):1663-86.

8. Sorensen RU, Klinger JD, Cash HA, Chase PA, Dearborn DG. In vitro inhibition of lymphocyte proliferation by *Pseudomonas aeruginosa* phenazine pigments. Infect Immun. 1983 Jul;41(1):321-30.

9. Muller M. Premature cellular senescence induced by pyocyanin, a redox-active *Pseudomonas aeruginosa* toxin. Free Radic Biol Med. 2006 Dec 1;41(11):1670-7.

10. Muller M, Li Z, Maitz PK. *Pseudomonas* pyocyanin inhibits wound repair by inducing premature cellular senescence: Role for p38 mitogen-activated protein kinase. Burns. 2009 Jun;35(4):500-8.

11. Nutman J, Berger M, Chase PA, Dearborn DG, Miller KM, Waller RL, et al. Studies on the mechanism of T cell inhibition by the *Pseudomonas aeruginosa* phenazine pigment pyocyanine. J Immunol. 1987 May 15;138(10):3481-7.

12. Campa M, Bendinelli M, Friedman H. *Pseudomonas aeruginosa* as an opportunistic pathogen. New York: Plenum Press; 1993.

13. Shellito J, Nelson S, Sorensen RU. Effect of pyocyanine, a pigment of *Pseudomonas aeruginosa*, on production of reactive nitrogen intermediates by murine alveolar macrophages. Infect Immun. 1992 Sep;60(9):3913-5.

14. Armstrong AV, Stewart-Tull DE. The site of the activity of extracellular products of *Pseudomonas aeruginosa* in the electron-transport chain in mammalian cell respiration. J Med Microbiol. 1971 May;4(2):263-70.

15. Stewart-Tull DE, Armstrong AV. The effect of 1-hydroxyphenazine and pyocyanin from *Pseudomonas aeruginosa* on mammalian cell respiration. J Med Microbiol. 1972 Feb;5(1):67-73.

16. Davis G, Thornalley PJ. Free radical production from the aerobic oxidation of reduced pyridine nucleotides catalysed by phenazine derivatives. Biochim Biophys Acta. 1983 Sep 30;724(3):456-64.

17. Atienza JM, Yu N, Kirstein SL, Xi B, Wang X, Xu X, et al. Dynamic and label-free cell-based assays using the real-time cell electronic sensing system. Assay Drug Dev Technol. 2006 Oct;4(5):597-607.

18. Muir D, Varon S, Manthorpe M. An enzyme-linked immunosorbent assay for bromodeoxyuridine incorporation using fixed microcultures. Anal Biochem. 1990 Mar;185(2):377-82.

19. Porstmann T, Ternynck T, Avrameas S. Quantitation of 5-bromo-2-deoxyuridine incorporation into DNA: An enzyme immunoassay for the assessment of the lymphoid cell proliferative response. J Immunol Methods. 1985 9/3;82(1):169-79.

20. Mosmann T. Rapid colorimetric assay for cellular growth and survival: Application to proliferation and cytotoxicity assays. J Immunol Methods. 1983 12/16;65(1-2):55-63.

21. Singh NP, McCoy MT, Tice RR, Schneider EL. A simple technique for quantitation of low levels of DNA damage in individual cells. Exp Cell Res. 1988 Mar;175(1):184-91.

22. Olive PL, Banath JP. The comet assay: A method to measure DNA damage in individual cells. Nat Protoc. 2006;1(1):23-9.

23. Dhawan A, Bajpayee M, Parmar D. Comet assay: A reliable tool for the assessment of DNA damage in different models. Cell Biol Toxicol. 2009 Feb;25(1):5-32.

24. Tice RR, Agurell E, Anderson D, Burlinson B, Hartmann A, Kobayashi H, et al. Single cell gel/comet assay: Guidelines for in vitro and in vivo genetic toxicology testing. Environ Mol Mutagen. 2000;35(3):206-21.

25. Xing JZ, Zhu L, Jackson JA, Gabos S, Sun XJ, Wang XB, et al. Dynamic monitoring of cytotoxicity on microelectronic sensors. Chem Res Toxicol. 2005 Feb;18(2):154-61.

26. Anderson D, Plewa MJ. The international comet assay workshop. Mutagenesis. 1998 Jan;13(1):67-73.

27. Zhou W, Lou L, Zhu L, Li Z, Zhu L. Formation and cytotoxicity of a new disinfection by-product (DBP) phenazine by chloramination of water containing diphenylamine. J Environ Sci (China). 2012;24(7):1217-24.

28. Forman S, Kas J, Fini F, Steinberg M, Ruml T. The effect of different solvents on the ATP/ADP content and growth properties of HeLa cells. J Biochem Mol Toxicol. 1999;13(1):11-5.

29. Maes J, Verlooy L, Buenafe OE, de Witte PA, Esguerra CV, Crawford AD. Evaluation of 14 organic solvents and carriers for screening applications in zebrafish embryos and larvae. PLoS One. 2012;7(10):e43850.

30. Villanueva CM, Cantor KP, Grimalt JO, Castano-Vinyals G, Malats N, Silverman D, et al. Assessment of lifetime exposure to trihalomethanes through different routes. Occup Environ Med. 2006 Apr;63(4):273-7.

31. Villanueva CM, Cantor KP, Grimalt JO, Malats N, Silverman D, Tardon A, et al. Bladder cancer and exposure to water disinfection by-products through ingestion, bathing, showering, and swimming in pools. Am J Epidemiol. 2007 Jan 15;165(2):148-56.

32. Villanueva CM, Cantor KP, Cordier S, Jaakkola JJ, King WD, Lynch CF, et al. Disinfection byproducts and bladder cancer: A pooled analysis. Epidemiology. 2004 May;15(3):357-67.

33. IARC Working Group on the Evaluation of Carcinogenic Risks to Humans. Some drinking-water disinfectants and contaminants, including arsenic. Lyon, France: International Agency for Research on Cancer Press (IARCPress); 2004.

34. Costet N, Villanueva CM, Jaakkola JJ, Kogevinas M, Cantor KP, King WD, et al. Water disinfection by-products and bladder cancer: Is there a European specificity? A pooled and meta-analysis of European case-control studies. Occup Environ Med. 2011 May;68(5):379-85.

35. Wilkening S, Stahl F, Bader A. Comparison of primary human hepatocytes and hepatoma cell line HepG2 with regard to their biotransformation properties. Drug Metab Dispos. 2003 Aug;31(8):1035-42.

36. Westerink WM, Schoonen WG. Phase II enzyme levels in HepG2 cells and cryopreserved primary human hepatocytes and their induction in HepG2 cells. Toxicol In Vitro. 2007 Dec;21(8):1592-602.

37. Brandon EF, Bosch TM, Deenen MJ, Levink R, van der Wal E, van Meerveld JB, et al. Validation of in vitro cell models used in drug metabolism and transport studies; genotyping of cytochrome P450, phase II enzymes and drug transporter polymorphisms in the human hepatoma (HepG2), ovarian carcinoma (IGROV-1) and colon carcinoma (CaCo-2, LS180) cell lines. Toxicol Appl Pharmacol. 2006 Feb 15;211(1):1-10.

38. Hart SN, Li Y, Nakamoto K, Subileau EA, Steen D, Zhong XB. A comparison of whole genome gene expression profiles of HepaRG cells and HepG2 cells to primary human hepatocytes and human liver tissues. Drug Metab Dispos. 2010 Jun;38(6):988-94.

39. Hanahan D, Weinberg RA. Hallmarks of cancer: The next generation. Cell. 2011 Mar 4;144(5):646-74.

40. Bull RJ, Awwa Research Foundation, United States. Environmental Protection Agency. Use of toxicological and chemical models to prioritize DBP research. Denver, CO: Awwa Research Foundation; 2006.

41. Boyd JM. Personal communication regarding phenazine concentrations in finished drinking water samples. 2013.

42. xCELLigence product list [Internet].; 2012. Available from: http://www.aceabio.com/productlist.aspx?cateid=265.

Chapter 3: The BJ/XPA RTCA *in vitro* assay[1]

3.1 Introduction

Endpoint-based *in vitro* assays are widely-used tools which examine many aspects of toxicity, including cytotoxicity, genotoxicity, and mutagenicity. However, as described in **Chapter 1, Section 1.7**, these assays may have several disadvantages. These may include destroying cells to perform analysis, obtaining data for only a single timepoint per experiment, measuring only a single parameter of cell health, and significant hands-on experimenter intervention or sample processing (1). These factors are a significant barrier to high-throughput screening, particularly when multiple assays are required to examine several aspects of toxicity.

Methods that simultaneously examine several aspects of toxicity have been developed to reduce the requirement for multiple time- and resource-dependent *in vitro* assays. One such method uses DNA damage repair-deficient and –proficient cells to examine genotoxicity and cytotoxicity in the same assay. The DRAG assay (2, 3) uses Chinese hamster ovary (CHO) cell lines with defects in several different DNA repair mechanisms. Responses of normal and DNA-repair deficient CHO cells to toxicants are examined using a microplate format and the endpoint-based Neutral Red assay. Cells are exposed to several concentrations of the toxicant for a set period (e.g. 1, 24, or 240 hours), depending on the agent, and then allowed to recover for a set period in fresh culture medium (48-120 hours) (2, 3). The Neutral Red dye incorporation assay (4) is then performed to assess cytotoxicity. Increased cytotoxicity in a particular repair-deficient cell type indicates a possible genotoxic mechanism for the test compound (2, 3). Examination of toxic effects on the normal cell line indicates the cytotoxic properties of the test compound. In this way, the DRAG assay tests

---

[1] Western blotting experiments in this chapter were performed in collaboration with Dr. Shengwen Shen, a postdoctoral fellow in the Division of Analytical & Environmental Toxicology at the University of Alberta.

simultaneously for cytotoxicity and genotoxicity using the established Neutral Red cytotoxicity assay. Although the DRAG assay can measure cytotoxicity and specific genotoxic lesions simultaneously, it is limited by the endpoint-based nature of the Neutral Red cytotoxicity assay, which requires lysis of the cells to measure dye retention (4).

As described in **Chapter 1, Section 1.7**, real-time cell analysis (RTCA) is an impedance-based cell sensing technology capable of continuous measurement of cell health without dyes or labels (5). Instead of destroying cells to obtain data, the RTCA system measures the electrical impedance caused by cells bound to gold microelectrodes on the bottom surface of multiwell plates (1, 5). This is reported as a unitless measurement called "cell index" (CI), which represents a blended measurement of cell number, proliferation, and cell morphological characteristics (6, 7). Increased CI indicates increased cell number, proliferation, and cell surface binding to the electrodes; decreased CI is due to cell death, detachment from the electrodes, reduced proliferation, and/or reduced cell-electrode contact. Thus, CI provides a more holistic evaluation of cell function in each well compared to other *in vitro* assays. This non-destructive approach permits the same plate of cells to be monitored continuously throughout the entire course of an experiment, and the multiwell plate design allows for high-throughput screening of up to 576 wells simultaneously (8). After the cells are treated with the desired toxicant, no further experimenter intervention is normally required; data are collected automatically.

To maximize the advantages of each approach, I have developed an *in vitro* assay using the RTCA system to examine the contribution of DNA damage to overall cytotoxicity in mammalian cell lines. Like the DRAG assay, this novel assay combines simultaneous assessment of cytotoxicity and genotoxicity through use of matched cell lines. However, this new assay incorporates the RTCA system, permitting improved non-invasive, continuous, and high-throughput assessment of cytotoxicity. Initial assay development has focused on the nucleotide excision repair (NER) pathway (see **Chapter 1, Section 1.8** for details). NER is the

primary repair mechanism for a wide array of DNA lesions, especially the formation of bulky adducts, crosslinking agents, and intercalating agents (9, 10). The NER pathway may also play an important role in the repair of oxidative DNA damage (11-13). The development of a NER-specific assay is a useful tool for *in vitro* toxicity assessment because many genotoxic substances cause NER-mediated lesions.

Assay development has utilized a pair of matched human skin fibroblast cell lines which are either proficient or deficient in performing NER. The BJ cell line (ATCC: CRL-2522) was derived from normal human infant foreskin fibroblasts and can perform NER. The XPA cell line (NIGMS: GM04312C) was derived from skin fibroblasts from a child with severe xeroderma pigmentosum (XP) (14), a genetic disorder characterized by an inability to perform NER. This cell line is unable to perform NER due to the lack of a functional XPA protein, which is required to detect NER-mediated DNA damage (9, 10). It is expected that a DNA lesion normally repaired by the NER pathway may be cytotoxic in XPA cells, because these cells will not be able to repair the lesion; the same lesion is likely not cytotoxic in the NER-functional BJ cells because it may be repaired. Comparing the responses of the BJ and XPA cells will provide information on the mechanism of toxicity; a greater cytotoxic response in XPA compared to BJ cells may indicate a NER-mediated genotoxic component to the overall toxicity. Because multiple non-genotoxic mechanisms may be involved in this system, it cannot provide unequivocal information solely on the genotoxicity of a test substance. However, comparing BJ and XPA response in the RTCA system will provide information on the contribution of NER-mediated genotoxicity to overall cytotoxicity, and may serve as an indicator for the need for further genotoxicity testing.

To validate the BJ/XPA *in vitro* assay, the XPA protein status of the BJ and XPA cell lines was verified via Western blotting. XPA protein was predicted to be present in BJ cells and absent in XPA cells. Next, the effect of ultraviolet (UVC, 254nm) light exposure to BJ and XPA cells was examined in the RTCA system.

77

UVC light is known to form DNA lesions such as cyclobutane pyrimidine dimers (such as T-T or C-C) and pyrimidine-pyrimidone photoproducts (such as T-C) which are repaired primarily by the NER pathway (9, 15). Therefore, XPA cells exposed to UVC light were expected to experience greater cytotoxicity than BJ cells exposed to the same UVC fluence ($\approx$ dose) because XPA cells lack the ability to repair this damage. In other words, UVC irradiated cells will serve as a positive control group for NER-mediated DNA damage, as the damage caused by UVC light is repaired by the NER pathway. Results of this experiment will determine the validity of the BJ/XPA pairing and assess the prediction that an inability to repair an NER-mediated lesion will result in greater cytotoxicity.

Because cytotoxic responses of BJ and XPA cells to NER-mediated genotoxicants will be compared in this assay, it is also necessary to examine basal sensitivity to substances which do not cause NER-mediated genotoxicity. To examine relative sensitivity to *non*-genotoxic cytotoxicants, the effects of Triton X-100 and gentamicin on BJ and XPA cell health was examined using the RTCA system. Triton X-100 is a non-ionic surfactant which disrupts membrane integrity in mammalian cells; it is frequently used as a positive control substance for cytotoxicity assays (16, 17). Gentamicin is an aminoglycoside antibiotic which is well-known for nephrotoxicity and ototoxicity (18), but is considered non-genotoxic (19). Based on these results, the effectiveness of the BJ/XPA pairing may be assessed; ideally, both cell lines should exhibit similar sensitivity to these agents.

3.2   Materials and Methods

3.2.1 Cell lines and culture conditions

The BJ cell line was obtained from ATCC (#CRL-2522), and the XPA cell line (NIGMS: GM04312C) was kindly provided by Dr. Michael Weinfeld at the University of Alberta. Cell lines were maintained in a humidified 37°C incubator, with 5% CO_2, in Eagle's Minimum Essential Medium (ATCC; #30-2003) supplemented with 10% fetal bovine serum (Sigma; #F1051) and 1% of 10000 U penicillin/10000 µg streptomycin solution (Gibco; #15140-122). Cells were

subcultured when confluence was 80-95%, and culture medium was refreshed at least twice per week. Cell line passage numbers were restricted (≤15 passages per set of cell cultures) to minimize effects of genetic drift. All manipulations of cell cultures were performed in a biosafety cabinet (Thermo Scientific Forma Class 2 A2; #1284) under aseptic conditions. Manipulation of cell lines was performed in compliance with the University of Alberta "Working with Biohazardous Materials" policy and laboratory personnel received both institutional and site-specific biosafety training.

3.2.2 Protein extraction & quantification

Protein extraction on untreated BJ and XPA cells was performed using the Total Protein Extraction Kit (EMD Millipore; #2140). Briefly, cells were harvested, suspended and lysed in extraction buffer, as per kit protocol. The solution was rotated at 4°C for 20 minutes, and then centrifuged at 11,000 rpm at 4°C for 20 minutes. The resulting supernatant was collected and frozen at -80°C until use. Protein concentrations in BJ and XPA cell extracts were determined by the Bradford assay (20), using a Quick Start Bradford Protein Assay Kit 1 (Bio-Rad; #500-0201) and a Smart-Spec Plus[TM] spectrophotometer (Bio-Rad; #170-2525). A standard absorbance curve at 595 nm was constructed using bovine serum albumin solution provided in the kit. BJ and XPA protein extracts were diluted 1:50 in the provided 1x dye reagent and measured at 595 nm. Absorbance readings were compared to the standard curve and corrected for dilution to determine the protein concentration of the extracts.

3.2.3 Western blotting

Western blotting experiments were performed in collaboration with Dr. Shengwen Shen, a postdoctoral fellow in the Division of Analytical & Environmental Toxicology at the University of Alberta. Protein extracts from BJ and XPA cells, as described above, as well as nuclear extract from MCF7 mammary

adenocarcinoma cells (Santa Cruz Biotechnology; #sc-2149), representing an XPA positive control group, were analyzed by Western blotting. Separation of 20 µg protein per well was performed on a 12% SDS-PAGE gel, run at a constant voltage of 200 V. Protein molecular weight was confirmed with a prestained protein marker (Cell Signaling Technology, Inc.; #7720) pipetted into the leftmost well in use. Proteins were transferred to 0.45 µM nitrocellulose membranes (Bio-Rad; #162-0115) using a Mini Trans-Blot® Electrophoretic Transfer Cell (Bio-Rad; #170-3930) run at a constant 80 V for 2 hours. Blocking was performed on a rocking platform at room temperature for 1h in PBST + 5% milk solution. A 1:200 dilution of mouse monoclonal (IgG1) antibody to full-length human XPA protein (Santa Cruz Biotechnology; # sc-28353) was then applied in a PBST + 5% milk solution and the blot was incubated at 4°C on a rocking platform overnight. The next day, the blot was rinsed three times in PBST + 5% milk solution for 10 minutes per rinse. A 1:10000 dilution of a horseradish-peroxidase-conjugated secondary goat anti-mouse antibody (Jackson ImmunoResearch; #115-035-003) in PBST + 5% milk solution was applied and the blot was agitated at room temperature for 1 hour. Protein detection was performed using a chemiluminescent detection kit (ECL Western Blotting System, GE Healthcare Life Sciences, # RPN2108) and blots were digitally photographed using an ImageQuant LAS 4000 system (GE Healthcare Life Sciences, #28-9558-10). After protein detection, equal protein loading was confirmed by Ponceau S staining (21).

3.2.4 Cytotoxicity investigations

Triton X-100 (Fisher Scientific Canada; #BP151-100) and gentamicin sulphate (Sigma; #G-3632) were dissolved in Eagle's Minimum Essential Medium (ATCC; #30-2003) at concentrations of 0.0002-0.2% v/v and 0.03-30 mg/mL, respectively. Care was taken to thoroughly wipe excess Triton X-100 from pipette tips while making stock solutions. Solutions were sterile-filtered through 0.2 µM

nylon syringe filters (Fisherbrand; #09-719C) prior to use. Fresh treatment solutions were prepared for each experimental replicate immediately prior to use.

3.2.5 RTCA cytotoxicity assay

BJ and XPA cells were harvested using a 0.05% trypsin-0.53 mM EDTA solution (Gibco; #25300-05) and plated into 16-well RTCA E-plates at a density of 4000 and 5000 cells per well, respectively. Both cell lines were used in each replicate, with half of the available wells plated with each cell type. Using built-in RTCA software (ACEA RT-CES SP v5.3, ACEA Biosciences), diagnostic assays were performed on all plates prior to use; if any well failed quality control tests, the results from that well were discarded. If multiple bad wells were found on a plate, the plate was discarded. The RTCA system was programmed to collect cell index (CI) measurements every hour. Cells were allowed to equilibrate in the E-plates without treatment until reaching a CI value of ~1, corresponding to ~40-50% confluence (7), within 36-48 hours post-plating. Any wells showing abnormal cell growth were not used for treatment or control groups. Plates were then removed from the incubator, and culture medium was removed. Each well was treated with a 200 µL aliquot of Triton X-100 solution, gentamicin solution, or culture medium (negative control group). The treatment layout was randomized for each replicate to avoid layout-related technical artifacts. After treatment, plates were returned to the RTCA unit in the incubator and monitored hourly until a growth plateau had been reached, ~72 hours post-treatment.

3.2.6 UVC light exposure

A UVC lamp (Phillips; #G30T8) in a biological safety cabinet was used to expose the cell lines to UVC light. The lamp produces UVC light at 253.7 nm. BJ and XPA cells were plated and allowed to equilibrate as described above. When CI of both cell types ≈ 1, RTCA plates were removed from the incubator, placed in the biosafety cabinet, the culture medium was aspirated, and 200 µL of sterile

phosphate-buffered saline (PBS) was added to each well. This step was performed to prevent interference from the phenol red indicator present in the culture medium. Covers were removed, and the plates were placed in the middle of the cabinet work surface. Plates were oriented the same way and in the same position for each experimental replicate, but the left-to-right ordering of the plates for each exposure time was randomized to avoid positional effects. The UV lamp was activated and plates were irradiated for the appropriate time period. After irradiation, the PBS in each well was aspirated, and 200 µL of fresh culture medium was placed in each well. The plates were then returned to the RTCA unit in the incubator for 72 hours, with hourly monitoring of cell index.

3.2.7 Measurement of UVC fluency

A handheld UV meter (UVP Radiometer; #97-0015-02) and sensor (UVP UVX-25; #97-0016-01) was used to measure UVC fluency. The meter was zeroed manually as per product instructions, and the sensor was placed in the biosafety cabinet at the positions used for RTCA plate exposure. Three sets of measurements were obtained; an average intensity measurement was used to calculate fluency. This value was corrected for time exposed for each treatment group in order to obtain total UVC exposure. UVC exposure corresponded to a fluence of $\cong 116$ J/m^2 for the 1 minute groups, and $\cong 232$ J/m^2 for the 2 minute groups. The formula used to perform the conversions (22) was:

$$\frac{J}{m^2} = \frac{intensity\ in\ \frac{\mu W}{cm^2}}{100} \times t_{sec}$$

Where:

J = joules

m^2 = square metres

$intensity\ in\ \frac{\mu W}{cm^2}$ = average UV reading obtained from the UV meter

t_{sec} = UV exposure time in seconds

3.2.8 RTCA data analysis

Statistical analyses were performed with Prism® software (GraphPad Software) and Microsoft Excel (Microsoft Corporation). Results from all experiments were exported into Microsoft Excel, organized, and imported into Prism. At least three replicates were performed for each experiment; mean values from these combined replicates were used for data analysis. Data for RTCA experiments were analyzed via log-transformation of the concentration values, normalization to the solvent control group results, and fitting of a non-linear sigmoidal dose-response curve. IC_{50} values over time were calculated from this curve, where possible. To determine if IC_{50} values for BJ and XPA cells were significantly different over time, IC_{50} values for each timepoint were compared with unpaired t-tests, using the Holm-Šídák correction for multiple comparisons, with a significance level of $p<0.05$.

3.3   Results

3.3.1 Western blotting

As seen in **Figure 3-1**, bands corresponding to the molecular weight of the XPA protein (~40 kDa) were observed in the lanes containing BJ and MCF7 protein extract, but not in the lane containing XPA protein extract.
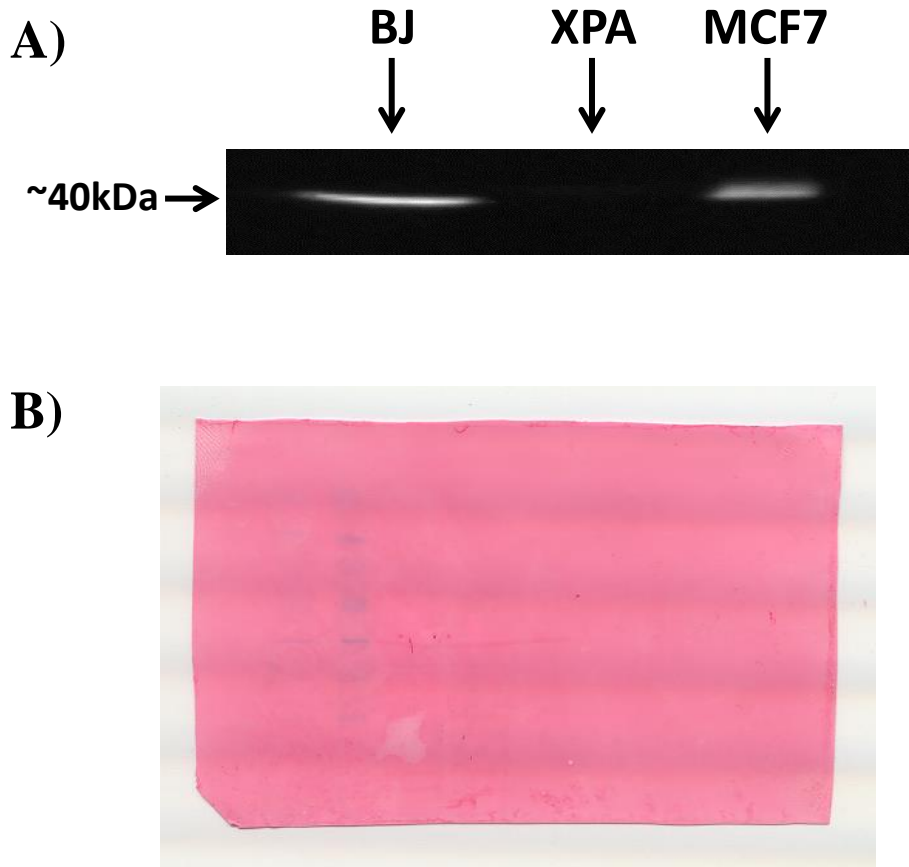
Figure 3-1: Western blotting for XPA protein in BJ, XPA, and MCF7 protein extracts

Chemiluminescent signal corresponding to presence of XPA protein in BJ, XPA, and MCF7 protein extracts (**A**). 20 µg of protein from each cell line was used in each well. MCF7 cell extract was obtained from Santa Cruz Biotechnology (# sc-2149) and was used as a positive control sample for XPA protein. Blots were probed with a 1:200 dilution of a primary mouse monoclonal (IgG1) antibody to full-length human XPA protein (Santa Cruz Biotechnology; # sc-28353) and a 1:10000 dilution of a goat anti-mouse horseradish peroxidase conjugated secondary antibody. Equal protein loading was confirmed by Ponceau S staining (**B**).

3.3.2 UVC exposure and RTCA monitoring

As observed in **Figure 3-2**, XPA cells showed a fluence-dependent peak and decline in cell index, commencing at approximately 3 hours post-treatment. After approximately 36 hours post-treatment, cell index of UVC-exposed XPA cells declined to zero, indicating near-complete cell death. This observation was confirmed by visual inspection of the UVC-exposed XPA cells; most cells had detached from the plate surface and were floating freely in the culture medium. XPA cells which were not exposed to UVC light experienced a steady increase in cell index throughout the course of the experiment. BJ cells exposed to UVC light did experience a fluence-dependent depression in cell index which persisted over the course of the experiment, but some gradual recovery of cell index values was observed over the course of the experiment.
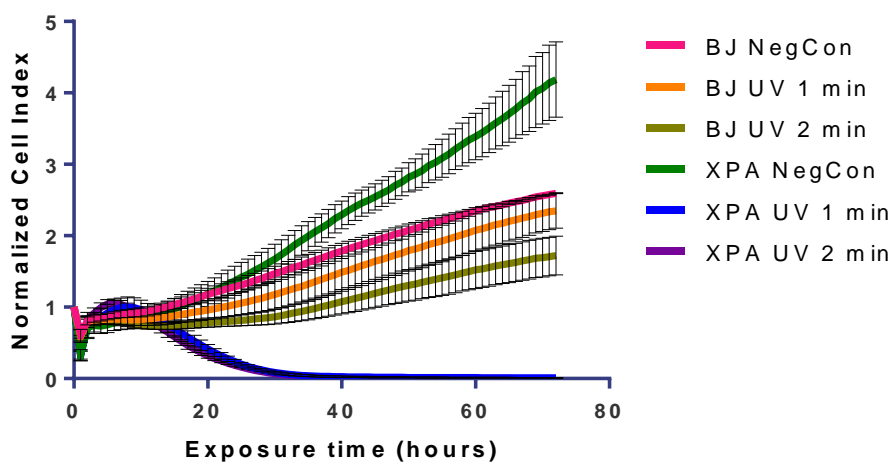
Figure 3-2: Effect of UVC irradiation on BJ and XPA cell lines, measured by RTCA

RTCA data were obtained from BJ and XPA cells exposed to germicidal UVC light, as well as negative control (NegCon) cells not exposed to UVC light. Exposure times are equivalent to $\cong 116$ J/m^2 for 1 minute, and $\cong 232$ J/m^2 for 2 minutes. Data shown represent the mean of three independent experiments with error bars representing the standard error of the mean (SEM). XPA cells show an apparent fluence-dependent peak and sharp decline in CI after UVC exposure, likely indicating cell death (confirmed by visual observation). Although BJ cells demonstrate a depressed CI after UVC exposure, the CI continues to increase over the course of the experiment, indicating that the cells are able to recover after the genotoxic insult. (Note that the initial decrease and recovery of CI at ~1 hour of exposure is an artifact of the treatment process and does not represent an experimental result.)

3.3.3 Non-genotoxic cytotoxicity assessment with RTCA

As shown in **Figures 3-3** (gentamicin) and **3**-**4** (Triton X-100), BJ and XPA cells responded in a generally similar manner to these non-genotoxic cytotoxicants. As seen in **Figure 3-3**, the highest concentration of gentamicin (30 mg/mL) produced near-complete reduction in cell index shortly after treatment in both cell types. Conversely, the lower concentrations of gentamicin produced little effect

compared to the untreated control groups. The IC_{50} values of gentamicin over time for both cell types were nearly identical throughout the exposure period, and no significant differences in IC_{50} value were observed between BJ and XPA cells at any timepoint. In **Figure 3-4**, both cell types experienced severe cytotoxicity at the highest concentration of Triton X-100 (0.02% v/v) and little cytotoxicity at the lowest concentration (0.00002% v/v). However, XPA cells appeared to show greater cytotoxicity at intermediate concentrations of Triton X-100 compared to BJ cells; this is reflected in the comparison of the IC_{50} values over time for both cell types. XPA IC_{50} values for Triton X-100 were significantly lower ($p<0.05$) than those for BJ cells at 20-23 hours exposure. However, the shapes of the IC_{50} curves over time are similar for both cell lines.

A)

B)

C)
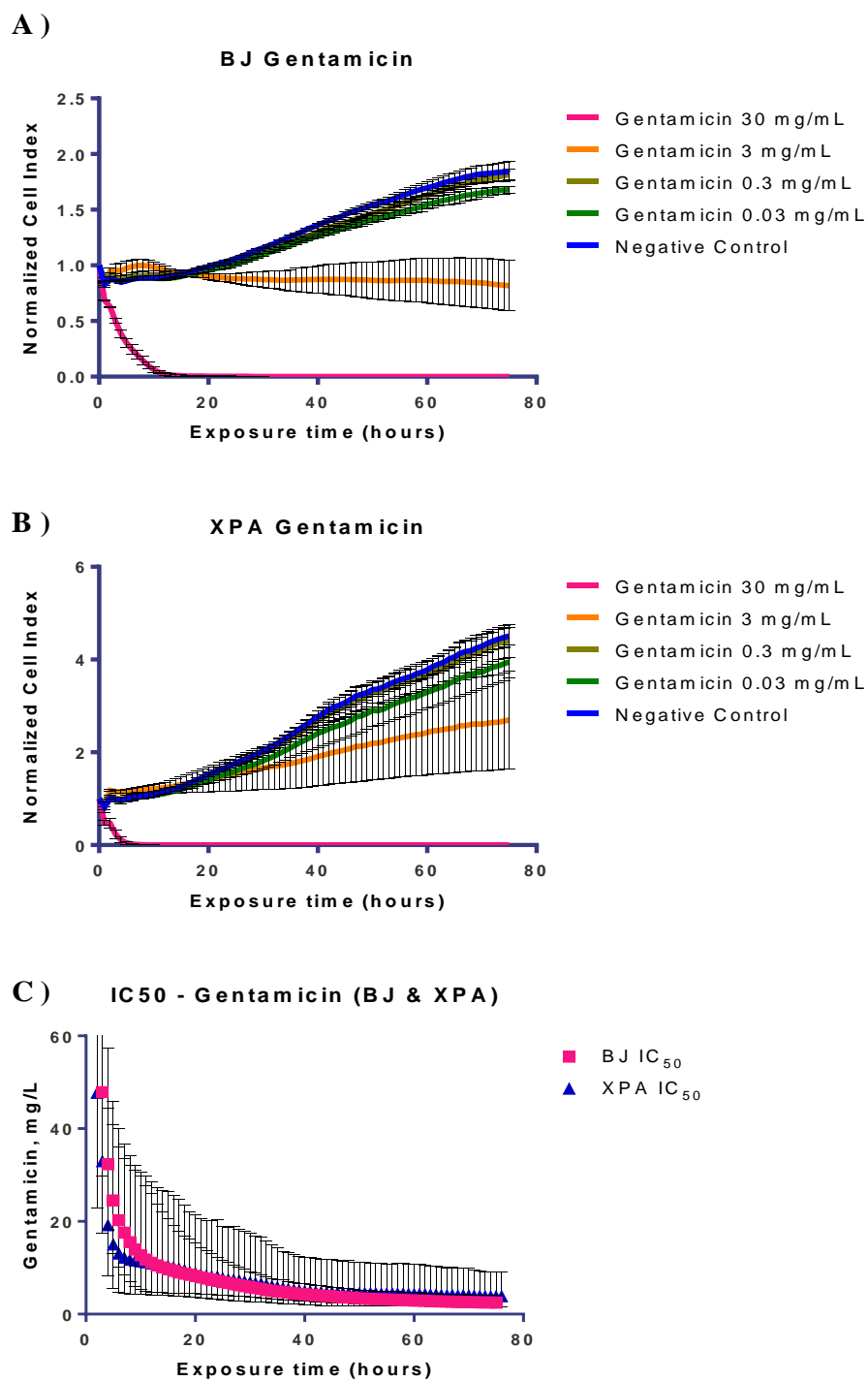
Figure 3-3: Effect of non-genotoxic cytotoxicant gentamicin on BJ and XPA cells, measured by RTCA

RTCA data were obtained from BJ (**A**) and XPA (**B**) cells exposed to gentamicin, with comparison of IC_{50} values (**C**). Negative control cells received culture

medium alone. Data shown represent the mean of three independent experiments, with error bars representing the standard error of the mean (SEM) in Panels A & B, and 95% confidence intervals in Panel C. No statistically significant differences in IC_{50} values between BJ and XPA cells were observed in Panel C.
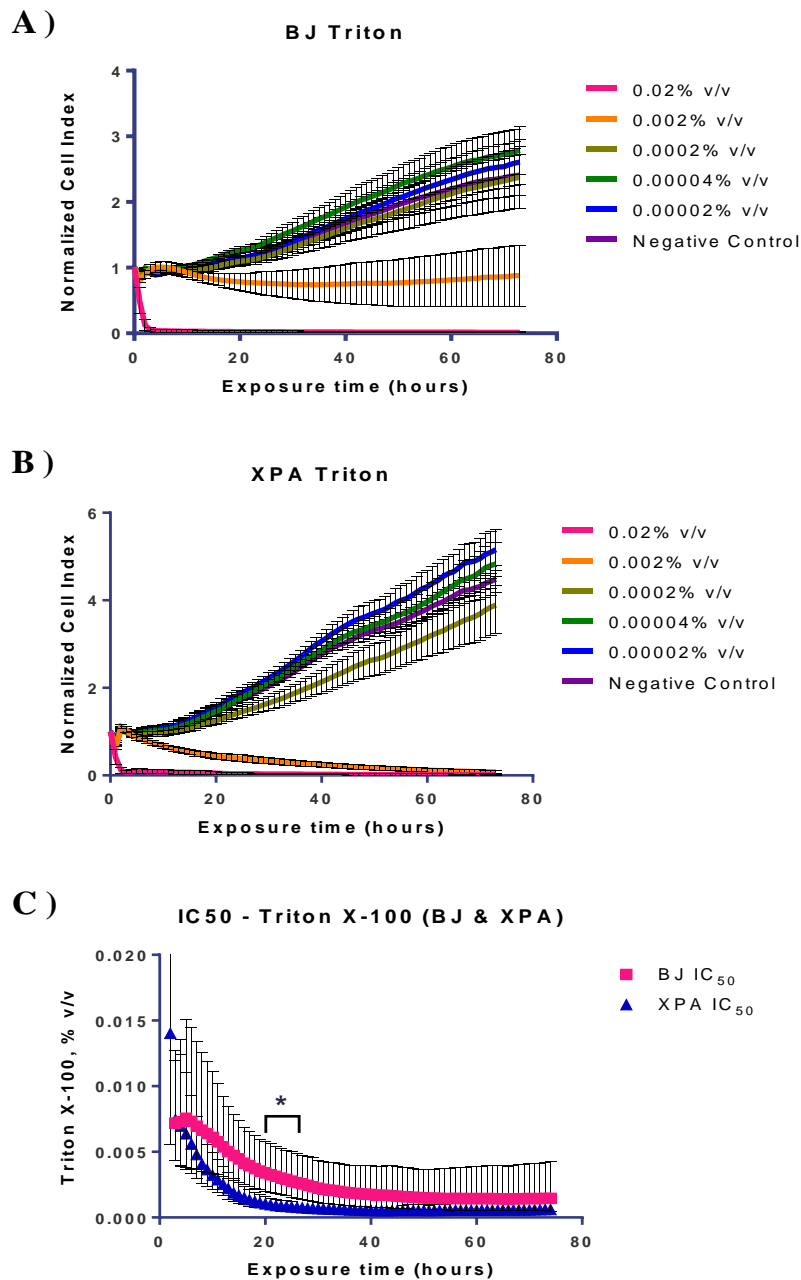
Figure 3-4: Effect of non-genotoxic cytotoxicant Triton X-100 on BJ and XPA cells, measured by RTCA

RTCA data were obtained from BJ (**A**) and XPA (**B**) cells exposed to Triton X-100, with comparison of IC_{50} values (**C**). Negative control cells received culture medium alone. Data shown represent the mean of three independent experiments, with error bars representing the standard error of the mean (SEM) in Panels A & B, and 95% confidence intervals in Panel C. Significantly different IC_{50} values

were observed in BJ and XPA cells at 20-23 hours exposure, as shown in Panel C
(* = p<0.05).

3.4   Discussion

As shown by the experimental results, the BJ/XPA assay was successfully
validated and is capable of detecting NER-mediated lesions. Western blotting
clearly indicates that the XPA protein is present in the normal BJ cells but absent
in the XPA cell line (**Figure 3-1**), which confirms the identity of the XPA cell
line and verifies that the XPA protein is present in the BJ cell line. This particular
XP cell line (NIGMS: GM04312C) is appropriate for use as a NER-deficient
model because it contains a mutation which prevents production of functional
XPA protein (14). As XPA protein is required for all forms of nucleotide excision
repair (9, 10), an XPA-deficient cell line was selected for use in this assay. Cell
lines with deficiencies in other XP proteins (e.g. XPC) may still perform some
forms of NER (e.g. transcription-coupled NER); therefore, they would be
unsuitable for use in this assay (see **Chapter 1, Section 1.8**). Likewise, as the BJ
cell line contains a functional XPA protein, is a skin fibroblast cell line like the
XPA cell line, and has a long lifespan in culture (23), it is an appropriate choice
for a normal cell line in this assay. The BJ and XPA response to UVC light
(**Figure 3-2**) confirms the differing DNA repair capabilities of each cell line. The
increased cytotoxicity observed in XPA cells is consistent with the prediction that
NER-mediated lesions (such as the cyclobutane pyrimidine dimers produced by
UVC light) would be more lethal to XPA cells because they lack the capacity to
repair these lesions. Therefore, these results confirm the identity and NER
capacity of the BJ and XPA cell lines, and support their use in the RTCA system.

The appropriateness of the BJ/XPA pairing in this assay is further supported by
the similar results obtained from the non-genotoxic cytotoxicity experiments
(**Figures 3-3 and 3-4**). These experiments were designed to ensure that BJ or
XPA cell lines were not simply inherently more sensitive to the effects of
toxicants, even those which do not act via a NER-mediated mechanism.

Generally, the responses to gentamicin and Triton X-100 were similar between each cell line, as measured by the calculated IC_{50} values. No significant difference in IC_{50} values between BJ and XPA cells were observed when exposed to gentamicin (**Figure 3-3**). XPA cells were significantly more sensitive to Triton X-100 compared to BJ cells between 20-23 hours of exposure, but IC_{50} values were not significantly different for any other measured time periods (**Figure 3-4**). Despite some transient difference in the IC_{50} values, the cell lines appear to respond to the Triton X-100 in a similar overall fashion (in contrast to the different responses observed in the UVC experiments in **Figure 3-2**). This finding exemplifies the utility of using the RTCA system for determining cytotoxicity as opposed to more traditional endpoint-based methods; if the latter methods were used during the periods of significantly different IC_{50} values, the BJ/XPA pairing might be rejected as unsuitable based on data collected at only one timepoint. However, the RTCA results over time demonstrate that the BJ and XPA cells show a similar response to Triton X-100 for the remainder of the exposure time. Based on these data, BJ and XPA cells show generally similar response to two non-genotoxic cytotoxicants and are a suitable pairing for this assay.

As these results have demonstrated, the BJ/XPA RTCA *in vitro* assay represents a rapid and simple method for simultaneously examining the cytotoxicity and NER-mediated genotoxicity of a test substance. Expansion of this concept with additional cell lines is readily accomplished if adherent cells are used. (Suspension cells are not suitable for the RTCA assay as they do not adhere to the plate microelectrodes.). Several Chinese hamster ovary (CHO) cell lines with deficiencies in the nucleotide excision repair (UV4, UV5) and base excision repair pathways (EM9) are used in the DRAG assay discussed previously (2, 3). The RTCA method described here could be adapted to use these CHO cell lines to investigate the effects of non-NER-mediated genotoxicants. As inter-species differences in toxicant metabolism may exist (24), human cell lines should be used where possible. However, as many DNA repair pathways are highly conserved, the use of non-human mammalian cell lines should be acceptable; some DNA repair-deficient mutations are lethal even during embryonic

development (25) so these cell lines must be obtained *in utero* from experimental animals. Assay development with cell lines with different DNA repair deficiencies could produce a comprehensive, simultaneous *in vitro* screening assay for several types of DNA lesions.

There are also other alternatives to using commercially available cell lines in the RTCA system. To produce "matched" cell lines which are more closely related, it is theoretically possible to either transfect DNA-repair deficient cell lines with a functional gene or mRNA to repair the deficiency (26), or to silence a functional DNA-repair gene or mRNA in a repair-proficient cell line (27). This approach has the distinct advantage of producing a pair of cell lines which are identical except for the transfected or silenced gene. However, extensive optimization of this system would be required to ensure that the transfected or silenced gene is functioning as expected, to test the stability of the manipulation over time, to determine any detrimental effects on the cell as a consequence of transfection or silencing, and to ensure that the correct gene was transfected or silenced. There is evidence that some methods of RNA silencing may be "diluted" due to cell division (28) or that the knockdown of gene function may not be complete or have "off-target" effects (29). While the development of such a system would prove a valuable addition to this method, there exist substantial challenges to optimization and validation.

Although the experiments described above have confirmed the functionality of the BJ/XPA RTCA *in vitro* method, further validation is possible if desired. A series of RTCA experiments with a chemical compound known to cause NER-mediated DNA damage could be performed with BJ and XPA cells to complement the experiments performed with UVC light. A possible candidate for these experiments would be benzo(a)pyrene (BaP), which may form metabolites known to cause bulky DNA adducts (30) repaired by the NER system. Other compounds causing NER-mediated DNA damage (e.g. 4-nitroquinoline 1-oxide (31)) may also be possible validation candidates. As with the UVC experiments, it would be expected that XPA cells would experience greater cytotoxicity compared to BJ

cells when exposed to toxicants producing NER-mediated genotoxic lesions. Additional non-genotoxic cytotoxic substances could be tested in the BJ/XPA *in vitro* assay to more completely determine the relative sensitivities of each cell line to a variety of substances with differing toxic mechanisms of action. While the two cell lines are unlikely to respond identically to all non-genotoxic substances because they are derived from different individuals, ideally the sensitivity to most compounds will be similar. Additional validation will increase the confidence that observed differences in response are due to NER-mediated lesions as opposed to inherent differences in sensitivity.

The BJ/XPA *in vitro* assay represents an improvement to existing *in vitro* genotoxicity assays. As previously discussed, the advantages of using the RTCA system to measure cytotoxicity include continuous, real-time measurement; dye- and label-free cytotoxicity assessment; a more complete assessment of cell health due to the blended cell number, proliferation, and morphology measurement; and a high-throughput format capable of testing many samples at one time (1, 5). Due to the small toxicant volumes required (~200 μL of the desired concentration per well), this assay is also well-suited for situations where test compound availability is limited. The use of a blended cell number/proliferation/morphology measurement in the RTCA system may allow detection of more subtle effects that may precede cell death (e.g. changes in cell morphology from reduced adherence of cells to culture plate surface, which may indicate imminent cell death). Using BJ and XPA cell lines with the RTCA system represents a powerful combination that can provide substantial toxicity data with each experimental replicate.

Several aspects of experimental design must be considered when developing future experiments with the BJ/XPA RTCA *in vitro* assay. Because RTCA provides continuous monitoring, choosing individual exposure periods is less of an issue compared to more traditional endpoint-based assays. Continuous exposure can permit assessment of toxicity throughout the entire cell cycle for most proliferative cell types, which provides additional data on how a toxicant may affect cellular function. However, if the inclusion of a toxicant-free recovery

period is desired (such as in the DRAG assay (2, 3)), it can easily be added by simply replacing the toxicant solution with cell culture medium at the desired exposure time. Some optimization of the exposure time prior to a recovery period would need to be performed, to ensure that the toxicant would have adequate time to exert a toxic effect. Further discussion of this optimization is beyond the scope of this chapter, but it should be noted that the effect of exposure time and individual toxicant characteristics should be considered when incorporating a recovery period into the BJ/XPA RTCA *in vitro* assay.

Other considerations related to the further development, validation, and use of the BJ/XPA *in vitro* assay include concentration of test toxicants and interpretation of results. Toxicant concentrations which are too high or too low could cause false positive or negative results, respectively. Optimization with the test agent should be performed to determine a range of concentrations suitable for testing, with generation of accurate IC_{50} values as an important aspect of experimental design. Interpreting assay results is also important; that is, how much of a difference in response between the two cell lines should be considered "significant"? Small differences in response could be attributed to inherent variation between the BJ and XPA cell lines (particularly considering the variation observed with Triton X-100 treatment in **Figure 3-4**), but moderate differences may be more difficult to categorize. In determining a potential genotoxic mechanism of action, it would be necessary to take into account statistical significance of the results as well as differences between IC_{50} values for both cell types over time and over a range of toxicant concentrations. Further assay development may be required to define criteria for a "positive" and "negative" result, bearing in mind that experimental design could have a strong impact on potential results.

This assay has attempted to control for differences in inherent variation by comparing toxicity of known NER-mediated genotoxic and non-genotoxic cytotoxicants in BJ and XPA cells. However, it is important to note that the purpose of this system is not to provide unequivocal evidence that a test compound is genotoxic via an NER-mediated mechanism. There may be other

95

underlying factors which could explain a difference in sensitivity between the two cell types. Follow-up experiments to confirm NER-mediated genotoxicity should be performed if a compound is suspected to act through this mechanism. Likewise, this assay does not provide stand-alone data adequate for human health risk assessment decisions. At present, *in vitro* assays are not sophisticated enough to model the complex interactions which occur *in vivo*. Rather, the BJ/XPA RTCA *in vitro* assay should be considered a rapid, high-throughput screening tool which may help identify toxicants of concern and provide direction for future testing. It may be used to triage a large number of potential toxicants for NER-mediated genotoxicity, prioritizing potentially genotoxic compounds for more time- and resource-intensive *in vitro* and *in vivo* testing. In this way, scarce testing resources can be directed to potentially toxic compounds, limiting unnecessary testing of compounds unlikely to be toxic.

In summary, the results of these experiments have shown: 1) XPA protein is present in BJ but absent in XPA cells, explaining the inability of XPA cells to perform NER; 2) XPA cells experience greater cytotoxicity in the RTCA assay compared to BJ cells when exposed to UVC light; this finding is expected as UVC light damage is repaired by the NER pathway, which is non-functional in XPA cells; and 3) BJ and XPA cells generally respond similarly in the RTCA assay to non-genotoxic cytotoxic agents (gentamicin & Triton X-100), suggesting that cell lines have similar susceptibility to non-genotoxic agents. While additional optimization and validation is required before this assay can be used in a regulatory context, these results suggest that the BJ/XPA *in vitro* assay could serve as a useful screening tool for determining NER-mediated genotoxic effects.

3.5   References

1. Atienza JM, Zhu J, Wang X, Xu X, Abassi Y. Dynamic monitoring of cell adhesion and spreading on microelectronic sensor arrays. J Biomol Screen. 2005 Dec;10(8):795-805.

2. Helleday T, Johansson F, Jenssen D. The DRAG test: An assay for detection of genotoxic damage. Altern Lab Anim. 2001 May-Jun;29(3):233-41.

3. Johansson F, Allkvist A, Erixon K, Malmvarn A, Nilsson R, Bergman A, et al. Screening for genotoxicity using the DRAG assay: Investigation of halogenated environmental contaminants. Mutat Res. 2004 Sep 12;563(1):35-47.

4. Borenfreund E, Puerner JA. Toxicity determined in vitro by morphological alterations and neutral red absorption. Toxicol Lett. 1985 Feb-Mar;24(2-3):119-24.

5. Atienza JM, Yu N, Kirstein SL, Xi B, Wang X, Xu X, et al. Dynamic and label-free cell-based assays using the real-time cell electronic sensing system. Assay Drug Dev Technol. 2006 Oct;4(5):597-607.

6. Solly K, Wang X, Xu X, Strulovici B, Zheng W. Application of real-time cell electronic sensing (RT-CES) technology to cell-based assays. Assay Drug Dev Technol. 2004 Aug;2(4):363-72.

7. Xing JZ, Zhu L, Jackson JA, Gabos S, Sun XJ, Wang XB, et al. Dynamic monitoring of cytotoxicity on microelectronic sensors. Chem Res Toxicol. 2005 Feb;18(2):154-61.

8. xCELLigence product list [Internet].; 2012. Available from: http://www.aceabio.com/productlist.aspx?cateid=265.

9. Friedberg EC, Walker GC, Siede W. DNA repair and mutagenesis. Washington, D.C.: ASM Press; 1995.

10. Nouspikel T. DNA repair in mammalian cells : Nucleotide excision repair: Variations on versatility. Cell Mol Life Sci. 2009 Mar;66(6):994-1009.

11. Moller P, Wallin H. Adduct formation, mutagenesis and nucleotide excision repair of DNA damage produced by reactive oxygen species and lipid peroxidation product. Mutat Res. 1998 Jun;410(3):271-90.

12. Brooks PJ, Wise DS, Berry DA, Kosmoski JV, Smerdon MJ, Somers RL, et al. The oxidative DNA lesion 8,5'-(S)-cyclo-2'-deoxyadenosine is repaired by the nucleotide excision repair pathway and blocks gene expression in mammalian cells. J Biol Chem. 2000 Jul 21;275(29):22355-62.

13. Kuraoka I, Bender C, Romieu A, Cadet J, Wood RD, Lindahl T. Removal of oxygen free-radical-induced 5',8-purine cyclodeoxynucleosides from DNA by the nucleotide excision-repair pathway in human cells. Proc Natl Acad Sci U S A. 2000 Apr 11;97(8):3832-7.

14. GM04312 [Internet].; 2009. Available from: http://ccr.coriell.org/sections/Search/Sample_Detail.aspx?Ref=GM04312&PgId= 166.

15. Novarina D, Amara F, Lazzaro F, Plevani P, Muzi-Falconi M. Mind the gap: Keeping UV lesions in check. DNA Repair (Amst). 2011 Jul 15;10(7):751-9.

16. Dayeh VR, Chow SL, Schirmer K, Lynn DH, Bols NC. Evaluating the toxicity of triton X-100 to protozoan, fish, and mammalian cells using fluorescent dyes as indicators of cell viability. Ecotoxicol Environ Saf. 2004 Mar;57(3):375-82.

17. Weyermann J, Lochmann D, Zimmer A. A practical note on the use of cytotoxicity assays. Int J Pharm. 2005 Jan 20;288(2):369-76.

18. Karasawa T, Steyger PS. Intracellular mechanisms of aminoglycoside-induced cytotoxicity. Integr Biol (Camb). 2011 Sep;3(9):879-86.

19. European Agency for the Evaluation of Medicinal Products - Veterinary Medicines and Inspections. Committee for veterinary medicinal products: Gentamicin. London: 2001. Report No.: EMEA/MRL/803/01.

20. Bradford MM. A rapid and sensitive method for the quantitation of microgram quantities of protein utilizing the principle of protein-dye binding. Anal Biochem. 1976 May 7;72:248-54.

21. Romero-Calvo I, Ocon B, Martinez-Moya P, Suarez MD, Zarzuelo A, Martinez-Augustin O, et al. Reversible Ponceau staining as a loading control alternative to actin in Western blots. Anal Biochem. 2010 Jun 15;401(2):318-20.

22. Pamphilon DH, Alnaqdy AA, Godwin V, Preece AW, Wallington TB. Studies of allogeneic bone marrow and spleen cell transplantation in a murine model using ultraviolet-B light. Blood. 1991 May 1;77(9):2072-8.

23. CRL-2522™ [Internet].; 2013. Available from: http://www.atcc.org/ATCCAdvancedCatalogSearch/ProductDetails/tabid/452/Default.aspx?ATCCNum=CRL-2522&Template=cellBiology.

24. Martignoni M, Groothuis GM, de Kanter R. Species differences between mouse, rat, dog, monkey and human CYP-mediated drug metabolism, inhibition and induction. Expert Opin Drug Metab Toxicol. 2006 Dec;2(6):875-94.

25. Friedberg EC, Meira LB. Database of mouse strains carrying targeted mutations in genes affecting cellular responses to DNA damage: Version 3. Mutat Res. 1999 Mar 10;433(2):69-87.

26. Rabinovich PM, Weissman SM. Cell engineering with synthetic messenger RNA. Methods Mol Biol. 2013;969:3-28.

27. Fire A, Xu S, Montgomery MK, Kostas SA, Driver SE, Mello CC. Potent and specific genetic interference by double-stranded RNA in *Caenorhabditis elegans*. Nature. 1998 Feb 19;391(6669):806-11.

28. Bartlett DW, Davis ME. Insights into the kinetics of siRNA-mediated gene silencing from live-cell and live-animal bioluminescent imaging. Nucleic Acids Res. 2006 Jan 12;34(1):322-33.

29. Hannon GJ, Rossi JJ. Unlocking the potential of the human genome with RNA interference. Nature. 2004 Sep 16;431(7006):371-8.

30. Geacintov NE, Yoshida H, Ibanez V, Harvey RG. Non-covalent intercalative binding of 7,8-dihydroxy-9,10-epoxybenzo(a)pyrene to DNA. Biochem Biophys Res Commun. 1981 Jun;100(4):1569-77.

31. Bailleul B, Daubersies P, Galiegue-Zouitina S, Loucheux-Lefebvre MH. Molecular basis of 4-nitroquinoline 1-oxide carcinogenesis. Jpn J Cancer Res. 1989 Aug;80(8):691-7.

Chapter 4: Cytotoxicity and mutagenicity of halobenzoquinone drinking water disinfection byproducts[1]

4.1 Introduction

Halobenzoquinone (HBQ) drinking water disinfection byproducts (DBPs) were recently identified as potentially carcinogenic compounds requiring toxicity testing. These compounds consist of a single benzoquinone ring with one or more halogenated substituents attached to the ring; they are distinct from the polycyclic aromatic carbons that are called "haloquinones". Halobenzoquinone compounds were initially predicted to form from common raw water precursor compounds and were predicted to be toxic using quantitative-structure toxicity relationship (QSTR) modeling (1, 2). These models predict that many HBQs are carcinogenic, with predicted chronic lowest observed adverse effect levels (LOAELs) <1 mg/kg/day (2). As discussed in **Chapter 1, Section 1.5**, currently-regulated DBPs (haloacetic acids and trihalomethanes) appear to be insufficiently potent and not present in sufficient amounts to account for the excess bladder cancer risk associated with chlorinated water consumption (3-6). Therefore, identification of DBPs with sufficient potency and carcinogenicity to account for this risk is a priority (1, 2). The low predicted chronic LOAELs and structural similarity to known carcinogens of HBQ DBPs suggest that they may represent a cancer risk, specifically for bladder cancer (2). Consequently, the investigation of the toxic effects of HBQs was designated a high priority.

Several HBQ compounds have been detected as DBPs in treated North American drinking water, including 2,6-dibromo-1,4-benzoquinone (2,6DBBQ); 2,6-dichloro-1,4-benzoquinone (DCBQ); 2,6-dichloro-3-methyl-1,4-benzoquinone (DCMBQ); and 2,3,6-trichloro-1,4-benzoquinone (TCBQ) (7). QSTR analysis

---

[1] Ames test experiments in this chapter were performed on a contract basis by HydroQual Laboratories, Inc. of Calgary, Alberta, Canada.

does not predict that any of these compounds will be mutagens, but does predict that DCMBQ and TCBQ will be carcinogens. The predicted chronic LOAELs for these HBQs are 0.159 (2,6DBBQ), 0.049 (DCBQ), 0.079 (DCMBQ), and 0.033 (TCBQ) mg/kg/day (2). Although DCMBQ has a higher predicted LOAEL than some other HBQs, it was identified as the HBQ with the greatest potential to be a bladder carcinogen due to its chemical structure and relative similarity to known bladder carcinogens (1, 2). However, few empirical toxicological data are available for HBQs, and QSTR predictions of toxicity are hampered by limited toxicological data for compounds with similar structures in prediction databases (1, 2).

Generally, benzoquinone substances are known to cause toxicity through several mechanisms, including the formation of adducts with cell macromolecules (DNA, protein, lipids) and the generation of reactive oxygen species (ROS) with subsequent oxidative damage to cell macromolecules (8-12). The severity and nature of benzoquinone toxicity are highly dependent on the bioactivating metabolic pathway. A two-electron reduction via DT-diaphorase (quinone reductase) results in the generally less toxic hydroquinone form, while a one-electron reduction via NADPH-cytochrome P450 reductase leads to the formation of a semiquinone radical. As the semiquinone radical is capable of auto-oxidation, redox cycling may occur. The continuous reduction and regeneration of the parent quinone result in depletion of intracellular oxygen, NADPH, and reducing agents such as glutathione. This process generates reactive oxygen species, which may cause both cytotoxicity and genotoxicity (8, 9). However, quinones are electrophilic Michael acceptors, and may also directly alkylate or arylate cellular macromolecules, including proteins and DNA (8, 9). Other potential mechanisms of quinone toxicity include disruption of cellular respiration (via effects on mitochondria) and intercalation of DNA (10). Evidence suggests that substitutions on the quinone ring may affect the mechanism of toxicity of the resulting compounds (10, 13).

Limited cytotoxicity data exist for the HBQs examined here or their related compounds. The majority of toxicity data for HBQ compounds comes from chloranil (tetrachloro-1,4-benzoquinone), which is a metabolic product of the wood preservative pentachlorophenol. 2,5-dichloro-1,4benzoquinone (2,5DCBQ) and chloranil caused cytotoxicity in both primary rat hepatocytes and adrenal carcinoma cells, with generation of ROS and depletion of glutathione observed in both cell types (13). Depletion of intracellular glutathione was also observed in rat platelets exposed to chloranil, with a simultaneous anti-aggregative effect (14). Chloranil also inhibited mouse cytosolic glutathione-*S*-transferase activity (15). Chloranil and 2,5DCBQ were both shown to have inhibitory effects on rat liver mitochondrial function *in vitro* (16). Likewise, chloranil also inhibited succinoxidase activity in heavy beef heart mitochondria and demonstrated redox cycling with generation of reactive oxygen species (ROS) *in vitro* (17). In both rats and mice, chloranil formed adducts with both cytosolic and nuclear hepatic proteins (18). A major metabolite of halogenated benzene compounds was found to be the corresponding halobenzoquinone, and these compounds may be hepatotoxic in rodents (19). Halogenated benzene-derived HBQs can also be reduced to the less toxic halohydroquinone form, conjugated with glutathione, and transported to the kidney, where they can cause nephrotoxicity in rodents (19). This finding is similar to a study which found that glutathione-conjugated 1,4-hydroquinone (a metabolite of 1,4-benzoquinone) caused nephrotoxicity in rats (20). The glutathione conjugates of 2,5DCBQ and chloranil also caused renal proximal tubular necrosis in male rats (21). From the toxicity data available for HBQ compounds, it appears they are capable of causing cytotoxicity via several mechanisms, including ROS production, glutathione depletion, and interference with mitochondrial function.

Some evidence suggests that halogenated benzoquinone compounds are capable of causing genotoxic effects as well. 2,5DCBQ, 2,6DCBQ, and chloranil were shown to cause decomposition of the lipid peroxidation product 13-HPODE into genotoxic metabolites (22). ROS generation was also observed in the V79 Chinese hamster lung cell line upon exposure to chloranil, with formation of 8-
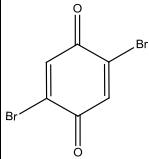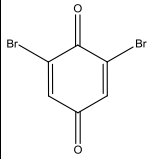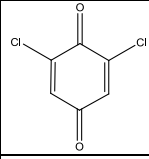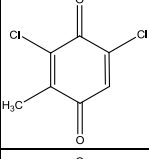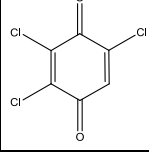
hydroxydeoxyguanosine (8OHdG) DNA lesions and single-stranded DNA breaks (23). When exposed to nucleosides and calf thymus DNA, chloranil preferentially formed adducts with deoxyguanosine, but would also form adducts with deoxycytidine and deoxythymidine (24). Exposure of immobilized DNA on a biosensor to chloranil and tetrafluoro-1,4-benzoquinone revealed that both compounds caused DNA damage, possibly by forming covalent adducts or through an oxidative damage mechanism (25). Previous experiments in our research group showed that HBQs are capable of binding to single- or double-stranded oligodeoxynucleotides, as measured by electrospray ionization mass spectrometry. The ranking of binding affinities was TCBQ ≈ DCMBQ < DCBQ << 2,6DBBQ, and binding was thought to occur through a non-covalent mechanism characterized by H-bonding and partial intercalation (26). In summary, HBQ compounds appear to cause genotoxicity through several different mechanisms, including direct adduct formation and reactive oxygen species production.

Members of this research group recently examined the toxicity of HBQ substances on the T24 human bladder cancer cell line (27). HBQs were examined for cytotoxicity, ROS production, and ability to cause oxidative lesions to DNA, proteins, and lipids. Cytotoxicity ranking of HBQs using the 24-hour MTS assay was TCBQ (IC_{50}: 150.7 µM) < DBBQ (IC_{50}: 142.0 µM) < DCMBQ (IC_{50}: 110.1 µM) < DCBQ (IC_{50}: 94.5 µM). Cytotoxicity of HBQs was greatly reduced with concomitant addition of N-acetylcysteine (NAC), a ROS scavenger. All HBQs were capable of producing ROS in a concentration-dependent manner, with TCBQ producing the greatest increase in ROS. However, DCMBQ appeared to produce the greatest increase in oxidative DNA lesions, as measured by 8OHdG production. Protein carbonylation, indicative of oxidative damage, was observed for all tested HBQs, but significantly increased lipid peroxidation was not observed for any tested HBQ. These results indicate that HBQs are capable of causing both cytotoxicity and genotoxicity in a human cancer cell line, likely due at least in part to an oxidative damage mechanism.

Although evidence suggests that related HBQ compounds and benzoquinones may be both cytotoxic and genotoxic, more toxicity data are needed for the newly-discovered HBQ DBPs. To address this knowledge gap, we propose to use the BJ/XPA *in vitro* assay developed in the previous chapter to examine the cytotoxic and genotoxic effects of selected HBQ DBPs on human cells *in vitro*. The response of normal BJ cells will be compared to that of nucleotide excision repair (NER)-deficient XPA cells to investigate if NER-mediated genotoxicity is potentially involved in HBQ toxic mechanisms of action. As opposed to the previous studies with HBQ compounds, this study will incorporate the use of intact normal (non-carcinoma) human cell lines and the impedance-based RTCA system, which will permit monitoring of cytotoxicity and potential NER-mediated genotoxicity over time. To examine mutagenicity of these substances, the Ames test/ bacterial reverse mutation assay will be used. Assessing the cytotoxicity, genotoxicity, and mutagenicity of these HBQs will provide much-needed toxicological data and allow assessment of earlier QSTR predictions (1, 2).

The simultaneous testing of specific HBQs in the BJ/XPA *in vitro* system permits analysis of toxicity based on chemical properties. In order to investigate the effects of chemical structure on HBQ toxicity, the HBQ DBPs identified in drinking water samples (2,6DBBQ; DCBQ; DCMBQ; and TCBQ) (7) will be tested, as well as the closely-related compound 2,5-dibromo-1,4-benzoquinone (2,5DBBQ) (see **Table 4-1**). While they all share the benzoquinone ring structure, these compounds differ in the number, position, and composition of ring substitutions. Therefore, these experiments will explore the effect of chlorinated vs. brominated substitutions, the number of substitutions on the ring structure, the presence and absence of a methyl substitution, and the positioning of substitutions on the parent ring structure.

Table 4-1: Chemical properties of selected HBQ DBPs

Halobenzoquinone	CAS #	Molecular Formula	Molecular Weight (g/mol)	Source and Purity	log P_{OW}	Chemical Structure
2,5-dibromo-1,4-benzoquinone (2,5DBBQ)	1633-14-3	$C_6H_2Br_2O_2$	265.89	ALDRICH, 98%	2.03	
2,6-dibromo-1,4-benzoquinone (2,6DBBQ)	19643-45-9	$C_6H_2Br_2O_2$	265.89	INDOFINE Chemical Company, ≥98%	2.03	
2,6-dichloro-1,4-benzoquinone (DCBQ)	697-91-6	$C_6H_2Cl_2O_2$	176.98	ALDRICH, 98%	1.768	
2,6-dichloro-3-methyl-1,4-benzoquinone (DCMBQ)	40100-98-9	$C_7H_4Cl_3O_2$	191.0125	Shanghai Acana Pharmtech Co., ≥98%	2.145	
2,3,6-trichloro-1,4-benzoquinone (TCBQ)	634-85-5	$C_6HCl_3O_2$	211.4311	Shanghai Acana Pharmtech Co., ≥98%	2.374	

Log P_{OW} values were calculated using Molinspiration software (www.molinspiration.com). Chemical structures and molecular weight values were produced with ChemDraw software (PerkinElmer).

4.2 Materials and Methods

4.2.1 Cell lines and culture conditions

The BJ cell line was obtained from ATCC (#CRL-2522), and the XPA cell line (NIGMS: GM04312C) was kindly provided by Dr. Michael Weinfeld at the University of Alberta. Cell lines were maintained in a humidified 37°C incubator, with 5% CO_2, in Eagle's Minimum Essential Medium (ATCC; #30-2003) supplemented with 10% fetal bovine serum (Sigma; #F1051) and 1% of 10000 U penicillin/10000 µg streptomycin solution (Gibco; #15140-122). Cells were

subcultured when confluence was 80-95%, and culture medium was refreshed at least twice per week. Cell line passage numbers were restricted (≤15 passages per individual set of cell cultures) to minimize effects of genetic drift. All manipulations of cell cultures were performed in a biosafety cabinet (Thermo Scientific Forma Class 2 A2; #1284) under aseptic conditions. Manipulation of cell lines was performed in compliance with the University of Alberta "Working with Biohazardous Materials" policy and laboratory personnel received both institutional and site-specific biosafety training.

4.2.2 Preparation of halobenzoquinone compounds

Halobenzoquinone compounds were obtained from Aldrich (DCBQ, 2,5DBBQ), Indofine Chemical Company (2,6DBBQ), and Shanghai Acana Pharmtech Company (TCBQ, DCMBQ) (see **Table 4-1**). All compounds were ≥98% purity. Stock solutions were made by dissolving the solid HBQ compound in 100% methanol. Stock solutions were stored in a -20°C freezer, protected from light. On the day of the experiment, the stock solutions were removed from the freezer and were diluted to appropriate concentrations in culture medium. A methanol-spiked sample of culture medium, equivalent to the volume of the most concentrated HBQ solution, was used as a solvent control treatment.

4.2.3 RTCA cytotoxicity assay

BJ and XPA cells were harvested using a 0.05% trypsin-0.53 mM EDTA solution (Gibco; #25300-05) and plated into 16-well RTCA E-plates at a density of 4000 and 5000 cells per well, respectively. Both cell lines were used in each replicate, with half of the available wells plated with each cell type. Using built-in RTCA software (ACEA RT-CES SP v5.3, ACEA Biosciences), diagnostic assays were performed on all plates prior to use; if any well failed quality control tests, the results from that well were discarded. If multiple bad wells were found on a plate, the plate was discarded. The RTCA system was programmed to collect cell index

(CI) measurements every hour. Cells were allowed to equilibrate in the E-plates without treatment until reaching a CI value of ~1, corresponding to ~40-50% confluence (28), within 36-48 hours post-plating. Any wells showing abnormal cell growth were not used for treatment or control groups. Plates were then removed from the incubator, and culture medium was removed. Each well was treated with a 200 µL aliquot of halobenzoquinone solution, methanol control solution, or culture medium (negative control group). The treatment layout was randomized for each replicate to avoid layout-related technical artifacts. After treatment, plates were returned to the RTCA unit in the incubator and monitored hourly until a growth plateau had been reached, usually ~72 hours post-treatment.

4.2.4 Ames test/bacterial reverse mutation assay

The standard plate incorporation Ames test/bacterial reverse mutation assay was performed as previously described (29-31) with variations described below, by HydroQual Laboratories Ltd. in Calgary, Alberta. The *Salmonella typhimurium* strains TA98 (frameshift mutation) and TA100 (substitution mutation) were used (32), as well as the *Escherichia coli* WP2 uvrA strain (a repair-deficient strain that detects mutations at AT sites) (33). Cultures of each strain were mixed with molten top agar (containing a small amount of histidine for *Salmonella* or tryptophan for *E. coli*), rat S9 mix (if used; tests were performed with and without S9), and appropriate concentrations of the test HBQs, including a solvent control plate treated with methanol equivalent to the volume of the most concentrated HBQ sample. This mixture was poured onto glucose minimal agar medium plates and allowed to harden. The test plates were then inverted and incubated at 37°C for 5 days (TA98, TA100, *E. coli* +S9) or 10 days (*E. coli* −S9). Revertant bacterial colonies on each plate were counted and recorded.

4.2.5 Data analysis

Statistical analyses were performed with Prism$^{®}$ software (GraphPad Software) and Microsoft Excel (Microsoft Corporation). Results from all experiments were exported into Microsoft Excel, organized, and imported into Prism. At least three independent replicates were performed for each experiment; mean values from these combined replicates were used for data analysis. Data for RTCA experiments were analyzed via log-transformation of the concentration values, normalization to the solvent control group results, and fitting a non-linear sigmoidal dose-response curve (variable slope) to the data. IC$_{50}$ values over time were calculated from this curve, where possible. While all RTCA experiments were conducted with a negative control (consisting only of culture medium), these results were virtually identical to those of the solvent group; therefore, only the solvent control data are shown. For the Ames test, <u>all</u> of the following criteria were required for statistical significance: a statistically significant elevation in revertants of a treatment group, compared to the corresponding control group, as determined by Student's t-test (significance at p<0.05); the presence of at least a two-fold increase in revertant numbers (29, 32); <u>and</u> increased revertants appearing in ≥2 consecutive concentrations, unless increased revertants were observed only at the highest tested concentration or cytotoxicity was reported at the next highest tested concentration. Elevated revertant numbers in a single isolated concentration were not considered significant.

4.3   Results

4.3.1 RTCA HBQ cytotoxicity

Figures 4-1 to 4-5 demonstrate the cytotoxic effects of HBQs in the BJ/XPA *in vitro* assay. The decrease in cell index (CI) values in **Figure 4-1** demonstrates the cytotoxic effect of 2,5DBBQ on both BJ and XPA cells at 50 μM. The cytotoxic effect on XPA cells is more pronounced than that observed in BJ cells; this is reflected in the graph of IC$_{50}$ values over time. IC$_{50}$ values for BJ cells range from 51-68 μM over the exposure period. IC$_{50}$ values for XPA cells over the same period range from 42-55 μM. **Figure 4-2** demonstrates that 2,6DBBQ had no

toxic effect on BJ cells at any tested concentration, and only a slight decrease in CI is seen in XPA cells treated with 50 µM. In **Figure 4-3**, DCBQ exerts little cytotoxic effect on either BJ or XPA cells; while a slight decrease in CI is observed for the two lowest DCBQ concentrations (5 and 12.5 µM) in XPA cells, no decrease in CI is observed for the highest concentrations (25 and 50 µM). **Figure 4-4** indicates that BJ cells experience a decrease in CI when exposed to 50 µM DCMBQ. Conversely, a clear concentration-dependent decrease in cell index values is observed at 12.5-50 µM DCMBQ in XPA cells. IC_{50} values for DCMBQ in BJ cells are ~49-69 µM and ~14-35 µM in XPA cells. TCBQ had no cytotoxic effect in either BJ or XPA cells, as seen in **Figure 4-5**. No meaningful IC_{50} values could be calculated for 2,6DBBQ, DCBQ, or TCBQ in either cell line due to a lack of cytotoxicity.

Figure 4-1: Effect of 2,5DBBQ on cell index and IC$_{50}$ values of BJ and XPA cells, measured by RTCA

RTCA data were obtained from BJ (top panel) and XPA (middle panel) cells exposed to 2,5DBBQ, with comparison of IC_{50} values (bottom panel). A solvent control group was treated only with methanol (MeOH Control) at the highest concentration used in the treatment groups. Data shown are an average of three independent experiments, with error bars representing the standard error of the mean (SEM) for cell index values, and 95% confidence intervals for IC_{50} values. Note that ≥45 hours of exposure in BJ cells, 95% confidence intervals for the IC_{50} values could not be calculated due to extremely large confidence interval values. IC_{50} values for XPA cells are lower than those for BJ cells throughout the course of the experiment, with significantly lower IC_{50} values at 25-32 hours post-exposure, as measured by unpaired t-tests at each timepoint, using the Holm-Šídák correction for multiple comparisons and a significance level of $p<0.05$.

BJ 2,6DBBQ

Legend:
- MeOH Control
- 5uM 2,6DBBQ
- 12.5uM 2,6DBBQ
- 25uM 2,6DBBQ
- 50uM 2,6DBBQ

XPA 2,6DBBQ

Legend:
- MeOH Control
- 5uM 2,6DBBQ
- 12.5uM 2,6DBBQ
- 25uM 2,6DBBQ
- 50uM 2,6DBBQ
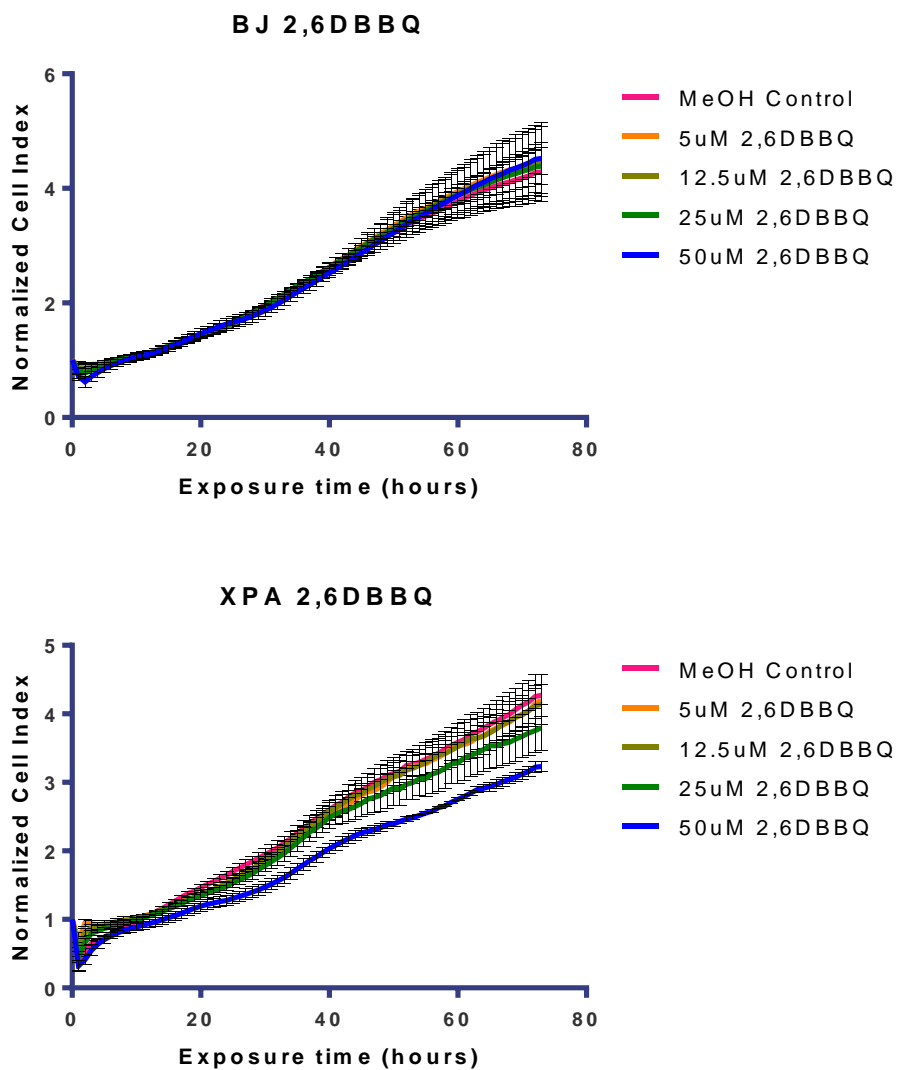
Figure 4-2: Effect of 2,6DBBQ on cell index values of BJ and XPA cells, measured by RTCA

RTCA data were obtained from BJ (top panel) and XPA (bottom panel) cells exposed to 2,6DBBQ. A solvent control group was treated only with methanol (MeOH Control) at the highest concentration used in the treatment groups. Data shown are an average of three independent experiments, with error bars representing the standard error of the mean (SEM). No meaningful IC_{50} values could be calculated for 2,6DBBQ in either BJ or XPA cells due to lack of cytotoxicity.
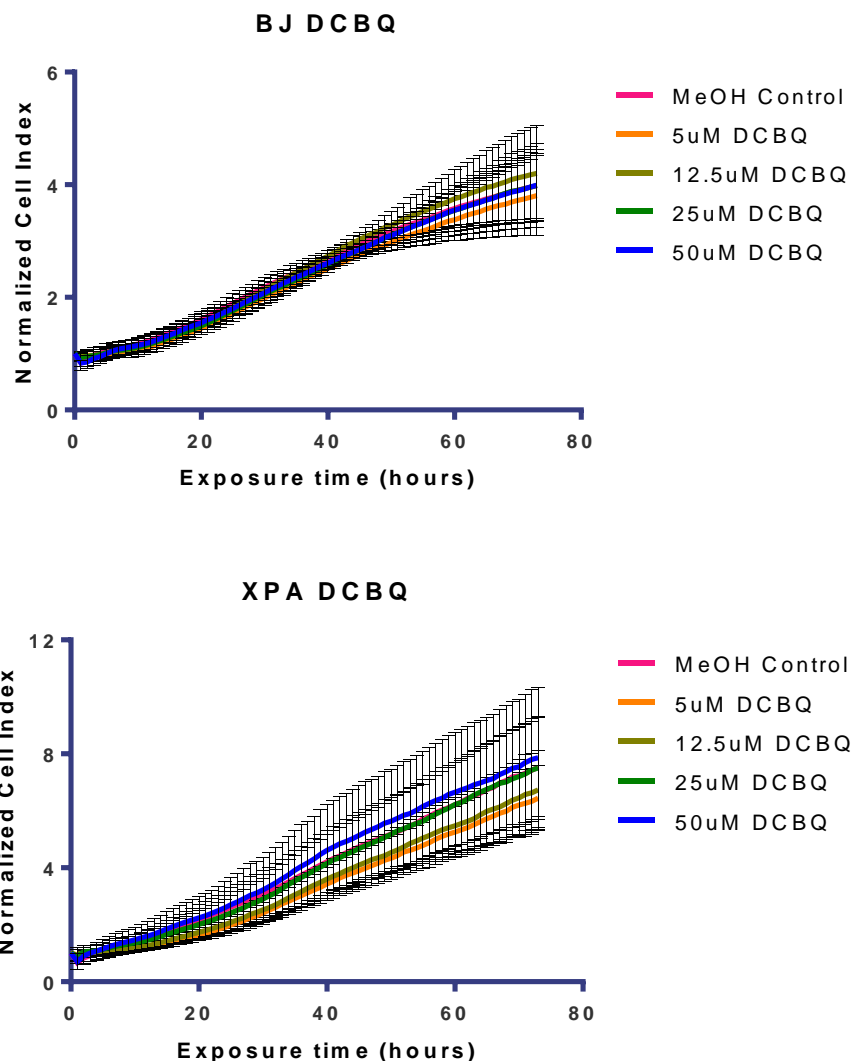
Figure 4-3: Effect of DCBQ on cell index values of BJ and XPA cells, measured by RTCA

RTCA data were obtained from BJ (top panel) and XPA (bottom panel) cells exposed to DCBQ. A solvent control group was treated only with methanol (MeOH Control) at the highest concentration used in the treatment groups. Data shown are an average of three independent experiments, with error bars representing the standard error of the mean (SEM). No meaningful IC_{50} values could be calculated for DCBQ in either BJ or XPA cells due to lack of cytotoxicity.
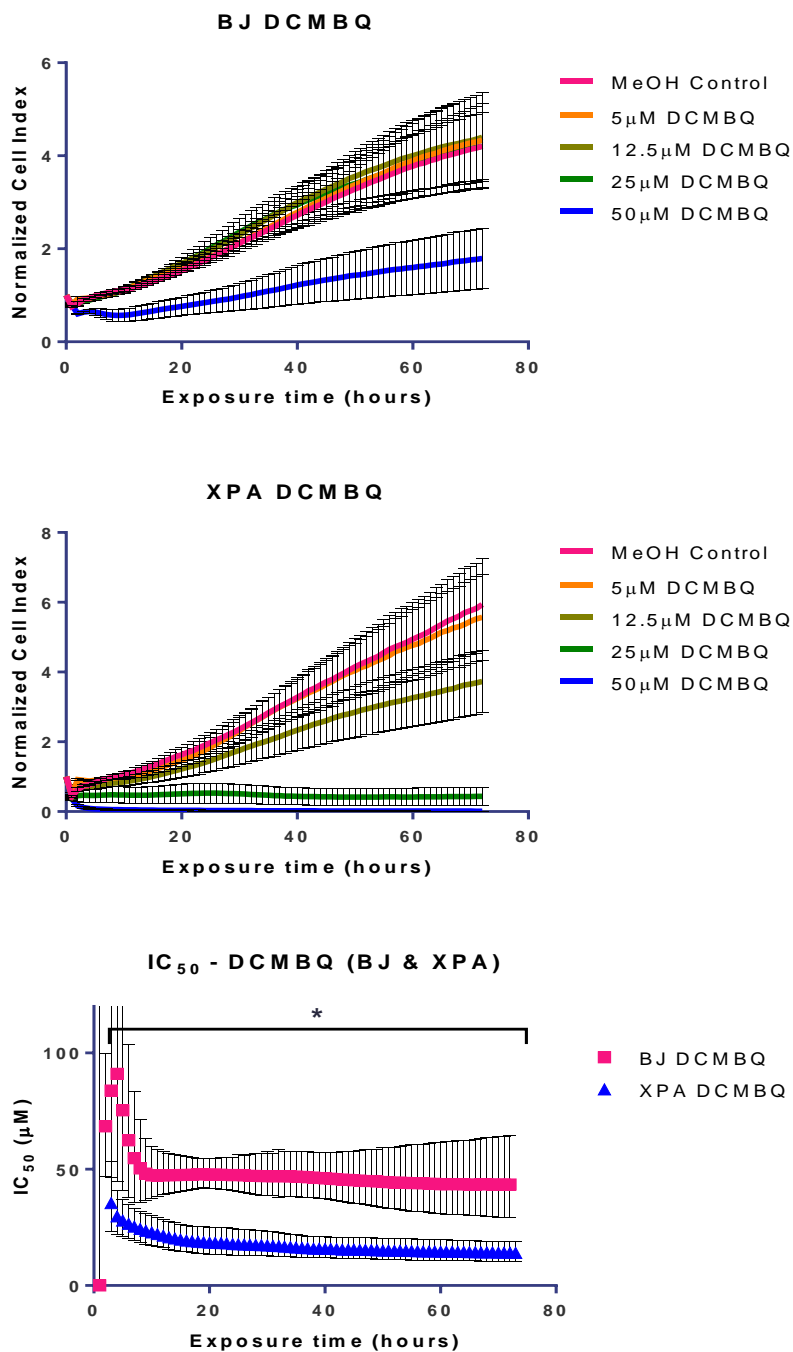
Figure 4-4: Effect of DCMBQ on cell index and IC$_{50}$ values of BJ and XPA cells, measured by RTCA

RTCA data were obtained from BJ (top panel) and XPA (middle panel) cells exposed to DCMBQ, with comparison of IC$_{50}$ values (bottom panel). A solvent control group was treated only with methanol (MeOH Control) at the highest

concentration used in the treatment groups. Data shown are an average of three independent experiments, with error bars representing the standard error of the mean (SEM) for cell index values, and 95% confidence intervals for IC_{50} values. IC_{50} values for XPA cells are lower than those for BJ cells throughout the course of the experiment, with significantly lower IC_{50} values at 3-72 hours post-exposure, as measured by unpaired t-tests at each timepoint, using the Holm-Šídák correction for multiple comparisons and a significance level of $p<0.05$.

BJ TCBQ

- MeOH Control
- 5uM TCBQ
- 12.5uM TCBQ
- 25uM TCBQ
- 50uM TCBQ

XPA TCBQ
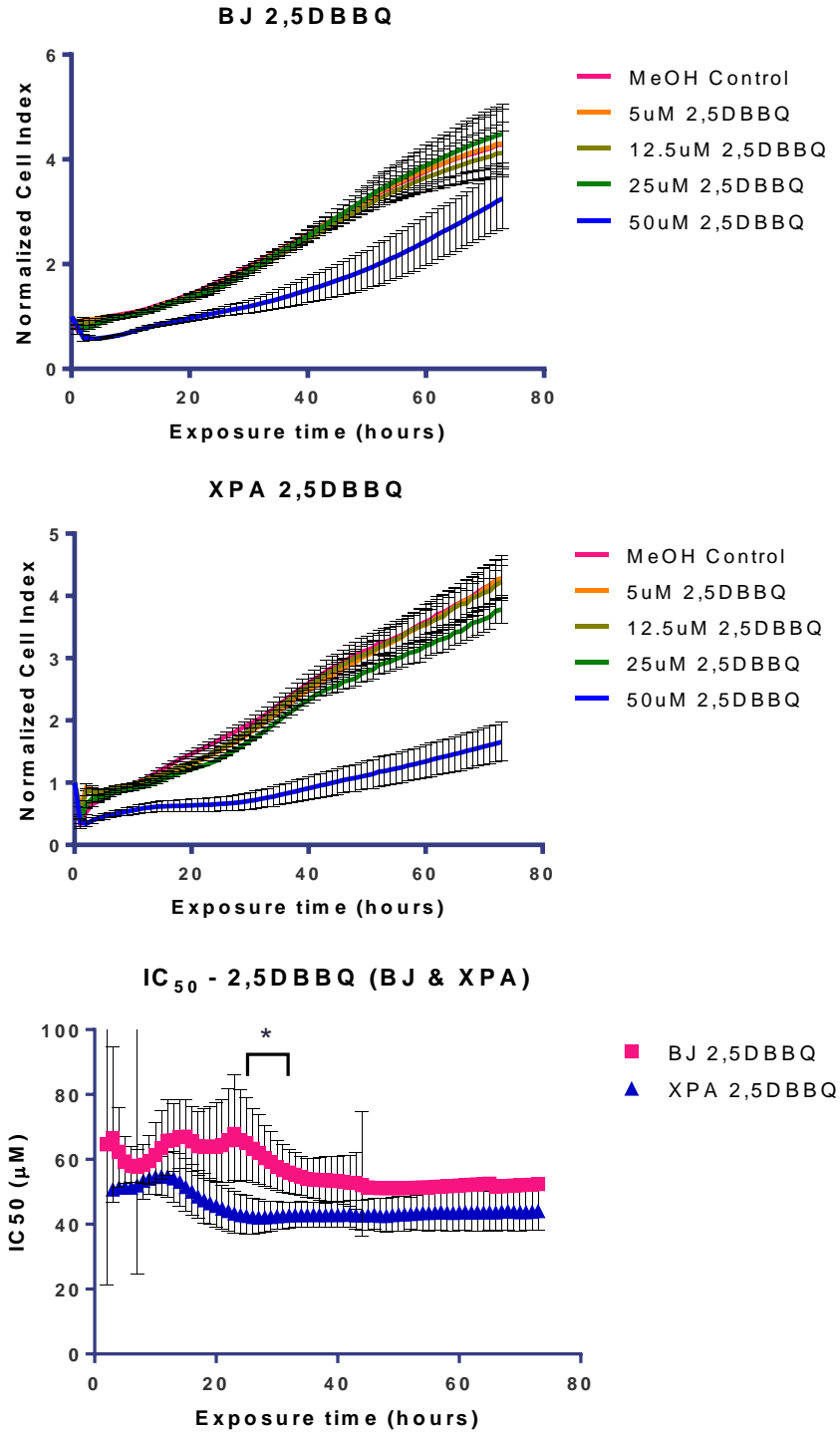
- MeOH Control
- 5uM TCBQ
- 12.5uM TCBQ
- 25uM TCBQ
- 50uM TCBQ
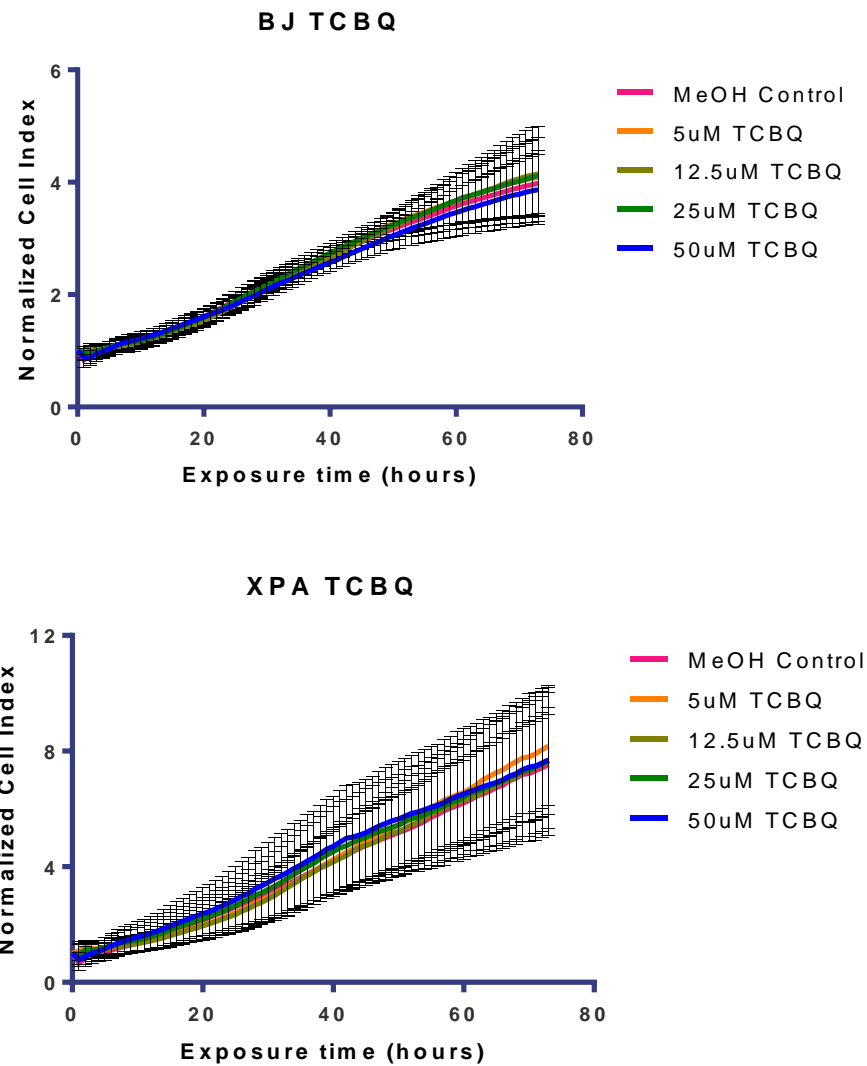
Figure 4-5: Effect of TCBQ on cell index values of BJ and XPA cells, measured by RTCA

RTCA data were obtained from BJ (top panel) and XPA (bottom panel) cells exposed to TCBQ. A solvent control group was treated only with methanol (MeOH Control) at the highest concentration used in the treatment groups. Data shown are an average of three independent experiments, with error bars representing the standard error of the mean (SEM). No meaningful IC_{50} values could be calculated for TCBQ in either BJ or XPA cells due to lack of cytotoxicity.

4.3.2 Ames test/bacterial reverse mutation assay

Results are displayed in **Table 4-2**. Acute cytotoxicity is observed in the *E. coli* WP2 <u>uvrA</u> strain with all HBQs without S9, in TA98 exposed to 2,6DBBQ without S9, and in TA100 exposed to 50 µM DCMBQ without S9. No mutagenicity or cytotoxicity is detected for *E. coli* WP2 <u>uvrA</u> or TA98 exposed to any HBQ with S9, for TA100 exposed to 2,6DBBQ with S9, or TA100 exposed to TCBQ without S9. Significantly elevated numbers of colonies compared to the control group, indicative of mutagenicity, are observed in TA100 exposed to 2,5DBBQ (-S9: 12.5-25 µM; +S9: 25-50 µM), DCBQ (-S9: 12.5-50 µM; +S9: 25-50 µM), and DCMBQ (-S9: 3.1-25 µM; +S9: 25-50 µM) with or without S9; 2,6DBBQ without S9 (12.5-50 µM), and TCBQ (25-50 µM) with S9.

Table 4-2: Results of Ames mutagenicity test of HBQs

	TA98 (frameshift)		TA100 (substitution)		_E. Coli_ (AT site)	
	no S9	with S9	no S9	with S9	no S9	with S9
2,5DBBQ	No	No	Yes (12.5-25µM)	Yes (25-50µM)	*	No
2,6DBBQ	*	No	Yes (12.5-50µM)	No	*	No
DCBQ	No	No	Yes (12.5-50µM)	Yes (25-50µM)	*	No
DCMBQ	No	No	Yes (3.1-25µM), cytotoxicity at 50µM	Yes (25-50µM)	*	No
TCBQ	No	No	No	Yes (25-50µM)	*	No

Table indicates results for treated bacteria compared with untreated control plates. HBQs were tested at concentrations of 3.1, 6.3, 12.5, 25, and 50 µM. "Yes" refers to statistically significantly (p<0.05) greater numbers of revertants in the designated concentrations of HBQs compared to the untreated control group (as determined by Student's t-test), with at least a two-fold increase in revertant colonies compared to the corresponding control group, in ≥2 consecutive concentrations (unless only the highest concentration showed significantly elevated revertants). An asterisk ("*") designates groups where cytotoxicity was observed in ≥2 consecutive concentrations. "No" refers to either no significant difference in the number of revertants per plate compared to the control group, or to cytotoxicity or an increased number of revertants at only one HBQ concentration <50 µM.

4.4 Discussion

The RTCA results (**Figures 4-1 through 4-5**) clearly indicate that the HBQs are capable of producing different degrees of cytotoxicity, including some differences between BJ and XPA cell response. The relative ranking of cytotoxicity is TCBQ $\approx$ 2,6DBBQ $\approx$ DCBQ < 2,5DBBQ < DCMBQ for BJ cells and TCBQ $\approx$ DCBQ < 2,6DBBQ < 2,5DBBQ < DCMBQ for XPA cells. TCBQ and DCBQ show essentially no cytotoxicity in either cell line at concentrations from 5-50 μM. 2,6DBBQ is mildly cytotoxic at 50 μM in XPA cells but not BJ cells. Both 2,5DBBQ and DCMBQ are toxic to BJ and XPA cells, but in the XPA cells, the depression of cell index values is more pronounced and/or present at lower HBQ concentrations. IC_{50} values could be calculated for 2,5DBBQ (BJ: 51-68 μM; XPA: 42-55 μM) and DCMBQ (BJ: 43-91 μM; XPA: 14-35 μM), but not for TCBQ, DCBQ, and 2,6DBBQ due to lack of toxicity.

The use of the BJ/XPA *in vitro* assay may permit some insight into the mechanism of toxicity of HBQ compounds by measuring cell-dependent toxicity. As described in **Chapter 3**, a greater cytotoxic response in XPA cells compared to BJ cells may indicate the involvement of nucleotide excision repair (NER)-mediated DNA damage. I chose to use the BJ/XPA *in vitro* assay to examine the cyto- and genotoxicity of these HBQs because one potential mechanism of quinone toxicity involves the formation of bulky adducts to cell macromolecules, including DNA (11), and bulky adducts are primarily repaired by NER (34, 35), While BJ and XPA cells generally responded in a similar manner to most of the HBQs, the cytotoxic effect was more pronounced in XPA compared to BJ cells for 12.5-50 μM DCMBQ, as well as 50 μM 2,5DBBQ and 2,6DBBQ (**Figures 4-1, 4-2, 4-4**). As seen in **Figure 4-1**, the IC_{50} values for 2,5DBBQ range between 51-68 μM for BJ cells and 42-55 μM for XPA cells. 2,5DBBQ IC_{50} values are consistently lower in XPA cells compared to BJ cells, and are significantly lower between 25-32 hours post-exposure. Unfortunately, the difficulty in fitting proper BJ IC_{50} 95% confidence intervals after 44 hours of exposure precludes statistical comparisons $\geq$45 hours. For DCMBQ (**Figure 4-4**), calculated IC_{50} values range

from 43-91 µM for BJ cells and 14-35 µM for XPA cells. The IC_{50} values for XPA cells exposed to DCMBQ are significantly lower than those for BJ cells throughout the majority of the exposure period (3-72 hours). This difference may indicate that these compounds have a genotoxic mechanism of action, and that the lesion(s) produced are repaired by the NER pathway. While the BJ/XPA *in vitro* assay cannot provide unequivocal evidence that these HBQs cause NER-mediated DNA damage, it would be prudent to perform further investigation of these compounds to determine any genotoxic potential.

Due to the different HBQs used in these experiments, the role of structure-dependent cytotoxicity may be explored. From the results described above, it is evident that the position, type, and number of substitutions affects the cytotoxicity and mutagenicity of HBQ compounds. For example, inclusion of 2,6DBBQ and 2,6DCBQ allows comparison of the effects of brominated and chlorinated substitutions at the same position. **Figures 4-2 and 4-3** illustrate that neither compound was profoundly cytotoxic to either BJ or XPA cells, with no cytotoxic effect observed in BJ cells with either compound. However, in XPA cells, some cytotoxicity was observed at 50 µM of 2,6DBBQ. It appears that bromine substitutions are slightly more toxic than chlorine substitutions at the 2,6 positions on the benzoquinone ring, although the differences between toxic responses are minor. A possible reason for this variation in toxicity is the difference in electronegativity for bromine (2.8) compared to chlorine (3.0), which could affect steric hindrance or stability of the molecule. Additional testing would be required to explore this hypothesis. The calculated log P_{OW} value for 2,6DBBQ is 2.03, greater than that of DCBQ at 1.768 (**Table 4-1**); indicating that 2,6DBBQ is more lipophilic and may more easily cross cell membranes via passive diffusion. Increased penetration of cell membranes may contribute to its increased cytotoxicity. The finding of greater toxicity of brominated HBQs compared to chlorinated HBQs is consistent with previous investigations of halogenated DBPs, which also found that halogen substitutions followed a general pattern of Cl << Br << I for increasing cytotoxicity and genotoxicity in CHO cells (36). More

121

extensive testing would be required before a general conclusion on the relative toxicities of brominated versus chlorinated HBQs could be reached.

Comparison of the isomers 2,5DBBQ and 2,6DBBQ indicates that the bromine substitution position on the benzoquinone ring also appears to affect toxicity. Cytotoxicity results for these compounds indicate that 2,5DBBQ caused a greater depression in CI than 2,6DBBQ, for both BJ and XPA cells, but only at the highest concentration (50 μM) (**Figures 4-1 & 4-2**). The reason for this effect is unknown, but likely relates to the different electron distribution of the molecules due to the differing positions of the bromine substitutions. The exact effect of this difference is unknown, but it may change susceptibility to detoxification/bioactivation, stability, or steric hindrance effects. It is unlikely that unequal penetration of cell membranes would play a role, as both compounds have the same calculated log P_{OW} (**Table 4-1**). Although this effect was only investigated with brominated HBQs, if the effect is related to steric hindrance or increased stability the same may hold true for isoforms of chlorinated HBQs as well. Additional testing with multiple isomers of both brominated and chlorinated compounds is advised.

For both cell lines, DCMBQ was much more cytotoxic than DCBQ, indicating the methyl group present in DCMBQ highly influences the observed toxicity (**Figures 4-3 & 4-4**). One possible explanation for the difference in toxicity could be differing log P_{OW} values for the two compounds.. As displayed in **Table 4-1**, the calculated log P_{OW} values for DCBQ and DCMBQ are 1.768 and 2.145, respectively, indicating that DCMBQ is more lipophilic than DCBQ and could penetrate cell membranes more easily. Another potential explanation involves the distribution of electrons within each chemical structure. Because chlorine is electronegative, the chlorine substitutions on the ring are electron-*withdrawing* groups that will pull electrons away from the centre ring structure. However, the methyl group found on DCMBQ is an electron-*donating* group which would cause electrons to flow toward the centre ring structure. This combination of electron withdrawing and donating groups appears to increase cytotoxicity,

122

though the exact mechanism by which it does so is unknown. Electron donating and withdrawing groups are known to affect the ability to reduce quinones to the less toxic hydroquinone form (10); it is possible that the combination of chlorine and methyl groups in DCMBQ confers greater stability, increased resistance to detoxification, or greater bioactivation. It is also possible that DCMBQ ring substituents cause steric hindrance effects which block the quinone-detoxifying enzyme DT-diaphorase. Increased $t_{1/2}$ for DT-diaphorase-mediated reduction (detoxification) of benzoquinone compounds with both electron-withdrawing and electron-donating substituents has been reported (37). While additional experimentation is required, it appears likely that the combination of increased lipophilicity and possibly increased stability or resistance to detoxification is responsible for the greater cytotoxicity of DCMBQ compared to DCBQ.

Little difference in cell index values was observed between DCBQ and TCBQ (**Figures 4-3 & 4-5**), suggesting that the addition of a third chlorine substitution did not appreciably affect cytotoxicity in either BJ or XPA cells. This is somewhat puzzling, as the predicted log P_{OW} values for the compounds are 1.768 for DCBQ and 2.374 for TCBQ. Thus, it would be expected that TCBQ would more easily cross the plasma membrane of cells, and could potentially have comparatively greater opportunity to interact with cell macromolecules. It is possible that the presence of the additional chlorine group adds greater steric hindrance, preventing interaction with cell macromolecules, or somehow contributes to increased detoxification or reduced bioactivation. One way to further investigate the effect of multiple chlorine substitutions would be to examine a tetra-chlorobenzoquinone compound (2,3,5,6-trichloro-1,4-benzoquinone; chloranil) in the same assay; this could provide further information on how the number and position of substitutions affects cytotoxicity. Because no tri-bromobenzoquinone substances were examined in these experiments, it is uncertain whether the observations of di- and tri-chlorobenzoquinone cytotoxicity are generalizable to bromobenzoquinone substances as well. Addition of a tri-bromobenzoquinone in this assay would be useful in further cytotoxicity

experiments to further understand the mechanism of HBQ toxicity. However, it is unknown if such substances are actually present in drinking water.

Useful comparisons may be made between these results and those from previous HBQs toxicity studies. However, these other studies have used different test organisms, experimental design, exposure periods, and methods to assess toxicity. Therefore, an assessment of the general trends of each study is likely to be more useful than a direct comparison of the results. A previous study found the binding affinity of HBQs to oligodeoxynucleotides (ODNs) was TCBQ ≈ DCMBQ < DCBQ << 2,6DBBQ. Binding affinity for ODNs was suggested to correlate with the potential toxicity of these HBQs (26). The BJ/XPA *in vitro* assay identified DCMBQ as the most cytotoxic and likely genotoxic HBQ due to its differential toxicity in BJ and XPA cells. However, DCMBQ showed relatively low binding affinity in the HBQ-ODN assay (26). This difference may be explained by the different experimental designs of the two studies. In the HBQ-ODN study, the compounds were exposed directly to naked DNA, without the presence of other cellular components. In the BJ/XPA *in vitro* assay, the HBQ compounds must cross the cell membrane to access the DNA and cause genotoxicity. The HBQs would also be subject to metabolism and could interact with other cell macromolecules in intact BJ and XPA cells; none of these components are present in the HBQ-ODN system, but could contribute significantly to both cytotoxicity and genotoxicity. Based on previous research on these and similar compounds (see **Section 4.1**), HBQs are likely capable of causing toxicity through both genotoxic and non-genotoxic mechanisms. Therefore, binding to ODNs may not accurately represent all potential mechanisms of toxicity. While the interaction of HBQs and ODNs may be useful for identifying the mechanism and strength of HBQ-DNA adduct formation, the BJ/XPA *in vitro* assay may be more useful for determining the biological significance of HBQ exposure because it represents a more biologically relevant system.

Our research group recently examined *in vitro* cytotoxicity and genotoxicity of HBQs in the T24 bladder cancer cell line (27). The cytotoxicity ranking of HBQs

124

in that work was TCBQ < 2,6DBBQ < DCMBQ < DCBQ (2,5DBBQ was not tested), which was determined by the MTS cell viability assay after 24 hours of exposure. These results confirm my assessment that TCBQ is the least cytotoxic of the tested HBQs. While DCBQ was the most potent cytotoxic HBQ in T24 cells, it did not produce cytotoxicity in either BJ or XPA cells at the concentration range used in these experiments. Although both studies found DCMBQ to be cytotoxic, the calculated IC_{50} values for DCMBQ in these experiments are dissimilar. For T24 cells, the 24 hour IC_{50} value is 110.1 µM (95% confidence interval: 106.5−113.8 µM) (27). In BJ cells, the corresponding 24 hour DCMBQ IC_{50} value is 47.5 µM (95% confidence interval: 40.8-55.3 µM), and for XPA cells it is 17.8 µM (95% confidence interval: 13.0-24.3 µM). This variation is likely due to the different cell function parameters measured by the cytotoxicity assays in each experiment (mitochondrial dehydrogenase function for MTS, and electrical impedance via cell-electrode contact for RTCA). Because the cell lines come from different individuals and tissues, some inherent variation in response is expected. Each cell line will have unique characteristics, such as metabolic capacity and metabolic enzyme profiles. Because DCMBQ may cause NER-mediated DNA damage, it may be particularly cytotoxic to XPA cells, which lack the capacity to repair these lesions. This finding illustrates the benefit of using DNA repair-proficient and −deficient cell lines in cytotoxicity testing, as it may provide clues to the mechanism of toxicity. While the two datasets are not identical in their assessment of HBQ toxicity, the characteristics of the cell lines used and the method of measuring cytotoxicity likely account for much of this variation.

Based on the results of the Ames test (**Table 4-2**), all tested HBQs appear to be mutagenic under specific conditions. Statistically significant elevations in mutation were only observed in the TA100 group, indicating that the HBQs primarily produce substitution mutations as opposed to frameshift mutations (TA98) or mutations which occur at AT sites (*E. coli* WP2 uvrA). This finding is consistent with previous research, which showed that non-halogenated p-benzoquinone produced single-base substitution mutations in mammalian cell

lines, as measured by the *supF* forward mutation assay (38). Cytotoxicity was observed in all *E. coli* WP2 uvrA groups exposed to HBQs without S9, but no significant cytotoxicity or mutagenicity was observed under the same conditions when S9 was present. This suggests that enzymes present in the S9 fraction may have detoxified the HBQs. Cytotoxicity was also observed in TA98 cells exposed to 2,6DBBQ, but this effect was negated by addition of S9. All HBQs tested in this experiment were capable of producing significant mutations in TA100 cells in at least two consecutive concentrations, either with or without S9; for 2,5DBBQ, DCBQ, and DCMBQ, significant mutations were seen both with and without S9. The addition of S9 in TA100 experiments appeared to have a slight detoxifying effect for most HBQs, increasing the concentration required for a mutagenic effect (2,5DBBQ, DCBQ, DCMBQ) or eliminating the mutagenic effect altogether (2,6DBBQ). However, for TA100 exposed to TCBQ, addition of S9 fraction appeared to bioactivate the compound, leading to a mutagenic effect. Because there are no standardized methods for determining a significant result in the Ames test (39), interpretation of results can be challenging. However, we feel that by combining a standard statistical test with the more traditional two-fold increase criteria (29), and requiring that an increase in revertants be observed in two consecutive test concentrations, we can reduce the possibility that the observed effects are due solely to chance.

An interesting comparison between previous QSTR predictions (2) and these findings is the apparent presence of a mutagenic effect of these HBQs when none was predicted to exist. Each HBQ subjected to the Ames test was able to produce statistically significant substitution mutations either with, without, or both with and without the presence of S9 fraction (**Table 4-2**). This discrepancy may reflect the difficulty of predicting toxicity with QSTR models when limited toxicological data are available for similar compounds in the resource databases. The QSTR predictions also indicated that DCMBQ and TCBQ were potential carcinogens (1, 2). The BJ/XPA *in vitro* assay is unable to test carcinogenicity of substances, so no direct assessment of the prediction of DMCBQ and TCBQ carcinogenicity can be made. However, both DCMBQ and TCBQ were shown to be mutagenic in the

Ames test, and DCMBQ also showed differing cytotoxicity in BJ and XPA cells in RTCA assays, leading to the possibility that DCMBQ produces a NER-mediated genotoxic lesion. TCBQ showed little cytotoxicity in either cell type, but this does not preclude a genotoxic mechanism of action; the BJ/XPA *in vitro* assay only examines NER-mediated genotoxicity, and other mechanisms of DNA damage are possible. These observations indicate that DCMBQ and TCBQ could possibly be carcinogenic, but as non-genotoxic carcinogens exist, and mutagenicity or genotoxicity does not necessarily mean a compound is carcinogenic, further assays specific to carcinogenesis are required to test these predictions.

Direct comparison between the LOAELs predicted by QSTR (1, 2) and data obtained via *in vitro* methods is not possible because these data represent different endpoints. The QSTR prediction is based on a database of *in vivo* studies of similar compounds in rodents, is reported as a predicted chronic LOAEL of mg/kg/day, and includes a variety of endpoints, including carcinogenicity (1, 2), while the BJ/XPA *in vitro* assay data described here is based on cytotoxicity experiments with human cell lines, with an exposure time of ~72 hours and toxicant concentrations measured in the micromolar range. However, some overall comparisons may be made. In general, the QSTR data (1, 2) and the current experiment set agree that DCMBQ is a potentially potent toxicant. Even though DCMBQ did not have the lowest predicted LOAEL in the QSTR testing, it was identified as the most likely bladder carcinogen in the tested set. DCMBQ was the most potent cytotoxic and mutagenic HBQ in the BJ/XPA *in vitro* and Ames test assays, respectively. While it is very important to remember that cytotoxicity, genotoxicity, and mutagenicity do not necessarily imply carcinogenicity, our results appear to agree that DCMBQ has the greatest overall toxicological potential out of our tested set of HBQs. Considering the results of these assays, previously published toxicity data (27), and the QSTR predictions (1, 2), we echo the call for urgent toxicity testing and risk assessment of HBQ DBPs, particularly DCMBQ, due to their apparent cytotoxic, genotoxic, and mutagenic potential.

In conclusion, based on the BJ/XPA *in vitro* assay results, the cytotoxicity ranking of the tested HBQs is: TCBQ ≈ 2,6DBBQ ≈ DCBQ < 2,5DBBQ < DCMBQ for BJ cells and TCBQ ≈ DCBQ < 2,6DBBQ < 2,5DBBQ < DCMBQ for XPA cells. XPA cells demonstrated significantly greater cytotoxicity than BJ cells when exposed to DCMBQ and 2,5DBBQ. IC_{50} values ranged from between 51-68 µM for BJ cells and 42-55 µM for XPA cells for 2,5DBBQ and between 43-91 µM for BJ cells and 14-35 µM for XPA cells for DCMBQ. Due to the nature of the BJ/XPA pairing, this may indicate that DCMBQ and 2,5DBBQ act at least in part by a NER-mediated genotoxic mechanism. Ames bacterial mutagenicity testing revealed that all HBQs were capable of producing significantly elevated substitution mutations under at least some of the assay conditions. The addition of S9 fraction generally appeared to have a weakly detoxifying effect in the Ames test but caused the bioactivation of TCBQ. While previous QSTR calculations did not predict the mutagenicity of these HBQs, these data are in agreement that DCMBQ is a potentially potent toxicant. Due to its cytotoxic, mutagenic, and potential genotoxic and carcinogenic effects, DCMBQ in particular urgently requires further *in vitro* and *in vivo* toxicity assessment.

4.5   References

1. Bull RJ, Awwa Research Foundation, United States. Environmental Protection Agency. Use of toxicological and chemical models to prioritize DBP research. Denver, CO: Awwa Research Foundation; 2006.

2. Bull RJ, Reckhow DA, Li X, Humpage AR, Joll C, Hrudey SE. Potential carcinogenic hazards of non-regulated disinfection by-products: Haloquinones, halo-cyclopentene and cyclohexene derivatives, N-halamines, halonitriles, and heterocyclic amines. Toxicology. 2011 Aug 15;286(1-3):1-19.

3. Villanueva CM, Cantor KP, Cordier S, Jaakkola JJ, King WD, Lynch CF, et al. Disinfection byproducts and bladder cancer: A pooled analysis. Epidemiology. 2004 May;15(3):357-67.

4. Villanueva CM, Cantor KP, King WD, Jaakkola JJ, Cordier S, Lynch CF, et al. Total and specific fluid consumption as determinants of bladder cancer risk. Int J Cancer. 2006 Apr 15;118(8):2040-7.

5. Villanueva CM, Cantor KP, Grimalt JO, Malats N, Silverman D, Tardon A, et al. Bladder cancer and exposure to water disinfection by-products through ingestion, bathing, showering, and swimming in pools. Am J Epidemiol. 2007 Jan 15;165(2):148-56.

6. IARC Working Group on the Evaluation of Carcinogenic Risks to Humans. Some drinking-water disinfectants and contaminants, including arsenic. Lyon, France: International Agency for Research on Cancer Press (IARCPress); 2004.

7. Zhao Y, Qin F, Boyd JM, Anichina J, Li XF. Characterization and determination of chloro- and bromo-benzoquinones as new chlorination disinfection byproducts in drinking water. Anal Chem. 2010 Jun 1;82(11):4599-605.

8. Casarett LJ, Doull J, Klaassen CD. Casarett and Doull's toxicology: The basic science of poisons. 6th ed. New York: McGraw-Hill Medical Pub. Division; 2001.

9. O'Brien PJ. Molecular mechanisms of quinone cytotoxicity. Chem Biol Interact. 1991;80(1):1-41.

10. Monks TJ, Hanzlik RP, Cohen GM, Ross D, Graham DG. Quinone chemistry and toxicity. Toxicol Appl Pharmacol. 1992 Jan;112(1):2-16.

11. Bolton JL, Trush MA, Penning TM, Dryhurst G, Monks TJ. Role of quinones in toxicology. Chem Res Toxicol. 2000 Mar;13(3):135-60.

12. Monks TJ, Jones DC. The metabolism and toxicity of quinones, quinonimines, quinone methides, and quinone-thioethers. Curr Drug Metab. 2002 Aug;3(4):425-38.

13. Siraki AG, Chan TS, O'Brien PJ. Application of quantitative structure-toxicity relationships for the comparison of the cytotoxicity of 14 p-benzoquinone congeners in primary cultured rat hepatocytes versus PC12 cells. Toxicol Sci. 2004 Sep;81(1):148-59.

14. Kim SR, Lee JY, Lee MY, Chung SM, Bae ON, Chung JH. Association of quinone-induced platelet anti-aggregation with cytotoxicity. Toxicol Sci. 2001 Jul;62(1):176-82.

15. Fruetel JA, Sparks SE, Quistad GB, Casida JE. Adducts of dienochlor miticide with glutathione, glutathione S-transferases, and hemoglobins. Chem Res Toxicol. 1994 Jul-Aug;7(4):487-94.

16. Lundberg P, Renberg L, Arrhenius E, Sundstrom G. Detoxication disturbances and uncoupling effects in vitro of some chlorinated guaiacols, catechols and benzoquinones. Chem Biol Interact. 1980 Nov;32(3):281-90.

17. Pritsos CA, Pointon M, Pardini RS. Interaction of chlorinated phenolics and quinones with the mitochondrial respiration: A comparison of the o- and p-chlorinated quinones and hydroquinones. Bull Environ Contam Toxicol. 1987 May;38(5):847-55.

18. Lin PH, Waidyanatha S, Pollack GM, Swenberg JA, Rappaport SM. Dose-specific production of chlorinated quinone and semiquinone adducts in rodent livers following administration of pentachlorophenol. Toxicol Sci. 1999 Jan;47(1):126-33.

19. den Besten C, Brouwer A, Rietjens IM, van Bladeren PJ. Biotransformation and toxicity of halogenated benzenes. Hum Exp Toxicol. 1994 Dec;13(12):866-75.

20. Lau SS, Hill BA, Highet RJ, Monks TJ. Sequential oxidation and glutathione addition to 1,4-benzoquinone: Correlation of toxicity with increased glutathione substitution. Mol Pharmacol. 1988 Dec;34(6):829-36.

21. Mertens JJ, Temmink JH, van Bladeren PJ, Jones TW, Lo HH, Lau SS, et al. Inhibition of gamma-glutamyl transpeptidase potentiates the nephrotoxicity of glutathione-conjugated chlorohydroquinones. Toxicol Appl Pharmacol. 1991 Aug;110(1):45-60.

22. Qin H, Huang CH, Mao L, Xia HY, Kalyanaraman B, Shao J, et al. Molecular mechanism of metal-independent decomposition of lipid hydroperoxide 13-HPODE by halogenated quinoid carcinogens. Free Radic Biol Med. 2013 Oct;63:459-66.

23. Dahlhaus M, Almstadt E, Henschke P, Luttgert S, Appel KE. Oxidative DNA lesions in V79 cells mediated by pentachlorophenol metabolites. Arch Toxicol. 1996;70(7):457-60.

24. Vaidyanathan VG, Villalta PW, Sturla SJ. Nucleobase-dependent reactivity of a quinone metabolite of pentachlorophenol. Chem Res Toxicol. 2007 Jun;20(6):913-9.

25. Jia S, Zhu BZ, Guo LH. Detection and mechanistic investigation of halogenated benzoquinone induced DNA damage by photoelectrochemical DNA sensor. Anal Bioanal Chem. 2010 Jul;397(6):2395-400.

26. Anichina J, Zhao Y, Hrudey SE, Le XC, Li XF. Electrospray ionization mass spectrometry characterization of interactions of newly identified water disinfection byproducts halobenzoquinones with oligodeoxynucleotides. Environ Sci Technol. 2010 Nov 11.

27. Du H, Li J, Moe B, McGuigan CF, Shen S, Li XF. Cytotoxicity and oxidative damage induced by halobenzoquinones to T24 bladder cancer cells. Environ Sci Technol. 2013 Mar 19;47(6):2823-30.

28. Xing JZ, Zhu L, Jackson JA, Gabos S, Sun XJ, Wang XB, et al. Dynamic monitoring of cytotoxicity on microelectronic sensors. Chem Res Toxicol. 2005 Feb;18(2):154-61.

29. Ames BN, Mccann J, Yamasaki E. Methods for detecting carcinogens and mutagens with the *Salmonella*/mammalian-microsome mutagenicity test. Mutat Res. 1975 Dec;31(6):347-64.

30. Hubbard SA, Green MHL, Gatehouse D, Bridges JW. The fluctuation test in bacteria. In: Kilbey BJ, Legator M, Nichols W, Ramel C, editors. Handbook of Mutagenicity Test Procedures. Amsterdam ; New York: Elsevier Science Publishers BV; 1984. p. 141.

31. Maron DM, Ames BN. Revised methods for the *Salmonella* mutagenicity test. In: Kilbey BJ, Legator M, Nichols W, Ramel C, editors. Handbook of

Mutagenicity Test Procedures. Amsterdam ; New York: Elsevier Science Publishers BV; 1984. p. 93.

32. Mortelmans K, Zeiger E. The Ames *Salmonella*/microsome mutagenicity assay. Mutat Res. 2000 Nov 20;455(1-2):29-60.

33. Mortelmans K, Riccio ES. The bacterial tryptophan reverse mutation assay with *Escherichia coli* WP2. Mutat Res. 2000 Nov 20;455(1-2):61-9.

34. Friedberg EC, Walker GC, Siede W. DNA repair and mutagenesis. Washington, D.C.: ASM Press; 1995.

35. Nouspikel T. DNA repair in mammalian cells : Nucleotide excision repair: Variations on versatility. Cell Mol Life Sci. 2009 Mar;66(6):994-1009.

36. Plewa MJ, Wagner ED, Muellner MG, Hsu KM, Richardson SD. Chapter 3: Comparative mammalian cell toxicity of N-DBPs and C-DBPs. In: Karanfil T, Krasner SW, Westerhoff P, Xie YF, editors. Disinfection by-products in drinking water: occurrence, formation, health effects, and control. Washington, DC; New York: American Chemical Society; 2008. p. 36-50.

37. Fourie J, Oleschuk CJ, Guziec F,Jr, Guziec L, Fiterman DJ, Monterrosa C, et al. The effect of functional groups on reduction and activation of quinone bioreductive agents by DT-diaphorase. Cancer Chemother Pharmacol. 2002 Feb;49(2):101-10.

38. Gaskell M, McLuckie KI, Farmer PB. Comparison of the repair of DNA damage induced by the benzene metabolites hydroquinone and p-benzoquinone: A role for hydroquinone in benzene genotoxicity. Carcinogenesis. 2005 Mar;26(3):673-80.

39. Kim BS, Margolin BH. Statistical methods for the Ames *Salmonella* assay: A review. Mutat Res. 1999 Jan;436(1):113-22.

Chapter 5: Mechanisms of DCMBQ toxicity

5.1   Introduction

Halobenzoquinone (HBQ) disinfection byproducts (DBPs) are an emerging concern due to their predicted low LOAELs and possible carcinogenicity. Previous quantitative structure toxicity relationship analysis identified 2,6-dichloro-3-methyl-1,4-benzoquinone (DCMBQ) as a HBQ of particular concern (1, 2). In the previous chapter, I demonstrated empirically that DCMBQ is cytotoxic and likely genotoxic in human cells, and is mutagenic in the Ames test. Therefore, I decided to further examine the toxic properties of DCMBQ in order to understand its toxic mechanism(s) of action.

In Chapter 4, RTCA experiments showed that DCMBQ was more cytotoxic to XPA cells than BJ cells (see **Figure 4-4**). Based on the model development detailed in **Chapter 3**, this finding may indicate that DCMBQ causes toxicity, at least in part, by creating a nucleotide excision repair (NER)-mediated DNA lesion. Formation of bulky adducts with cellular macromolecules, including DNA, is a potential mechanism of action of the quinone class (3). As bulky adducts are primarily repaired by the NER pathway, and XPA cells are not capable of performing NER (4, 5), the greater cytotoxicity observed in XPA cells compared to the normal, NER-proficient BJ cells may indicate that DCMBQ could form bulky DNA adducts *in vitro*. However, the quinone class is also well-known for producing reactive oxygen species (ROS) as a toxic mechanism of action (3). A proposed biotransformation pathway for DCMBQ, based on known biotransformation pathways of other quinones (3, 6) may be found in **Figure 5-1**; however, additional metabolic pathways, including Phase II metabolism, are also possible. A series of *in vitro* experiments examining cytotoxicity, ROS production, and genotoxicity were performed to determine which toxic mechanisms of action are active in DCMBQ toxicity, and their relative contributions to the overall toxic effect.
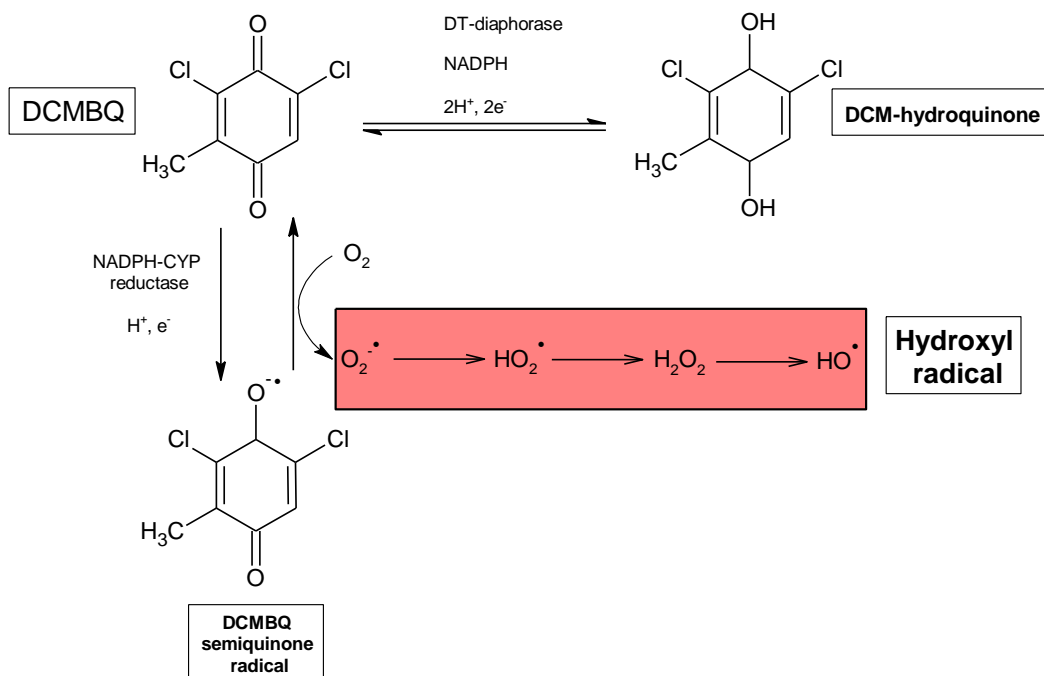
Figure 5-1: Proposed Phase I partial biotransformation pathway of DCMBQ

Two primary proposed partial biotransformation pathways for DCMBQ (based on known quinone biotransformation pathways (6)) are shown above. In the first pathway (shown horizontally), DCMBQ is reduced to its hydroquinone form in a two-electron reduction by DT-diaphorase, also known as NAD(P)H-quinone oxidoreductase, which is present in the cytosol. Hydroquinones are generally considered to be less toxic than other potential biotransformation products, but the hydroquinone product may auto-oxidize back to the parent quinone, leading to depletion of NADPH after repeated cycling (3). The second pathway (shown vertically) involves a single-electron reduction by NADPH-cytochrome P450 reductase to form an unstable semiquinone radical. Like the hydroquinone metabolite, this radical may auto-oxidize back to the parent quinone form, depleting NADPH and oxygen. Reactive oxygen species (highlighted in red above) are produced when molecular oxygen reacts with the semiquinone radical. The ultimate reactive oxygen species produced is likely the hydroxyl radical (HO$^{\bullet}$), which may then react with other cellular macromolecules, including lipids, proteins, and DNA. It is also possible that the semiquinone radical itself may form bulky adducts with cellular macromolecules (3). Note that this pathway does not

include Phase II metabolism, which may include processes such as glutathione conjugation (7).

Figure was generated using ACD/ChemSketch Freeware version 12.01 (Advanced Chemistry Development, Inc.).

Using the BJ/XPA *in vitro* RTCA assay described in **Chapter 3**, I have expanded the analysis of DCMBQ to further understand the mechanism of cytotoxicity. N-acetylcysteine, a reactive oxygen species scavenger, was added concomitantly to wells treated with concentrations of DCMBQ shown to be cytotoxic in **Figure 4-4**. By comparing the cell index responses of the treatment groups, the contribution of ROS to the cytotoxic response observed in **Chapter 4** can be determined. Next, the 2',7' –dichlorofluorescein diacetate (DCFDA) assay was used to examine the magnitude of ROS production via the formation of a fluorescent product. Because the DCFDA assay allows multiple measurements of each plate over time, these experiments allowed the determination of ROS production between cell types, over exposure time, and over increasing concentrations of DCMBQ.

To determine the genotoxic potential of DCMBQ, I performed the alkaline comet assay (single cell gel electrophoresis), which measures fragmentation of DNA, on BJ and XPA cells treated with appropriate concentrations of DCMBQ. This analysis was performed to confirm the recent discovery of the oxidative lesion 8OHdG in DCMBQ-treated T24 bladder cancer cells (8). As in **Chapter 2, Figure 2-8**, RTCA cytotoxicity data for BJ and XPA cells (**Chapter 4, Figure 4-4**) were used to determine appropriate concentrations for the comet assay. The comet assay requires ≥80% cell viability to prevent artifacts from excessive DNA fragmentation related to cell death (9, 10).

Initially, DCMBQ was tested in both cell lines for a 24 hour exposure without recovery to determine its genotoxic potential. Next, N-acetylcysteine (NAC), a

known ROS scavenger, was added concomitantly with the DCMBQ to determine if the presence of reactive oxygen species contributed to genotoxicity. The effect of adding a post-exposure 24-hour DCMBQ-free recovery period on tail moment values was also examined. DCMBQ exposure times of 4 hours, with or without a 24-hour recovery period, were used to compare the ability of BJ and XPA cells to handle the DCMBQ genotoxic insult in a shorter exposure period. To determine if residual DCMBQ was causing genotoxicity during the exposure period, cells were treated with DCMBQ for 4 hours and allowed to recover for 24 hours in DCMBQ-free culture medium, supplemented with NAC to scavenge residual ROS. Finally, to determine the ability of BJ and XPA cells to repair oxidative DNA damage, both cell lines were exposed to 0.003% v/v H_2O_2 with and without a 24-hour recovery period.

The goal of combining these approaches is to obtain more information on the mechanisms of DCMBQ toxicity, particularly the role of ROS production in both cyto- and genotoxicity, as well as the genotoxic mechanism of DCMBQ. These data will complement the RTCA and Ames test investigations I performed in **Chapter 4**, and can also be compared to the QSTR predictions of DCMBQ toxicity in the literature (1, 2). The experimental approach used here could be extended to other HBQ DBPs (such as the others described in **Chapter 4**), in order to explore their mechanisms of toxicity. However, as DCMBQ was determined to be the most toxic HBQ of the DBPs explored in **Chapter 4**, only DCMBQ will be investigated at this time.

5.2   Materials and Methods

5.2.1 Cell lines and culture conditions

The BJ cell line was obtained from ATCC (#CRL-2522), and the XPA cell line (NIGMS: GM04312C) was kindly provided by Dr. Michael Weinfeld at the University of Alberta. Cell lines were maintained in a humidified 37°C incubator, with 5% CO_2, in Eagle's Minimum Essential Medium (ATCC; #30-2003) supplemented with 10% fetal bovine serum (Sigma; #F1051) and 1% of 10000 U

penicillin/10000 µg streptomycin solution (Gibco; #15140-122). Cells were subcultured when confluence was 80-95%, and culture medium was refreshed at least twice per week. Cell line passage numbers were restricted (≤15 passages per individual set of cell cultures) to minimize effects of genetic drift. All manipulations of cell cultures were performed in a biosafety cabinet (Thermo Scientific Forma Class 2 A2; #1284) under aseptic conditions. Manipulation of cell lines was performed in compliance with the University of Alberta "Working with Biohazardous Materials" policy and laboratory personnel received both institutional and site-specific biosafety training.

5.2.2 Reagents and toxicant solutions

DCMBQ (≥98% purity) was obtained from Shanghai Acana Pharmtech Company (see **Table 4-1** for details). A stock solution was made by dissolving the solid DCMBQ in 100% methanol. Stock solutions were stored in a -20°C freezer, protected from light. A methanol-spiked sample of culture medium, equivalent to the volume of the most concentrated DCMBQ solution, was used as a solvent control treatment. N-acetylcysteine (#A9165, ≥99% purity) was obtained from Sigma-Aldrich and dissolved in deionized water, then pH-adjusted to ~7.4. The resulting neutral stock solution was sterile-filtered through a 0.2 µM nylon syringe filter (Fisherbrand; #09-719C), and stored in a -20°C freezer, protected from light. On the day of the experiment, the stock solutions of DCMBQ and NAC were removed from the freezer and were diluted to appropriate concentrations in culture medium (or phenol red-free medium, as described in the DCFDA ROS assay section).

5.2.3 RTCA cytotoxicity assay

BJ and XPA cells were harvested using a 0.05% trypsin-0.53 mM EDTA solution (Gibco; #25300-05) and plated into 16-well RTCA E-plates at a density of 4000 and 5000 cells per well, respectively. Both cell lines were used in each replicate,

138

with half of the available wells plated with each cell type. Using built-in RTCA software (ACEA RT-CES SP v5.3, ACEA Biosciences), diagnostic assays were performed on all plates prior to use; if any well failed quality control tests, the results from that well were discarded. If multiple bad wells were found on a plate, the plate was discarded. The RTCA system was programmed to collect cell index (CI) measurements every hour. Cells were allowed to equilibrate in the E-plates without treatment until reaching a CI value of ~1, corresponding to ~40-50% confluence (11), within 36-48 hours post-plating. Any wells showing abnormal cell growth were not used for treatment or control groups. Plates were then removed from the incubator, and culture medium was removed. Each well was treated with a 200 µL aliquot of DCMBQ solution, DCMBQ + NAC solution, methanol control solution, or culture medium (negative control group). The treatment layout was randomized for each replicate to avoid layout-related technical artifacts. After treatment, plates were returned to the RTCA unit in the incubator and monitored hourly until a growth plateau had been reached, usually ~72 hours post-treatment. All cell index values were "normalized" to a value of 1 at the time of treatment by the RTCA software in order to accurately compare relative differences in signal between the wells after treatment.

5.2.4 DCFDA ROS assay

This assay was performed using the DCFDA - Cellular Reactive Oxygen Species Detection Assay Kit from Abcam (#ab113851). BJ and XPA cells were suspended in Minimum Essential Medium without phenol red (Gibco, # 51200038), supplemented with 2mM L-glutamine (Gibco, # 25030149), 10% fetal bovine serum (Sigma; #F1051), and 1% of 10000 U penicillin/10000 µg streptomycin solution (Gibco; #15140-122). Phenol red-free medium was used to prevent interference with the fluorescent signal produced by DCFDA. Cells were plated in black-bottomed 96-well plates (Nunc, #137101) at a density of 25,000 cells/well and allowed to attach overnight. The next day, cells were washed with a 100 µL aliquot of DPBS (Gibco, #14190), and treated for 45 minutes at 37°C with 100 µL/well of DCFDA mix, prepared as directed. The plate was then gently washed

with 200 µL/well of the provided buffer solution, and 200 µL aliquots of DCMBQ +/- NAC (5-50 µM DCMBQ, 5 mM NAC), prepared in phenol red-free culture medium as described above, were added to the wells. Positive control wells were treated with 50 µM tert-butyl hydroperoxide (TBHP), negative control wells were treated with culture medium only, and solvent control wells were treated with a volume of methanol equal to that of the most concentrated treatment group. Plates were returned to the incubator and removed for analysis at 2, 4, 6, 24, 48, and 72 hours post-treatment. Plates were read in a multiwell plate fluorometer (Beckman Coulter, DTX 880) with an excitation wavelength of 485 nm and an emission wavelength of 535 nm. Blank wells, which included DCFDA but no cells, were included to determine non-specific binding of DCFDA to the plate; these values were subtracted from all treatment and control groups.

5.2.5 Alkaline comet assay

The alkaline comet assay was performed as previously described (12), using a CometAssay® kit (Trevigen, # 4250-050-K). Briefly, BJ and XPA cells were treated with compounds of interest (DCMBQ: 5-40 µM, NAC: 2 mM, H_2O_2: 0.003% v/v) and allowed to incubate for the desired exposure time. If a recovery period was used, the treatment solution was removed at the desired exposure time, plates were gently washed twice with DPBS, fresh culture medium was added, and the plates were returned to the incubator for the designated recovery period. Control groups included a negative control (culture medium only), solvent control (methanol volume equal to most concentrated treatment group), NAC control (2mM NAC only), and positive DNA damage control (cells exposed to 0.003% v/v hydrogen peroxide in culture medium for 20 minutes at 4°C). For the H_2O_2 recovery experiments, cells were exposed to 0.003% v/v H_2O_2 in culture medium for 20 minutes at 4°C, then washed twice with DPBS and returned to the 37°C incubator for 24 hours. In all other instances, the positive control group did not receive a recovery period, but was treated with 0.003% H_2O_2 at 4°C 20 minutes before analysis.

After treatment and optional recovery, BJ and XPA cells were harvested using a 0.05% trypsin-0.53 mM EDTA solution (Gibco; #25300-05) and suspended in ice-cold DPBS (Gibco, #14190) at a concentration of ~1 x 10^5 cells/mL. A 1:10 dilution of cell suspension was made in molten 37°C LMAgarose, and cells were spread on provided CometSlides™. Slides were incubated at 4°C for 30 minutes, immersed in the provided Lysis Solution for 45 minutes at room temperature, then incubated in a 200 mM NaOH + 1 mM EDTA solution for 40 minutes at room temperature. Electrophoresis was performed at 4°C with an opaque 20-slide comet assay horizontal electrophoresis tank (Scie-Plas, #QCOMET20), using a 200 mM NaOH + 1 mM EDTA electrophoresis solution. Slides were exposed to a constant voltage of 22V, with adjustment of solution level to produce current of ~300 mA, for 30 minutes. After electrophoresis, slides were immersed in deionized water for two 5 minute periods, then in 70% ethanol for 5 minutes. Slides were allowed to dry flat overnight, and were stored in a dry, dark environment until imaging, no longer than two weeks.

For imaging, cells were treated with 1x SYBR Green I (Life Technologies, #S-7563) in Tris-EDTA buffer (pH 7.5) and incubated at 4°C for 5 minutes. Excess SYBR Green I was removed and the slides were allowed to air-dry, protected from light. Imaging was performed on an inverted fluorescence microscope with a fluorescein filter (Axiovert 200M, Zeiss) and MetaMorph® software (MDS Analytical Technologies). 50 randomly selected comets from each treatment group were scored for tail moment values with CometScore™ software (Tri-Tek).

5.2.6 Data analysis

Statistical analyses were performed with Prism® software (GraphPad Software) and Microsoft Excel (Microsoft Corporation). Results from all experiments were exported into Microsoft Excel, organized, and imported into Prism. At least three replicates were performed for each experiment; mean values from these combined replicates were used for data analysis. A two-way ANOVA was used to analyze the effects of exposure time and DCMBQ concentration on both cell lines in the

DCFDA ROS assay, with values for all treatment groups compared to the methanol control group at that time period. Data for comet assay experiments were analyzed via one-way ANOVA with Dunnett's post-hoc analysis, using the methanol-treated group as the control group. Tukey's multiple comparisons test was used to compare treatment group values to one another (e.g. DCMBQ treatment with or without concomitant NAC addition). In all analyses, results were considered statistically significant if $p<0.05$. While all RTCA experiments were conducted with a negative control (consisting only of culture medium), these results were virtually identical to those of the solvent group; therefore, only the solvent control data are shown.

5.3   Results

5.3.1 RTCA cytotoxicity assay

As seen in **Figure 5-2**, profound decreases in cell index (CI) (indicative of cytotoxicity) were observed in both BJ and XPA cells exposed to high concentrations of DCMBQ, but concomitant addition of 2mM NAC resulted in CI values closer to, or in some cases exceeding, the solvent control group CI values. The addition of 2 mM NAC caused a small depression in CI values for both cell types, but a clear increase in CI values was observed when comparing the DCMBQ-treated groups to those treated with DCMBQ+NAC.

A)

B)
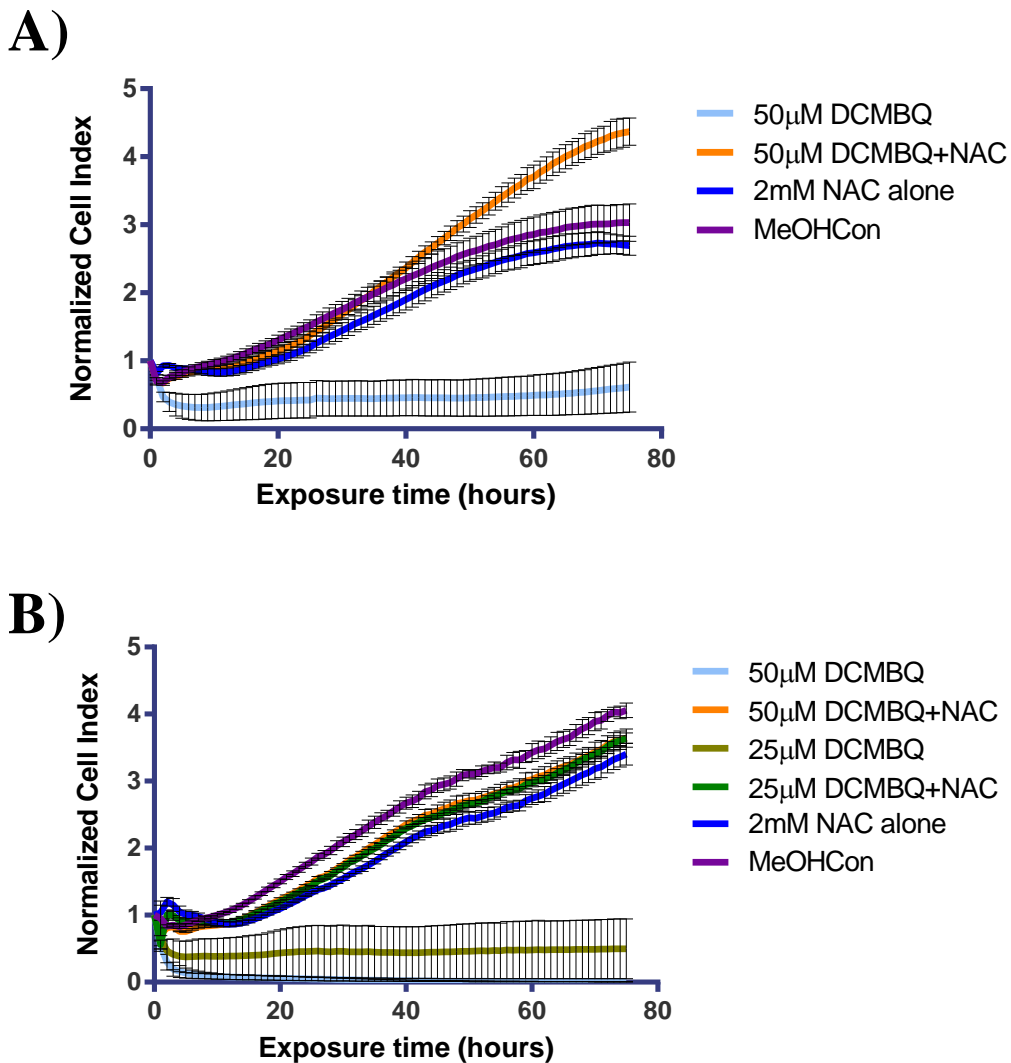
Figure 5-2: Effect of N-acetylcysteine addition on BJ and XPA cells exposed to DCMBQ, measured by RTCA

RTCA data were obtained from BJ (**A**) and XPA (**B**) cells exposed to DCMBQ, with and without concomitant addition of N-acetylcysteine (NAC). A solvent control group was treated only with methanol (MeOHCon) at the highest concentration used in the treatment groups. Data shown are an average of three independent experiments with error bars representing the standard error of the mean (SEM).

5.3.2 DCFDA ROS assay

A clear time- and concentration- dependent increase in fluorescence, indicative of ROS formation, is visible in both BJ and XPA cells exposed to DCMBQ (**Figure 5-3**). A significant, but not complete, reduction in fluorescent signal in both BJ and XPA cells exposed to 50 µM DCMBQ + 5 mM NAC was observed, compared to cells exposed to 50 µM DCMBQ alone. While the positive control substance TBHP increased fluorescence in exposed cells, this effect was minor compared to the fluorescence observed in the DCMBQ-treated groups (data not shown). A slight increase in solvent and negative control group fluorescence was observed over time. The magnitude of fluorescent signal for BJ and XPA cells was approximately equal overall. After analysis with two-way ANOVA (examining for effects of DCMBQ concentration and exposure time), ROS production was shown to increase proportionately with exposure time and DCMBQ concentration, with significantly elevated ROS production observed starting at 4h exposure (**Table 5-1**).

A)

B)
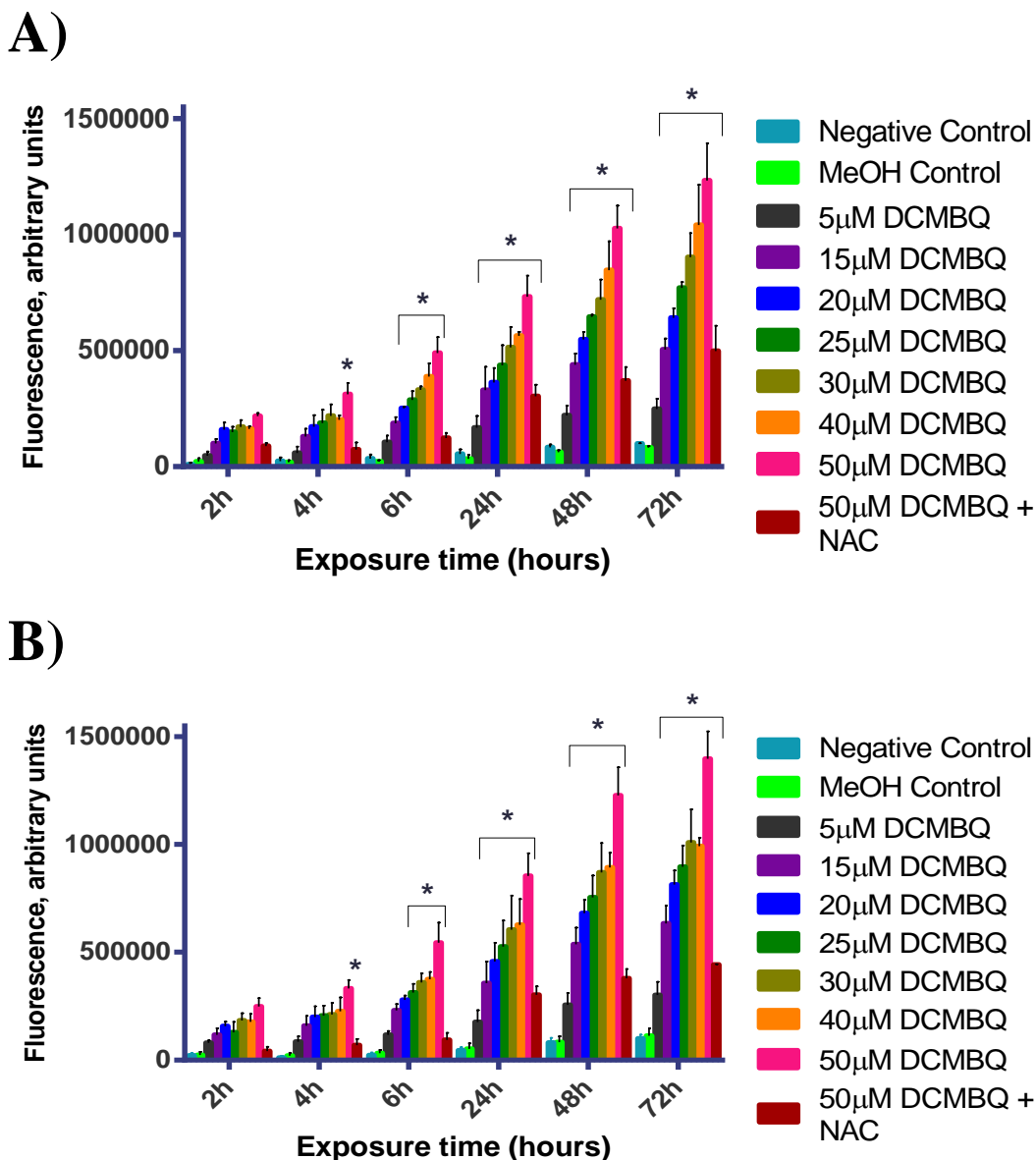
Figure 5-3: Effect of DCMBQ exposure on ROS production in BJ and XPA cells, measured by DCFDA assay

Fluorescence data were obtained from BJ (**A**) and XPA (**B**) cells exposed to DCMBQ for the time periods shown. Cells were incubated with DCFDA, washed, and treated with DCMBQ. Plates were removed from the incubator at the times shown, analyzed, and returned to the incubator. Blank wells (with DCFDA dye, without cells) were included on treatment plates; data shown here have had blank values subtracted. Control groups treated with solvent only (MeOH Control), and

culture medium only (Negative Control), were included. One set of wells was treated with 50 µM DCMBQ and concomitant addition of N-acetylcysteine (NAC), an ROS inhibitor. Data shown are an average of three independent experiments, with error bars representing the standard error of the mean (SEM). A two-way ANOVA to determine the effect of time and treatment on fluorescent signal was performed, using the MeOH Control group as the comparison (control) group.* = $p < 0.05$ (including all treatment groups under a bracket)

Table 5-1: Statistically significant values in the DCFDA ROS assay for BJ and XPA cells exposed to DCMBQ from 2-72 hours

	Exposure time					
Cell type	2h	4h	6h	24h	48h	72h
BJ	none	50 µM	20-50 µM	15-50 µM and 50µM+NAC	15-50 µM and 50µM+NAC	15-50 µM and 50µM+NAC
XPA	none	50 µM	25-50 µM	15-50 µM	15-50 µM	15-50 µM and 50µM+NAC

5.3.3 Alkaline comet assay

Both BJ and XPA showed significantly increased tail moment, indicative of DNA fragmentation, when exposed to DCMBQ for 24 hours without a recovery period (≥20 µM for BJ cells; ≥7.5 µM for XPA cells) (**Figure 5-4**). The increase in tail moment in BJ cells appears to be concentration-dependent, whereas XPA cells show a similar response from 7.5-20 µM DCMBQ. No significant increases in tail moment were observed in cells treated with 5 µM DCMBQ or the solvent control group in either cell line. When 2 mM NAC was added concomitantly with DCMBQ (**Figure 5-5**), a significant decrease in tail moment was observed in both BJ and XPA cells compared to cells treated only with DCMBQ. Addition of NAC, with or without the same volume of methanol present in the solvent control, did not significantly increase tail moment values.

After a 4-hour incubation period in DCMBQ (7.5 or 10 µM) without recovery, a non-significant elevation in tail moment values was observed for both BJ and

XPA cells compared to their respective solvent control groups (**Figure 5-6**). When cells were exposed to DCMBQ (7.5 or 10 µM) for 4 hours, washed, and allowed to recover for 24 hours in culture medium, tail moment values for all DCMBQ-treated cells in both cell lines were significantly elevated compared to their respective solvent control groups (**Figure 5-7**), and were also elevated compared to cells exposed to the same concentration of DCMBQ which were not allowed to recover (**Figure 5-6**). Cells exposed to DCMBQ (7.5 or 10 µM) for 4 hours and allowed to recover for 24 hours in culture medium containing 2 mM N-acetylcysteine experienced significantly elevated tail moment values compared to both the untreated control groups and cells exposed to the same DCMBQ concentrations for 4 hours without a recovery period (**Figure 5-8**). However, these tail moment values are generally smaller than those in cells exposed to the same conditions but allowed to recover in culture medium without NAC. Both BJ and XPA cells allowed to recover for 24 hours after exposure to 0.003% v/v H_2O_2 for 20 minutes at 4°C showed a highly significant reduction in tail moment values compared to cells which did not receive a recovery period (**Figure 5-9**). While post-recovery tail moment values were elevated for both cell lines compared to their respective negative control group, they were not significantly different. In almost all situations where both cell lines were exposed to the same concentration of DCMBQ, the tail moment values for XPA cells are greater than those of BJ cells (except **Figure 5-6**, where the BJ 7.5 µM tail moment is greater than the XPA 7.5 µM tail moment after 4 hours of DCMBQ exposure without recovery).

A)
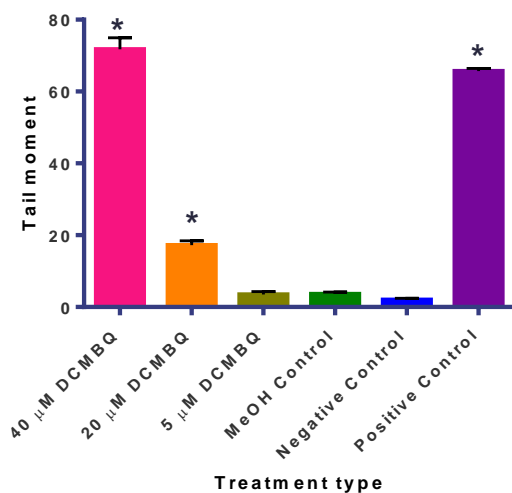
B)

Figure 5-4: Comet assay results of BJ and XPA cells exposed to DCMBQ for 24 hours, no recovery

Tail moment data were obtained from BJ (**A**) and XPA (**B**) cells exposed to DCMBQ for 24 hours. A solvent control group was treated only with methanol (MeOH Control) at the highest concentration used in the treatment groups. The negative control group was treated only with culture medium, and the positive control group was treated with 0.003% v/v hydrogen peroxide in culture medium for 20 minutes at 4°C to produce DNA fragmentation. Data shown represent the mean of three independent experiments, with error bars representing the standard error of the mean (SEM). Statistical significance was determined by performing a

one-way ANOVA with Dunnett's post-hoc analysis, using the MeOH Control group as the comparison (control) group. * = p<0.05 compared to MeOH Control group

A)

B)

Figure 5-5: Comet assay results of BJ and XPA cells exposed to DCMBQ for 24 hours, no recovery, with and without N-acetylcysteine

Tail moment data were obtained from BJ (**A**) and XPA (**B**) cells exposed to DCMBQ for 24 hours, with and without concomitant addition of N-acetylcysteine (NAC). A solvent control group was treated only with methanol (MeOH Control) at the highest concentration used in the treatment groups. The negative control group was treated only with culture medium. Data shown represent the mean of

three independent experiments, with error bars representing the standard error of the mean (SEM). Statistical significance was determined by performing one-way ANOVA with Dunnett's post-hoc analysis, using the MeOH Control group as the comparison (control) group. Tukey's multiple comparisons test was used to compare treatment groups to one another. * = $p<0.05$ compared to MeOH Control group; **a** = $p<0.05$ between the indicated groups
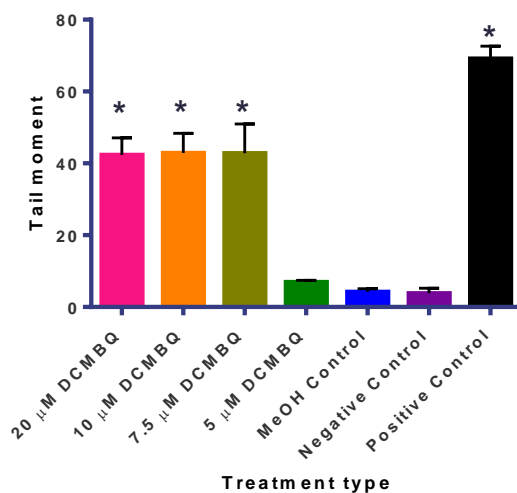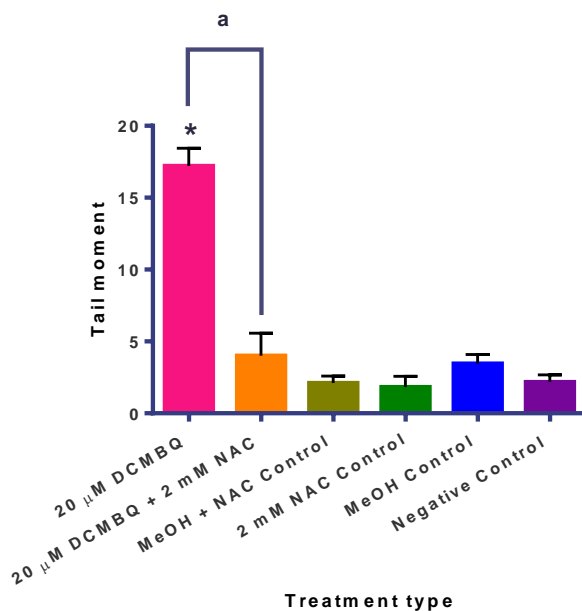
A)

B)
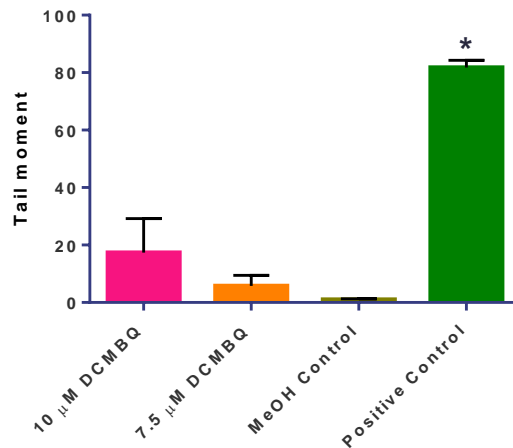
Figure 5-6: Comet assay results of BJ and XPA cells exposed to DCMBQ for 4 hours, no recovery

Tail moment data were obtained from BJ (**A**) and XPA (**B**) cells exposed to DCMBQ for 4 hours. A solvent control group was treated only with methanol (MeOH Control) at the highest concentration used in the treatment groups. The positive control group was treated with 0.003% v/v hydrogen peroxide in culture medium for 20 minutes at 4°C to produce DNA fragmentation. Data shown represent the mean of three independent experiments, with error bars representing the standard error of the mean (SEM). Statistical significance was determined by performing a one-way ANOVA with Dunnett's post-hoc analysis, using the MeOH Control group as the comparison (control) group. * = p<0.05 compared to MeOH Control group
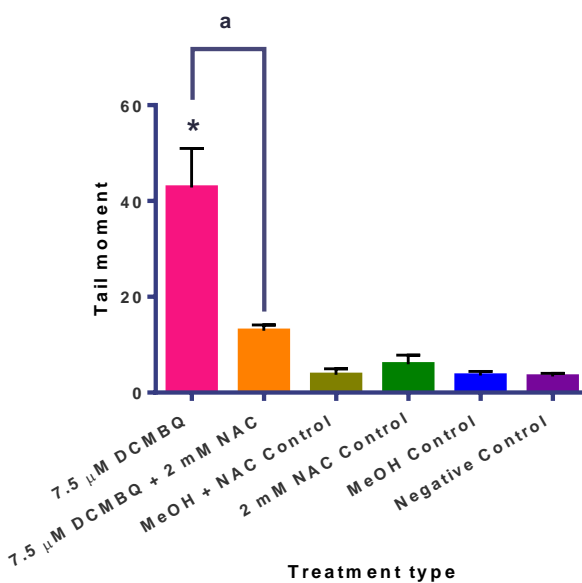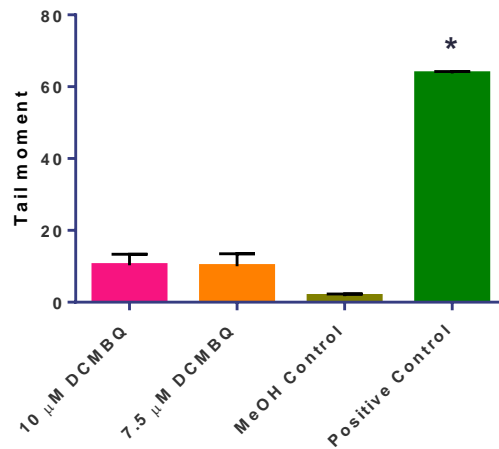
A)
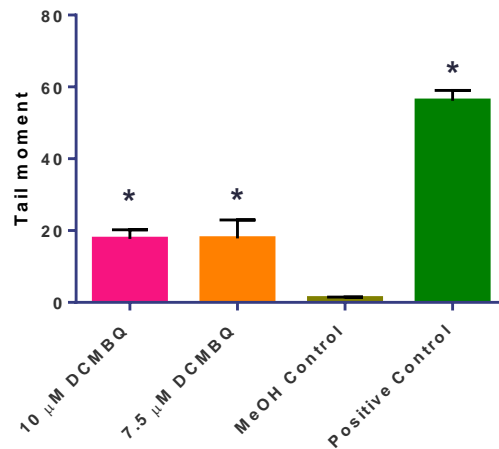
B)

Figure 5-7: Comet assay results of BJ and XPA cells exposed to DCMBQ for 4 hours, with 24h recovery

Tail moment data were obtained from BJ (**A**) and XPA (**B**) cells exposed to DCMBQ for 4 hours, washed with PBS, then allowed to recover in culture medium for 24 hours. A solvent control group was treated only with methanol (MeOH Control) at the highest concentration used in the treatment groups. The positive control group was treated with 0.003% v/v hydrogen peroxide in culture medium for 20 minutes at 4°C to produce DNA fragmentation; this group did not receive a recovery period. Data shown represent the mean of three independent experiments, with error bars representing the standard error of the mean (SEM).

Statistical significance was determined by performing a one-way ANOVA with Dunnett's post-hoc analysis, using the MeOH Control group as the comparison (control) group. * = p<0.05 compared to MeOH Control group

Figure 5-8: Comet assay results of BJ and XPA cells exposed to DCMBQ for 4 hours, with 24h recovery in presence of 2 mM NAC

Tail moment data were obtained from BJ (**A**) and XPA (**B**) cells exposed to DCMBQ for 4 hours, washed with PBS, then allowed to recover in culture medium supplemented with 2 mM NAC for 24 hours. A solvent control group was treated only with methanol (MeOH Control) at the highest concentration used in the treatment groups. The positive control group was treated with 0.003% v/v hydrogen peroxide in culture medium for 20 minutes at 4°C to produce DNA fragmentation; this group did not receive a recovery period. Data shown represent the mean of three independent experiments, with error bars representing the

155

standard error of the mean (SEM). Statistical significance was determined by performing a one-way ANOVA with Dunnett's post-hoc analysis, using the MeOH Control group as the comparison (control) group. * = p<0.05 compared to MeOH Control group
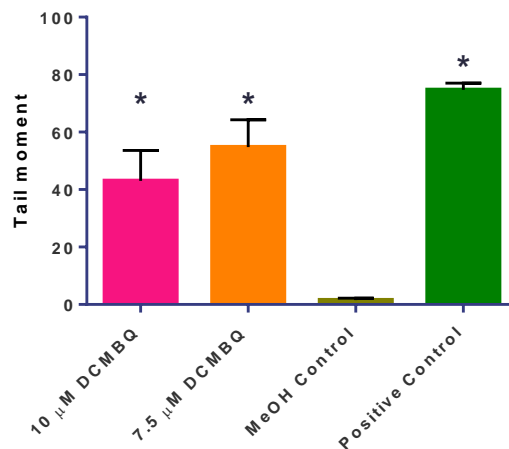
A)
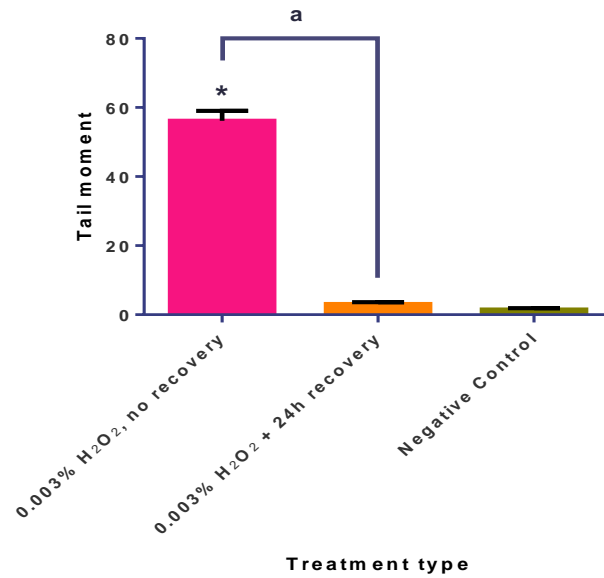
B)

Figure 5-9: Comet assay results of BJ and XPA cells exposed to H_2O_2, with and without recovery at 37°C

Tail moment data were obtained from BJ (**A**) and XPA (**B**) cells exposed to 0.003% v/v H_2O_2 for 20 minutes at 4°C, then analyzed immediately (no recovery) or washed with PBS and allowed to recover in culture medium for 24 hours

(recovery). Data shown are an average of three independent experiments, with error bars representing the standard error of the mean (SEM). Statistical significance was determined by performing a one-way ANOVA with Dunnett's post-hoc analysis, using the negative control group as the comparison group. Tukey's mult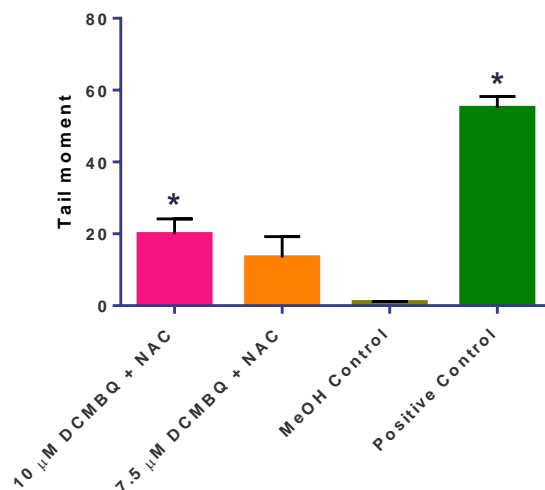iple comparisons test was used to compare treatment groups to one another. * = $p < 0.05$ compared to MeOH Control group; **a** = $p < 0.05$ between the indicated groups

5.4   Discussion

Based on these results, DCMBQ appears to be cytotoxic and genotoxic to both BJ and XPA cells, at least partially via the generation of reactive oxygen species. There is a highly significant correlation between DCMBQ concentration, exposure time, and ROS production, as seen in the DCFDA assay (**Figure 5-3**). The concomitant addition of N-acetylcysteine, a ROS scavenger, reduces both cytotoxicity and genotoxicity, as observed in the RTCA, DCFDA, and comet assays (**Figures 5-2, 5-3, 5-5, 5-8**). This finding is consistent with known mechanisms of toxicity of other benzoquinone substances, which are known to form semiquinone radicals that participate in futile redox cycling (**Figure 5-1**). This produces ROS which may damage cell macromolecules such as DNA (3, 6). A recent study by our research group also found that DCMBQ is cytotoxic to the T24 human bladder cancer cell line, and that this toxicity can be greatly reduced by the addition of NAC. DCMBQ was also shown to cause oxidative DNA damage in these cells, as measured by 8OHdG lesion formation (8). These findings support my observation that the cytotoxicity and genotoxicity of DCMBQ involves ROS production. Although benzoquinones are known to form other metabolites as well, the balance of evidence obtained in these experiments and from previous research suggests that the cyto- and genotoxicity of DCMBQ is, at least in part, due to the generation of ROS.

Another piece of supporting evidence for an ROS contribution to DCMBQ toxicity involves the Ames test/bacterial reverse mutation assay results discussed

in **Chapter 4, Table 4-2**. DCMBQ produced significantly elevated substitution mutations in the TA100 *Salmonella* strain. This finding is consistent with a previous study that found single-base substitution mutations in the *supF* forward mutation assay after treatment with p-benzoquinone (13). Substitution mutations (transitions/transversions) are consistent with a small modification to the DNA base, such as that arising from oxidative damage (14-16). Some benzoquinone compounds are also known to form adducts to cell macromolecules, including DNA (3, 6). If DCMBQ produced bulky DNA adducts, it might be expected to cause frameshift mutations, as the bulky adduct could be mistaken for an extra base by the DNA replication machinery (17). However, no significant frameshift mutations were observed in the TA98 *Salmonella* strain. Therefore, the results from the Ames test appear to point more strongly towards a possible ROS-mediated toxicity as opposed to the formation of bulky adducts. This finding is not sufficient in itself to indicate a mechanism of action involving ROS. However, when considered with the results from the RTCA, DCFDA, and comet assays described above, it provides additional evidence that DCMBQ toxicity likely involves the formation of ROS.

Since the balance of evidence suggests that ROS are largely responsible for the genotoxic effects of DCMBQ, why was a difference in cytotoxic response between BJ and XPA cells observed at high DCMBQ concentrations in the original RTCA assay (**Chapter 4, Figure 4-4**)? Furthermore, why are XPA tail moment values consistently larger than those observed in BJ cells when exposed to the same concentration of DCMBQ (**Figures 5-6 through 5-9**), if both cell lines are capable of oxidative DNA damage repair? While it is possible that the two cell lines had inherently different sensitivities to DCMBQ, another explanation is possible. Normally, the base excision repair (BER) pathway repairs small oxidative DNA lesions (5), and this pathway is functional in the XPA cell line. However, there is evidence that the NER pathway may have some role in the repair of oxidative damage as well. Individuals with severe xeroderma pigmentosum (XP Group A; the same subtype as the donor of the XPA cell line

(18)), a genetic disease where the NER pathway is non-functional, may experience a severe neurodegenerative syndrome thought to be due to buildup of unrepaired oxidative damage in the central nervous system (19, 20). This finding suggests that the NER pathway plays a role in the repair of oxidative damage, but that its exact function is unknown. Other researchers have proposed that NER acts as a "backup" (secondary) pathway for BER, activating to repair oxidative damage if the BER pathway is saturated (21). There is also some evidence that specific oxidative lesions are preferentially repaired by the NER pathway, as opposed to the BER pathway (22, 23). These findings may explain the differences in cytotoxicity observed between BJ and XPA cells exposed to DCMBQ (see **Chapter 4, Figure 4-4**). It is possible that, at these DCMBQ concentrations, enough ROS were produced to saturate the BER pathway, necessitating the activation of the "backup" NER pathway. Because XPA cells do not have a functional NER pathway, overwhelming oxidative damage resulted in cytotoxicity caused, at least in part, by oxidative DNA damage. Conversely, BJ cells experienced less cytotoxicity because the NER pathway was functional and able to supplement the BER pathway. This hypothesis may also explain the larger tail moment values observed in XPA cells compared to BJ cells exposed to the same concentrations of DCMBQ; the absence of the NER pathway could result in a larger number of unrepaired lesions. DCMBQ could also produce the type of oxidative lesions preferentially repaired by NER. It is entirely possible that NER-mediated bulky DNA adducts form concomitantly with the observed oxidative damage, which could also explain the difference between the BJ and XPA cytotoxic and genotoxic responses to DCMBQ. As the identity of lesions caused by DCMBQ are not known, additional information is required to confirm or refute these hypotheses.

An unexpected finding was the apparent *increase* in DNA damage found in both BJ and XPA cells exposed to DCMBQ for 4 hours and allowed to recover in DCMBQ-free medium for 24 hours, compared to cells exposed under the same conditions without recovery (**Figures 5-6 through 5-8**). Initially, I hypothesized

160

that the post-recovery increase in DNA damage suggests that an intracellular toxic mechanism is still occurring despite removal of exogenous DCMBQ. I further hypothesized that residual intracellular DCMBQ could be biotransformed to a charged semiquinone molecule (as in **Figure 5-1**) and would therefore be unable to exit cells. The semiquinone could then continue to participate in futile redox cycling, generating additional ROS and depleting intracellular oxygen and NADPH, even after the removal of extracellular DCMBQ. To test this hypothesis, a ROS scavenger (NAC) was added to the DCMBQ-free recovery medium with the intent that residual intracellular ROS and toxic DCMBQ metabolites would be scavenged. Although the addition of NAC during the recovery period generally produced smaller tail moment values compared to cells allowed to recover without NAC, these tail moment values were still greater than those measured immediately after the 4-hour exposure to DCMBQ (**Figures 5-6 & 5-8**). It appears that NAC somewhat reduces DNA damage during the recovery period, but not to the extent that DNA damage is reduced when NAC is added concomitantly with DCMBQ at the beginning of the exposure period (**Figure 5-5**). Therefore, it is unlikely that trapped toxic metabolites are primarily responsible for the increase in tail moment values during the recovery period.

Next, I hypothesized that DCMBQ may exert its toxic effect rapidly, with the majority of the genotoxic damage occurring before the end of the 4-hour incubation period. This could explain why the addition of NAC during recovery had little effect, as the damage would have already occurred by the start of the recovery period. However, this is not a sufficient explanation for the observed results. While it is true that ROS are known to have half-lives on the order of micro- or nanoseconds (24, 25), the DCFDA experiments have shown that DCMBQ is capable of producing ROS over a sustained period, far greater than the 4-hour exposure window used in the comet assay experiments. While rapid DNA damage explains why a recovery period might not produce any *decrease* in DNA damage (as the damage would have already occurred) it does not explain

161

why an *increase* in DNA damage was observed in both BJ and XPA cells exposed in the 4h exposure/24h recovery experiments (**Figures 5-7 & 5-8**).

A more plausible and comprehensive explanation is that part of the increase in apparent DNA damage observed in the comet assay during recovery is actually due to detection of transient DNA lesions caused by DNA repair processes, or unrepaired lesions still present after the recovery period. Others have shown that the transient lesions caused by DNA repair can be detected by the comet assay (26, 27). In both the NER and BER pathways, repair enzymes temporarily cause single-strand breaks in order to excise the damaged base(s) (see **Chapter 1, Section 1.8**). Also, an initial step in the BER pathway involves glycosylases removing the damaged base, creating an apurinic or apyrimidinic (AP) site (5); under high pH conditions, such as those found in the alkaline comet assay, these AP sites are converted to strand breaks and may also be detected in the comet assay (26). Therefore, if DCMBQ causes ROS-mediated genotoxicity, which is primarily repaired by BER, the AP sites and endonuclease-mediated strand breaks formed during repair, as well as the strand breaks caused directly by ROS, could be detected by the alkaline comet assay. Assuming this is the case, I hypothesized that the increased tail moment values observed after the recovery period are likely due to a combination of unrepaired DCMBQ-mediated DNA damage and transient DNA repair-mediated lesions.

It is also possible that some forms of oxidative damage may not be detected by the comet assay until the repair process has begun. ROS may produce several different DNA lesions, including single-stranded breaks and oxidative modification of individual bases (16, 28). While single-stranded breaks would be detected by the comet assay prior to repair, base modification in itself would likely not be detectable *unless* it caused a strand break or loss of the base. However, the repair process for oxidized bases (base excision repair) would produce lesions detectable by the comet assay, as described above. Therefore, oxidized bases may not be captured by the comet assay until the DNA repair

162

process has started, and the increased DNA fragmentation detected after the recovery period in these experiments may be due to the repair of oxidized bases caused by DCMBQ.

However, it is likely that DNA damage repair occurred both during the DCMBQ exposure period and the recovery period; DNA repair is generally a rapid process and BER has been shown to occur in minutes to hours after the damage has occurred (29). Why, then, is DNA damage detected after a 24-hour recovery period, when DNA repair might otherwise be expected to be complete? As shown in **Figure 5-9**, both BJ and XPA cells are capable of near-complete repair of DNA damage caused by hydrogen peroxide after a 24-hour recovery period. Hydrogen peroxide induces DNA damage via an oxidative/free radical mechanism (5), which is also the mechanism proposed for DCMBQ-induced DNA damage. The tail moment values produced by H_2O_2 exposure before recovery are larger than those produced by DCMBQ (**Figures 5-6 through 5-9**), indicating a greater degree of DNA fragmentation, yet the repair for H_2O_2 lesions appears to be far more efficient than those caused by DCMBQ. Although available evidence suggests that DCMBQ produces oxidative DNA damage, some other process or aspect must make DCMBQ-mediated DNA damage more refractory to repair.

A potential explanation for the refractory nature of DCMBQ-induced DNA lesions could be the conformation and proximity of the lesions to one another. A phenomenon known as oxidatively generated clustered DNA lesions (OGCLs) or locally multiply damaged sites (LMDS) has been reported in the literature (30-33). These lesions, caused by oxidative damage from ionizing radiation or radiomimetic chemical toxicants, occur in close proximity to one another (≥ 2 lesions within 1-2 helical turns of DNA), either on the same strand or on opposite strands (32, 34). The resulting lesion experiences reduced or delayed repair, depending on the proximity of other nearby lesions; some OGCLs are not repairable and can lead to cytotoxicity (31). The repair of some conformations of OGCLs is intentionally delayed in order to prevent the formation of potentially

163

cytotoxic double-stranded breaks as part of the repair process (34). Delayed repair periods of clustered lesions have been reported, up to several days after the damage occurred (30). The hydroxyl radical, which is predicted to be the ultimate reactive oxygen species produced by DCMBQ (**Figure 5-1**), is capable of producing OGCLs (31). There is also some evidence that the NER pathway, which is non-functional in XPA cells, preferentially repairs some specific OGCLs. At present, this has only been shown in bacteria (31). OGCLs also can lead to substitution mutations if the damage persists through DNA replication (31, 32); substitution mutations were also the primary mutation observed in the Ames test assay with DCMBQ in **Chapter 4** (**Table 4-2**).

Due to the similarities between characteristics of DCMBQ-induced lesions and OGCLs, it is possible that DCMBQ produced OGCLs in these experiments. Generation of complex DNA lesions, such as OGCLs, would explain why repair of DCMBQ might be delayed into the recovery period; it is also consistent with the proposed ultimate reactive oxygen species produced by DCMBQ (hydroxyl radical) and the substitution mutations observed in **Chapter 4, Table 4-2**. This hypothesis would also explain why H_2O_2 appears to cause more DNA fragmentation than DCMBQ, yet H_2O_2-induced damage is repaired more efficiently (**Figures 5-6 through 5-9**). A comparison of H_2O_2, which produces primarily simple single oxidative lesions, with ionizing radiation, which produces OGCLs (called LMDS in that manuscript) showed that a far smaller number of OGCLs are required to cause cell death compared to the simple oxidative lesions caused by H_2O_2 (33). A similar phenomenon may be occurring here, with fewer yet more complex DCMBQ lesions producing a more difficult challenge to BJ and XPA DNA repair processes, compared to the more numerous yet simpler oxidative lesions caused by H_2O_2. Formation of OGCLs would also be consistent with the post-recovery rise in tail moment values for *both* BJ and XPA cells exposed to DCMBQ, as this type of lesion would be expected to affect both cell lines. The consistently larger tail moment values in DCMBQ-exposed XPA cells compared to BJ cells (**Figures 5-6 through 5-9**) could be explained by possible

164

NER involvement in oxidative DNA damage repair, and/or the simultaneous formation of NER-mediated DNA lesions (e.g. bulky adducts). However, there is no direct evidence that DCMBQ causes OGCLs; further investigation is required to determine if this lesion type is involved in DCMBQ genotoxicity.

At present, there is insufficient data to definitively conclude the degree to which DNA repair processes influence the results of the comet assays performed here. The comet assay procedure used in these experiments is unable to distinguish between lesions caused by genotoxic agents and transient lesions caused by DNA repair enzymes; both would be detected as DNA damage. However, it seems plausible that DCMBQ-mediated DNA damage would be undergoing repair during the exposure and recovery periods, and that persistent DNA repair lesions would be captured by the comet assay after the recovery period. This could explain why DNA damage appeared to increase upon recovery, even with the addition of NAC (**Figures 4-6, 4-7, 4-8**). The DNA repair process would likely not be affected by NAC, but the addition of NAC ensures that any remaining intracellular DCMBQ or its toxic metabolites would be eliminated. The small decrease in tail moment values seen in recovery with NAC (**Figure 4-8**) compared to recovery without NAC (**Figure 4-7**) could indicate the contribution of trapped intracellular DCMBQ or its metabolites to the increase in tail moment values during the recovery period. However, much of the increase in tail moment values during the recovery period is likely from the transient DNA lesions which occur during the DNA repair process.

Several follow-up experiments could be performed to further determine the specific genotoxic effects of DCMBQ in this experimental system. The FLARE^{TM} (Fragment Length Analysis using Repair Enzymes) assay (Trevigen), a modified comet assay, could be used to determine the specific DNA lesions present after exposure to DCMBQ. The FLARE assay incubates the toxicant-exposed DNA with a repair enzyme specific to the lesion thought to be produced by the toxicant, then proceeds with the alkaline comet assay procedure. If cells incubated with the

repair enzyme show greater DNA fragmentation than cells exposed under the same conditions without repair enzyme, this indicates that the repair enzyme has cleaved the DNA to remove its corresponding lesion (thus producing a lesion detected by the comet assay). In this case, because I predict that DCMBQ causes oxidative lesions, the DNA should be incubated with human 8-oxoguanine DNA glycosylase 1 (hOGG1), which is specific for 8-oxoguanine and formamidopyrimidine moieties. Greater DNA fragmentation should be observed in cells incubated with hOGG1, as the ROS-mediated genotoxicity of DCMBQ would result in the formation of 8-oxoguanine lesions, causing hOGG1 to cleave the DNA at these sites. Another approach to confirming the presence of oxidative DNA damage would be to directly detect a representative lesion, such as 8-hydroxy-2'-deoxyguanosine (8OHdG), via a colorimetric or fluorimetric ELISA performed on DNA from treated cells. Indeed, significantly elevated 8OHdG has been detected in T24 human bladder cancer cells exposed to DCMBQ (8). For assessment of complex/clustered oxidative DNA lesions, high-performance liquid chromatography with electrospray ionization tandem mass spectrometry (HPLC ESI-MS/MS) methods have been developed, although further refinement is required to accurately identify these lesions (31). Although careful sample preparation is required for these approaches to prevent oxidative damage artifacts, they may prove useful in further mechanistic studies of *in vitro* DCMBQ toxicity.

Another surprising finding was the apparent plateau of DNA fragmentation found in the XPA cells exposed to DCMBQ for 24 hours (**Figure 5-4B**). DCMBQ concentrations of 20, 10, and 7.5 μM all produced approximately equal tail moment values in these cells (~42). This does not conform to the apparent concentration-response relationship observed in other assays (e.g. the DCFDA ROS assay, **Figure 5-3B**). The reason behind this plateau is unknown, but could be due to the saturation of the metabolic pathway(s) responsible for the bioactivation of DCMBQ. If the pathway(s) producing genotoxic metabolites was saturated, the remainder of the DCMBQ might be transformed by another metabolic pathway(s) which does not produce genotoxic products measurable by

the comet assay. This explanation is consistent with the finding that benzoquinone compounds are known to have multiple potential metabolic pathways (3, 6). Saturation of quinone metabolic pathways in *in vitro* mammalian cell cultures has been previously reported in the literature (35). However, this still does not explain why formation of ROS appears to increase over this concentration range yet tail moment values remain constant. Alternatively, excess DCMBQ may undergo partial metabolism, or remain present as the parent compound. At present, insufficient evidence exists to test this hypothesis; the specific metabolic pathways of DCMBQ and the chemical structure of its toxic products are unknown. Additional experiments to identify the metabolic products (e.g. analysis of intracellular contents and culture medium with high performance liquid chromatography/mass spectrometry) would be required to confirm this hypothesis.

It is important to remember that generation of reactive oxygen species is not the only potential pathway for DCMBQ toxicity. Although there is ample evidence suggesting an oxidative damage component to DCMBQ toxicity, this does not eliminate the possibility that DCMBQ simultaneously causes bulky adduct formation or other mechanisms of toxicity. Alkali-labile sites, which are DNA lesions susceptible to high pH, could also contribute to the tail moment values observed in the comet assay experiments; however, these lesions have not been chemically characterized so it is unknown whether they play a role in DCMBQ-induced genotoxicity. Also, other aspects of metabolism, such as Phase II metabolic processes, may play a role in DCMBQ toxicity. Evidence suggests that some quinone substances become more toxic upon glutathione conjugation, with toxicity increasing up to the third glutathione substitution (7). It is not known whether BJ and XPA cells are capable of, or are performing glutathione conjugation on DCMBQ in these experiments. The presence of the chlorine and methyl groups on the benzoquinone ring result in only one accessible ring carbon in the DCMBQ structure. It is unknown if only one GSH substitution is possible on this molecule, or if the functional groups will be cleaved during the

167

conjugation of additional GSH moieties. If these processes are occurring, the effect that they will have on the biological activity of DCMBQ or its metabolites is unclear. However, as shown in **Chapter 4, Figure 4-4**, the presence of the methyl group on the quinone ring appears to be central for DCMBQ toxicity, as DCBQ, a similar substance without the methyl substitution, is virtually non-toxic at the same concentrations to BJ and XPA cells in RTCA experiments (**Chapter 4, Figure 4-3**). Clearly, modifications to the basic quinone structure may have significant implications for the *in vitro* toxicity of the halobenzoquinone disinfection byproducts.

Based on these results, DCMBQ appears to cause cytotoxicity and genotoxicity in BJ and XPA cells at least in part due to ROS-mediated toxicity. Both cytotoxicity and genotoxicity of DCMBQ may be prevented with concomitant addition of N-acetylcysteine (NAC). DCMBQ is capable of generating ROS in both BJ and XPA cells in a time- and concentration-dependent manner over 72 hours, as observed in the DCFDA assay; measured ROS production decreases significantly with concomitant addition of NAC. Significantly elevated DNA fragmentation is observed when BJ and XPA cells are exposed to DCMBQ without recovery. A plateau of DNA damage appears to occur in XPA cells, which may be due to saturation of metabolic pathways. DNA fragmentation appears to increase after a 24-hour recovery period following a 4-hour incubation with DCMBQ in both BJ and XPA cells; addition of NAC during this recovery period has little effect. While DCMBQ likely causes oxidative DNA damage, the efficient repair of hydrogen peroxide-induced DNA damage shown by both BJ and XPA cells indicates that DCMBQ may cause a more complex form of oxidative damage, such as oxidatively generated clustered lesions (OGCLs). Therefore, I hypothesize that the increased DNA fragmentation observed after the recovery period is due to transient DNA damage caused by the normal repair processes of complex, refractory lesions caused by DCMBQ exposure. However, additional experimentation is required to test this hypothesis.

5.5   References

1. Bull RJ, Reckhow DA, Li X, Humpage AR, Joll C, Hrudey SE. Potential carcinogenic hazards of non-regulated disinfection by-products: Haloquinones, halo-cyclopentene and cyclohexene derivatives, N-halamines, halonitriles, and heterocyclic amines. Toxicology. 2011 Aug 15;286(1-3):1-19.

2. Bull RJ, Awwa Research Foundation, United States. Environmental Protection Agency. Use of toxicological and chemical models to prioritize DBP research. Denver, CO: Awwa Research Foundation; 2006.

3. Monks TJ, Hanzlik RP, Cohen GM, Ross D, Graham DG. Quinone chemistry and toxicity. Toxicol Appl Pharmacol. 1992 Jan;112(1):2-16.

4. Nouspikel T. DNA repair in mammalian cells : Nucleotide excision repair: Variations on versatility. Cell Mol Life Sci. 2009 Mar;66(6):994-1009.

5. Friedberg EC, Walker GC, Siede W. DNA repair and mutagenesis. 2nd ed. Washington, D.C.: ASM Press; 2006.

6. Casarett LJ, Doull J, Klaassen CD. Casarett and Doull's toxicology: The basic science of poisons. 6th ed. New York: McGraw-Hill Medical Pub. Division; 2001.

7. Lau SS, Hill BA, Highet RJ, Monks TJ. Sequential oxidation and glutathione addition to 1,4-benzoquinone: Correlation of toxicity with increased glutathione substitution. Mol Pharmacol. 1988 Dec;34(6):829-36.

8. Du H, Li J, Moe B, McGuigan CF, Shen S, Li XF. Cytotoxicity and oxidative damage induced by halobenzoquinones to T24 bladder cancer cells. Environ Sci Technol. 2013 Mar 19;47(6):2823-30.

9. Anderson D, Plewa MJ. The international comet assay workshop. Mutagenesis. 1998 Jan;13(1):67-73.

10. Tice RR, Agurell E, Anderson D, Burlinson B, Hartmann A, Kobayashi H, et al. Single cell gel/comet assay: Guidelines for in vitro and in vivo genetic toxicology testing. Environ Mol Mutagen. 2000;35(3):206-21.

11. Xing JZ, Zhu L, Jackson JA, Gabos S, Sun XJ, Wang XB, et al. Dynamic monitoring of cytotoxicity on microelectronic sensors. Chem Res Toxicol. 2005 Feb;18(2):154-61.

12. Singh NP, McCoy MT, Tice RR, Schneider EL. A simple technique for quantitation of low levels of DNA damage in individual cells. Exp Cell Res. 1988 Mar;175(1):184-91.

13. Gaskell M, McLuckie KI, Farmer PB. Comparison of the repair of DNA damage induced by the benzene metabolites hydroquinone and p-benzoquinone: A role for hydroquinone in benzene genotoxicity. Carcinogenesis. 2005 Mar;26(3):673-80.

14. Maynard S, Schurman SH, Harboe C, de Souza-Pinto NC, Bohr VA. Base excision repair of oxidative DNA damage and association with cancer and aging. Carcinogenesis. 2009 Jan;30(1):2-10.

15. Feig DI, Loeb LA. Mechanisms of mutation by oxidative DNA damage: Reduced fidelity of mammalian DNA polymerase beta. Biochemistry. 1993 Apr 27;32(16):4466-73.

16. Cooke MS, Evans MD, Dizdaroglu M, Lunec J. Oxidative DNA damage: Mechanisms, mutation, and disease. FASEB J. 2003 Jul;17(10):1195-214.

17. Sambamurti K, Callahan J, Luo X, Perkins CP, Jacobsen JS, Humayun MZ. Mechanisms of mutagenesis by a bulky DNA lesion at the guanine N7 position. Genetics. 1988 Dec;120(4):863-73.

18. GM04312 [Internet].; 2009. Available from: http://ccr.coriell.org/sections/Search/Sample_Detail.aspx?Ref=GM04312&PgId= 166.

19. Reardon JT, Bessho T, Kung HC, Bolton PH, Sancar A. In vitro repair of oxidative DNA damage by human nucleotide excision repair system: Possible explanation for neurodegeneration in xeroderma pigmentosum patients. Proc Natl Acad Sci U S A. 1997 Aug 19;94(17):9463-8.

20. Hayashi M. Roles of oxidative stress in xeroderma pigmentosum. Adv Exp Med Biol. 2008;637:120-7.

21. Moller P, Wallin H. Adduct formation, mutagenesis and nucleotide excision repair of DNA damage produced by reactive oxygen species and lipid peroxidation product. Mutat Res. 1998 Jun;410(3):271-90.

22. Kuraoka I, Bender C, Romieu A, Cadet J, Wood RD, Lindahl T. Removal of oxygen free-radical-induced 5',8-purine cyclodeoxynucleosides from DNA by the nucleotide excision-repair pathway in human cells. Proc Natl Acad Sci U S A. 2000 Apr 11;97(8):3832-7.

23. Brooks PJ, Wise DS, Berry DA, Kosmoski JV, Smerdon MJ, Somers RL, et al. The oxidative DNA lesion 8,5'-(S)-cyclo-2'-deoxyadenosine is repaired by the nucleotide excision repair pathway and blocks gene expression in mammalian cells. J Biol Chem. 2000 Jul 21;275(29):22355-62.

24. Wardman P. Fluorescent and luminescent probes for measurement of oxidative and nitrosative species in cells and tissues: Progress, pitfalls, and prospects. Free Radic Biol Med. 2007 Oct 1;43(7):995-1022.

25. Giorgio M, Trinei M, Migliaccio E, Pelicci PG. Hydrogen peroxide: A metabolic by-product or a common mediator of ageing signals? Nat Rev Mol Cell Biol. 2007 Sep;8(9):722-8.

26. Collins AR, Dobson VL, Dusinska M, Kennedy G, Stetina R. The comet assay: What can it really tell us? Mutat Res. 1997 Apr 29;375(2):183-93.

27. Collins AR. Investigating oxidative DNA damage and its repair using the comet assay. Mutat Res. 2009 Jan-Feb;681(1):24-32.

28. Haliwell B, Aruoma O, editors. DNA & free radicals. Sussex, UK: Ellis Horwood Ltd; 1993.

29. Lan L, Nakajima S, Oohata Y, Takao M, Okano S, Masutani M, et al. In situ analysis of repair processes for oxidative DNA damage in mammalian cells. Proc Natl Acad Sci U S A. 2004 Sep 21;101(38):13738-43.

30. Georgakilas AG. Processing of DNA damage clusters in human cells: Current status of knowledge. Mol Biosyst. 2008 Jan;4(1):30-5.

31. Cadet J, Ravanat JL, TavernaPorro M, Menoni H, Angelov D. Oxidatively generated complex DNA damage: Tandem and clustered lesions. Cancer Lett. 2012 Dec 31;327(1-2):5-15.

32. Sage E, Harrison L. Clustered DNA lesion repair in eukaryotes: Relevance to mutagenesis and cell survival. Mutat Res. 2011 Jun 3;711(1-2):123-33.

33. Ward JF, Evans JW, Limoli CL, Calabro-Jones PM. Radiation and hydrogen peroxide induced free radical damage to DNA. Br J Cancer Suppl. 1987 Jun;8:105-12.

34. Eccles LJ, O'Neill P, Lomax ME. Delayed repair of radiation induced clustered DNA damage: Friend or foe? Mutat Res. 2011 Jun 3;711(1-2):134-41.

35. Thor H, Smith MT, Hartzell P, Bellomo G, Jewell SA, Orrenius S. The metabolism of menadione (2-methyl-1,4-naphthoquinone) by isolated hepatocytes. A study of the implications of oxidative stress in intact cells. J Biol Chem. 1982 Oct 25;257(20):12419-25.

Chapter 6: Future Work and Conclusions

In the previous chapters, I have described my studies on the cytotoxicity, mutagenicity, and genotoxicity of phenazine and halobenzoquinones, which are recently identified drinking water disinfection byproducts (DBPs). These results have provided valuable information for the elucidation of their potential toxicity and possible effects on human health, as little or no toxicity data were previously available for these substances. I have also developed a new method for examining the *in vitro* toxicity of chemicals, which is applicable to DBPs as well as other classes of compounds. This new technique integrates BJ and XPA cell lines with an impedance-based instrument and is capable of continuous, real-time sensing of chemical-induced cytotoxicity and nucleotide excision repair-mediated DNA damage. The following sections describe in greater detail the contributions of this work to the pre-existing knowledge gap, a discussion of the environmental relevance and limitations of these findings, and suggestions for future research on this topic.

6.1 Contributions to new knowledge

The work in this thesis has contributed to filling the DBP knowledge gap by investigating the cytotoxicity of phenazine and selected HBQ DBPs, as little to no empirical data for these compounds were previously available. I have identified differential toxicity of phenazine in human cell lines, which manifested as an antiproliferative cytotoxic effect in HepG2 cells but a genotoxic effect in T24 cells. I also described a novel method for using RTCA cytotoxicity data to determine appropriate concentrations for the comet assay (**Chapter 2**). I examined selected HBQ DBPs for cytotoxicity, mutagenicity and NER-mediated genotoxicity, identifying DCMBQ as the most toxic compound. These data may be compared with the quantitative-structure toxicity relationship (QSTR)

modeling previously performed on HBQ DBPs (1, 2), to test the predictive ability of this model (see **Chapter 4** for a more comprehensive discussion). My results showed that all tested HBQs were mutagenic in the Ames test, despite the QSTR prediction that these HBQs would not be mutagenic (1, 2). As the HBQ DBPs were identified as a research priority in the QSTR results, the data presented here can be used to plan further experiments to determine if these compounds are toxic *in vivo* under environmentally relevant conditions. My research has also contributed to the understanding of the mechanisms of DCMBQ toxicity by identifying the contribution of reactive oxygen species (ROS) to the DCMBQ-induced cytotoxicity and genotoxicity. This finding confirms the recent work by other members of our research group, which found that DCMBQ generates ROS and oxidative DNA lesions in human bladder cancer cells (3). I have also proposed an explanation for the complex refractory DCMBQ-induced DNA lesions observed in **Chapter 5**, which could be investigated with further research.

Ultimately, these data could contribute to the hazard characterization of these DBPs as part of a regulatory agency's risk assessment process. It is important to note that these data are *not* sufficient in themselves as a basis for human health risk assessment; additional *in vivo* testing (e.g. acute and chronic rodent bioassays) is required for a complete hazard characterization. However, my *in vitro* results may be used to prioritize compounds for future *in vivo* testing, allowing for more efficient use of limited resources. For example, DCMBQ demonstrated higher cytotoxicity, mutagenicity and genotoxicity compared to other HBQs, suggesting that it warrants further *in vivo* studies.

Another original contribution of this work is the creation of the BJ XPA RTCA *in vitro* high-throughput screening method. Using this assay, cytotoxicity and nucleotide excision repair-mediated DNA damage can be continuously monitored in a single experiment, in real-time, with little or no hands-on interaction required after cell treatment. Although only nucleotide excision repair is examined here, this experimental design may be easily expanded to include other matched-pair

174

cell lines with other DNA-repair deficiencies (e.g. base excision repair). The development of new *in vitro* assays is vital to the future of toxicology and regulatory toxicity testing, as many jurisdictions are gradually phasing out or severely restricting *in vivo* testing. While the BJ/XPA RTCA method cannot replace *in vivo* testing, it could potentially reduce the number of animals required (by identifying toxicants of concern, leading to more targeted *in vivo* testing), and/or contribute to refinement of *in vivo* protocols (by determining possible mechanisms of action and appropriate initial *in vivo* dosing ranges). Because it provides real-time monitoring without use of dyes or labels, RTCA technology is particularly well-suited to the development of new *in vitro* assays. While traditional *in vitro* assays often measure only one parameter of cell function at a single time point, RTCA can provide continuous measurement of cell function over hours or days, including morphology, proliferation, and attachment (4). The availability of RTCA platforms capable of testing hundreds or even thousands of wells simultaneously, and their compatibility with automated handling systems, allows for high-throughput screening of potential toxicants with minimal experimenter intervention. This type of *in vitro* method is versatile for many other applications where high-throughput screening of multiple compounds is desired, such as drug discovery. As the BJ/XPA method is adaptable, high-throughput, and simple, further development of this method and similar *in vitro* methods is strongly recommended.

6.2   Environmental relevance and limitations

For all of these experiments, I have used toxicant concentrations above those which have been reported in actual finished water samples. This is because little to no toxicological information is available for these DBPs; therefore, I deliberately chose to use high concentrations to evoke toxicity. Most assays indicated that the tested DBPs provoked toxicity only at concentrations much greater than those known or projected to be found in finished drinking water. However, the experiments with phenazine (**Chapter 2, Figure 2-4**) demonstrated an antiproliferative effect in HepG2 cells at the lowest concentration tested (1.9

μM). Similarly, DCMBQ caused substitution mutations at concentrations as low as 3.1 μM in the Ames test in the absence of S9 fraction (**Chapter 4, Table 4-2**). In both cases, the measured or projected concentrations of these substances in finished drinking water is in the nano- or picomolar range (5, 6), indicating that these effects are approaching potential finished drinking water concentrations. Lower concentrations of these DBPs were not tested in their respective assays, so it is unknown if this effect persists at concentrations expected in finished drinking water. Also, occurrence data for these DBPs in finished drinking water samples is very limited, so the range of possible concentrations is unknown. However, considering the currently available occurrence data, further experimentation with phenazine and DCMBQ should be conducted to determine if their toxic effects persist at concentrations potentially present in finished drinking water.

Another important consideration for environmental relevance is the role of mixtures in DBP toxicology. In these experiments, single DBP compounds are tested; however, DBPs exist as a complex and constantly changing mixture in actual finished water. The composition of this mixture changes constantly based on factors such as raw water quality, choice of disinfectant(s), disinfection contact time, etc. Individual DBPs may be detected only under particular treatment conditions, or in some water systems but not others. Recent data obtained by our lab indicate that HBQ DBPs may be hydrolyzed at neutral pH (such as that found in cell culture medium), leading to a mixture of parent and hydrolyzed HBQ species (7, 8). My *in vitro* experiments also likely contained a mixture of parent and transformed HBQ DBPs; however, it is not known how quickly this transformation occurs nor to what degree the parent DBP compound is hydrolyzed. Due to these factors, it is difficult to determine what would constitute a representative DBP mixture in finished water, particularly because the majority of DBPs have not yet been identified. Additionally, because the toxicological properties of these DBPs are generally unknown, individual compounds were examined in order to provide preliminary information on their toxicity. Although testing these DBPs as a mixture is not feasible at this time, it would provide a

logical next step to determine the toxicological implications of interactions between DBPs and their metabolites. As additional information on DBP occurrence, composition, and stability becomes available, further testing with mixtures should be undertaken to better model environmental conditions.

Another important consideration is the biological systems used to perform these experiments. All of the experiments described here used immortalized human cell lines (except the bacterial strains used to perform the Ames tests in **Chapter 4**). Cancer-derived cell lines (HepG2 and T24) were used in the phenazine experiments in **Chapter 2**. The environmental relevance of cancer cell lines has been widely debated in the field of *in vitro* toxicology. It is true that cancer cells are, by definition, abnormal; they may have different regulation of cellular processes, such as cell cycle control, DNA repair, metabolism, and resistance to cell death (9). However, cancer cell lines are widely used in regulatory toxicity testing due to their readiness to proliferate *in vitro*, the availability of many different cell lines representing different target organs, and the absence of inter-individual variation within a cell line. In the phenazine experiments, HepG2 and T24 cells were used because they were derived from liver and bladder, respectively; these are suspected potential target organs for phenazine toxicity. As a matched pair of non-cancer nucleotide excision repair-proficient (BJ) and –deficient (XPA) skin fibroblast cell lines was available, I chose to use non-cancer cell lines in the BJ/XPA RTCA *in vitro* method. While these cells may avoid the issues associated with using abnormal cancer-derived cell lines, they likely do not represent a target organ for DBP toxicity. The trade-off between selecting a cell line that possesses more "normal" characteristics compared to a cell line that more closely represents the desired target organ/tissue should be carefully considered during the experimental design phase. Both approaches can be appropriate, depending on the desired investigation. A significant advantage of cell lines, whether or not they are cancer-derived, is the ability for multiple researchers to use the same cell line in a number of experiments, allowing the determination of the relative potency of compounds. This is particularly helpful in situations where

ranking of toxicity or prioritizing future toxicological investigation is required, such as in the investigation of DPB toxicity. Although *in vitro* cell lines are unable to fully model the complex interactions that would occur *in vivo*, they are valuable tools to create a standardized screening tool to identify DBPs requiring additional testing.

Although the preceding experiments indicate that potentially toxic byproducts may form during the disinfection of water, these results must be considered in context. While it is true that exposure to disinfected drinking water has been associated with an increased risk of some adverse health effects (particularly bladder cancer) (2), the disinfection of drinking water remains an important public health initiative. The risks of water-borne illness from untreated water far outweigh the risks associated with consumption of disinfected water. The estimated lifetime risk of bladder cancer due to consumption of chlorinated drinking water in the United States is between 5/1000 to 5/10000 (2); in contrast, 2 million people worldwide die each year from water-related diarrheal disease (10), much of which is likely preventable with adequate drinking water treatment. Morbidity and mortality may also occur from other water-borne illnesses, which further highlights the importance of adequate drinking water disinfection. The ultimate goal of drinking water disinfection byproduct research is to modify the disinfection procedure to reduce or eliminate potentially toxic DBPs while still maintaining adequate disinfection of drinking water. Therefore, the results of these experiments should not be construed as an argument against drinking water disinfection; rather, they indicate that some refinement in the disinfection procedure may be necessary to avoid formation of toxic byproducts.

6.3 Future work

There are many potential directions for future research arising from the current work. Most HBQ compounds described in this thesis were only subjected to preliminary assessment of *in vitro* toxicity (**Chapter 4**); therefore, future work could include testing these compounds with the same protocol used for DCMBQ

in **Chapter 5**. As discussed in **Chapter 4**, the role of the position of the substitution on the benzoquinone ring, the effects of chlorine vs. bromine substitutions, the effect of methyl substitutions, the number of substitutions, and other characteristics appear to influence the toxicity of HBQs. Performing more in-depth mechanistic testing on DBPs with different types and conformations of substitutions on the benzoquinone ring than those studied here could help clarify what role each of these characteristics plays in the toxicity of these compounds. For example, different HBQ compounds could be tested for ROS production using the DCFDA assay (see **Chapter 5**) to determine if substitutions on the benzoquinone ring affect ROS production. Likewise, testing of different HBQs with the comet assay (see **Chapter 5**) could reveal if the characteristics of ring substituents affect genotoxicity. As members of our research group have discovered that many other HBQ species are produced during water disinfection (7, 11), this testing could be expanded to other HBQ DBPs as they are discovered. Further characterization of the occurrence and concentrations of identified HBQs in finished water should also be performed to determine the possible exposure of the public to these compounds. Performing a hazard characterization of HBQ DBPs as well as a measure of potential public exposure will contribute to the risk assessment process for these compounds. Additionally, the methods described in the preceding chapters may be used to screen the hundreds, if not thousands, of other unknown DBP compounds as they are identified.

Although I explored some potential mechanisms of DBP toxicity in this work, additional mechanistic investigations may be performed. It was established in **Chapter 5** that DCMBQ can produce ROS *in vitro*, and that it was likely that these contributed to DNA damage. However, ROS may also react with other cellular macromolecules. Investigating potential formation of oxidized intracellular lipids and proteins in BJ and XPA cells may provide additional information on the mechanism of DCMBQ toxicity – a recent study from our lab found that DCMBQ caused protein oxidation but not lipid oxidation in a bladder cancer cell line (3). The nature of the DCMBQ-induced DNA lesions could be

explored further, particularly considering the possibility of complex or clustered oxidative DNA lesions as described in **Chapter 5**. Likewise, as quinones are known to have multiple potential mechanisms of toxicity (12), it may be helpful to explore non-ROS mediated mechanisms (e.g. direct macromolecule adduct formation, NADPH depletion, effect of GSH conjugation on metabolite toxicity etc.) to determine their role in DCMBQ and HBQ toxicity. Analysis of the effects of phenazine and HBQ DBPs on cell cycle progression with flow cytometry analysis might be useful, particularly as phenazine appeared to reduce proliferation in HepG2 cells (**Chapter 2**, **Figure 2-2A**). Flow cytometry analysis could also determine if phenazine and HBQ DBPs cause cell death via necrosis or apoptosis. Many other investigations are possible, depending on the desired mechanism of interest; these represent only a sample of potential future investigations for the DBPs discussed in this thesis.

Another avenue of further research involves the use of other testing systems and organisms, or modification of the assays described in the previous chapters. Many cell lines have different metabolic capacities than their equivalent *in vivo* tissues, or their metabolic properties are not well-characterized. Therefore, to examine the role of metabolism in DBP toxicity *in vitro*, metabolic enzymes could be added to cell cultures. (Initial metabolic modeling experiments were conducted by adding human hepatic S9 fraction to the BJ/XPA RTCA system described in **Chapter 3**; however, the cofactors required for enzyme function were toxic to the cells and further experimentation with S9 was abandoned.) Another approach would be to use primary cell cultures instead of immortalized cell lines for *in vitro* investigations. Primary cell cultures are thought to more directly model *in vivo* responses, including metabolic enzyme profiles. However, primary cells are not a feasible choice in the BJ/XPA RTCA model as many primary cell lines do not proliferate, have a very short life in culture (hours-days), and may require specialized culture techniques (e.g. sandwich culture) which prevent the cell-electrode contact required for the RTCA assay (13). Therefore, primary cell cultures may not be useful as a screening tool, but could be used for further

examination of potentially toxic DBPs identified during the screening process. Other *in vitro* culture techniques intended to produce more realistic exposure situations include 3D scaffolding and co-culturing with support cells (e.g. culturing hepatocytes together with Kupffer and stellate cells) (14), which could also be used on selected DBPs after the initial screening process. In order to provide adequate hazard characterization for regulatory agencies, DBPs identified as potentially toxic should also be examined with acute and chronic *in vivo* rodent bioassays. By using *in vitro* and *in vivo* methods together to investigate DBP toxicity, a more complete and environmentally relevant assessment of toxicity may be performed.

Further identification and quantification of DBP metabolites and transformation products may be accomplished with analytical chemistry techniques. Analysis of cell culture supernatant and cell lysates collected from DBP-treated cultures could determine the identity and location of DBP parent compounds and their metabolites or transformation products. As cell culture medium contains complex molecules and serum proteins which could confound the analysis, it is likely these experiments would need to be performed in a serum- or medium-free system, and sample concentration or specialized extraction techniques may be necessary. Optimization of treatment time, cell density, DBP concentration, and other experiment parameters would be necessary. A well-designed experiment could provide valuable information on *in vitro* DBP toxicokinetics and indicate the mechanisms of DBP detoxification or bioactivation by cellular enzymes. As members of our research group have developed methods for extracting, concentrating, identifying, and quantifying phenazine and halobenzoquinone DBPs, this represents an ideal opportunity for interdisciplinary collaboration.

6.4   Summary

Based on the findings in the previous chapters, I can conclude that phenazine and the tested HBQ DBPs are cytotoxic, mutagenic, and/or genotoxic under these experimental conditions. Phenazine is capable of producing an antiproliferative

effect in liver and bladder cell lines, and can cause DNA damage in bladder cells (**Chapter 2**). The BJ/XPA RTCA *in vitro* system, a high-throughput screening assay capable of assessing cytotoxicity and nucleotide excision repair-mediated DNA damage simultaneously, was developed and validated (**Chapter 3**). This system was successfully used to examine cytotoxicity of a selected group of halobenzoquinone disinfection byproducts; the assay detects differential cytotoxicity of the HBQs tested in normal BJ cells from the NER-deficient XPA cell line. Greater cytotoxicity in XPA cells compared to BJ cells may indicate formation of a nucleotide excision repair-mediated DNA lesion. These HBQs can also produce substitution mutations in the Ames test (**Chapter 4**). DCMBQ is the most potent HBQ compound tested in these experiments, demonstrating cytotoxicity, mutagenicity, and genotoxicity (**Chapters 4&5**). After further investigation, both the cytotoxic and genotoxic effects of DCMBQ appear to be mediated at least in part by the formation of reactive oxygen species (**Chapter 5**). These reactive oxygen species may produce DNA damage, potentially leading to mutagenesis or cellular dysfunction. DCMBQ may produce a type of complex DNA lesion known as oxidatively generated clustered lesions, which is more difficult to repair than other forms of oxidative damage. In light of these findings, DCMBQ warrants further *in vitro* and *in vivo* testing to fully characterize the effects it may have at environmentally relevant concentrations and exposure conditions. Deployment of a comprehensive *in vitro* screening protocol for new and recently-discovered DBPs is also necessary to identify and prioritize compounds for further testing. By identifying, screening, and minimizing the formation of potentially harmful DBPs, it will be possible to provide high-quality drinking water while minimizing risks from both biological and chemical contaminants.

6.5   References

1. Bull RJ, Reckhow DA, Li X, Humpage AR, Joll C, Hrudey SE. Potential carcinogenic hazards of non-regulated disinfection by-products: Haloquinones, halo-cyclopentene and cyclohexene derivatives, N-halamines, halonitriles, and heterocyclic amines. Toxicology. 2011 Aug 15;286(1-3):1-19.

2. Bull RJ, Awwa Research Foundation, United States. Environmental Protection Agency. Use of toxicological and chemical models to prioritize DBP research. Denver, CO: Awwa Research Foundation; 2006.

3. Du H, Li J, Moe B, McGuigan CF, Shen S, Li XF. Cytotoxicity and oxidative damage induced by halobenzoquinones to T24 bladder cancer cells. Environ Sci Technol. 2013 Mar 19;47(6):2823-30.

4. Atienza JM, Yu N, Kirstein SL, Xi B, Wang X, Xu X, et al. Dynamic and label-free cell-based assays using the real-time cell electronic sensing system. Assay Drug Dev Technol. 2006 Oct;4(5):597-607.

5. Huang R, Wang W, Qian Y, Boyd JM, Zhao Y, Li XF. Ultra pressure liquid chromatography-negative electrospray ionization mass spectrometry determination of twelve halobenzoquinones at ng/L levels in drinking water. Anal Chem. 2013 May 7;85(9):4520-9.

6. Boyd JM. Personal communication regarding phenazine concentrations in finished drinking water samples. 2013.

7. Zhao Y, Anichina J, Lu X, Bull RJ, Krasner SW, Hrudey SE, et al. Occurrence and formation of chloro- and bromo-benzoquinones during drinking water disinfection. Water Res. 2012 Sep 15;46(14):4351-60.

8. Qin F, Zhao YY, Zhao Y, Boyd JM, Zhou W, Li XF. A toxic disinfection by-product, 2,6-dichloro-1,4-benzoquinone, identified in drinking water. Angew Chem Int Ed Engl. 2010;49(4):790-2.

9. Hanahan D, Weinberg RA. Hallmarks of cancer: The next generation. Cell. 2011 Mar 4;144(5):646-74.

10. Facts and figures on water quality and health [Internet]. Geneva, Switzerland: World Health Organization; 2013. Available from: http://www.who.int/water_sanitation_health/facts_figures/en/index.html.

11. Wang W, Qian Y, Boyd JM, Wu M, Hrudey SE, Li XF. Halobenzoquinones in swimming pool waters and their formation from personal care products. Environ Sci Technol. 2013 Mar 13.

12. Monks TJ, Hanzlik RP, Cohen GM, Ross D, Graham DG. Quinone chemistry and toxicity. Toxicol Appl Pharmacol. 1992 Jan;112(1):2-16.

13. Castell JV, Jover R, Martinez-Jimenez CP, Gomez-Lechon MJ. Hepatocyte cell lines: Their use, scope and limitations in drug metabolism studies. Expert Opin Drug Metab Toxicol. 2006 Apr;2(2):183-212.

14. Kostadinova R, Boess F, Applegate D, Suter L, Weiser T, Singer T, et al. A long-term three dimensional liver co-culture system for improved prediction of clinically relevant drug-induced hepatotoxicity. Toxicol Appl Pharmacol. 2013 Apr 1;268(1):1-16.